Modelling of ionic interactions with organic components in wastewater

Sarah Westergreen

Date: December 2014

Supervisor: Dr. K.M. Foxon

Co-supervisor(s): Mr. CJ Brouckaert

Abstract

In current biological wastewater treatment models, physico-chemical processes (ionic speciation reactions, gas-liquid exchange, and liquid-solid interactions such as precipitation and adsorption) either are not explicitly considered, or are incorporated as simplified descriptions. This may result in an inaccurate prediction of digester behaviour. Specifically, the ionic behaviour of biomass is not explicitly included in standard models. The objectives of this study were to develop a model component that describes ionic behaviour of biomass, use this to predict the overall solution pH buffering capacity and determine its impact in an anaerobic digester's operating range (pH 6-8). The study hypothesises that the ionic behaviour of biomass can be described in terms of glycine equivalence; alternatively, it can be described by a model component consisting of functional groups characterised by concentration per unit mass of sludge and pK_a value for each group, either at equilibrium conditions, or considering kinetic effects.

The methodology involved constructing a mass balance / ionic speciation model capable of simulating alkaline and acidimetric experimental titrations with modifications for each hypothesis. Varying concentrations of glycine or suspensions of biomass (particulate organic matter) in background salt solutions were titrated and the model was fitted to the data by changing the parameters associated with the biomass description and, (where appropriate) associated kinetic terms, with associated estimation of parameter uncertainty.

A model component, UKZiNe was developed consisting of 4 functional groups; 2 carboxyl groups, 1 phosphate group and 1 amine group. Kinetic effects including carbon dioxide exchange and pH probe lag were explored.

The hypothesis that glycine could represent the ionic behavior of biomass was not supported. The alternate hypothesis, considering UKZiNe at equilibrium conditions, required further testing to evaluate the effects of kinetic reactions; the second alternate hypothesis that non-equilibrium effects significantly influence the measured experimental pH value, was supported.

All model formulations predicted that the biomass contribution to the overall buffer capacity in the operating region of an anaerobic digester was insignificant. The study implies that the inclusion of an ionic description of biomass does not considerably improve the pH prediction in digester simulations and can be excluded in future model development.

Preface

This dissertation presents the work performed by the author, Sarah Westergreen, in the School of Chemical Engineering at the University of KwaZulu-Natal, Durban, from January 2011 to December 2014, under the supervision of Dr Katherine Foxon and Mr Christopher Brouckaert.

The study is the original work by the author and has not been submitted in any form to any other university. Where use has been made of the work of others, it has been duly acknowledged in the text.

The publications resulting from the thesis work can be accessed in Water Science & Technology 65(6). 2012, pp: 1014 – 1020, doi:10.2166/wst.2012.922.

Acknowledgements

I would like to thank the Water Research Commission, the University of KwaZulu-Natal as well as the National Research Foundation for funding the research herewith. I would also like to thank the Pollution Research Group at UKZN as well as my supervisors Chris Brouckaert and Katherine Foxon for their continued support and supervision of this thesis and the work associated.

Declaration

I, ……., declare that

1. The research reported in this thesis, except where otherwise indicated, is my original research.

2. This thesis has not been submitted for any degree or examination at any other university.

3. This thesis does not contain other persons' data, pictures, graphs or other information, unless specifically acknowledged as being sourced from other persons.

4. This thesis does not contain other persons' writing, unless specifically acknowledged as being sourced from other researchers. Where other written sources have been quoted, then:

a. Their words have been re-written but the general information attributed to them has been referenced

b. Where their exact words have been used, then their writing has been placed in italics and inside quotation marks, and referenced.

5. This thesis does not contain text, graphics or tables copied and pasted from the Internet, unless specifically acknowledged, and the source being detailed in the thesis and in the References sections.

Signed

……

As the candidate's Supervisor I agree/do not agree to the submission of this thesis

1)	…….	…….	…….
	Name	**Signature**	**Date**
2)	…….	…….	…….
	Name	**Signature**	**Date**

Table of Contents

List of Figures

List of Tables

Nomenclature

Abbreviations

ASM	Activated sludge model
AD	Anaerobic digestion
ADM	Anaerobic digestion modelling
COD	Chemical oxygen demand
DOM	Dissolved organic matter
Exp	Experimental
FIM	Fisher Information Matrix
FSA	Free saline ammonia
IWA	International Water Association
LCFA	Long chain fatty acids
OP	Orthophosphate
PHA	Polyhydroxyalkanoates
RWQM	River water quality model
SCFA	Short chain fatty acids
SOM	Soluble organic matter
TP	Total phosphate
TS	Total solids
UCT	University of Cape Town
UKZN	University of KwaZulu-Natal
VFA	Volatile fatty acids
VS	Volatile solids
VSS	Volatile suspended solids

Symbols

μ	Viscosity
a	Activity
A	Site concentration
B	Equation constant

Symbols cont.

c	Concentration

cov	Covariance matrix
∂	Differential
f	Function
I	Ionic strength
J	Jacobian
k_a	Adsorption mass transfer coefficient
Kt	Thermodynamic equilibrium constant
K	Equilibrium constant
k_{CO3}	CO_2 exchange rate
κ	Conductivity
κ^0	Limiting solution conductivity
ΔH	Heat of reaction
N	Correction factor
p	Parameter/parameter set
P_{CO2}	Carbon dioxide partial pressure
pK_a	Log (Acid dissociation constant)
Q	Measurement error
S_{alk}	Alkalinity state
T	Temperature
t	Time
τ	Time constant
V	Volume
Y	Model value
Z	Charge
Δ	Differential
Σ	Sum
λ^o	Limiting solution activity
φ	Objective function
γ	Activity coefiicient

Chemical species & compounds

Ac^-	Acetate
Br^-	Butyrate
C	Carbon
Ca^{+2}	Calcium

CH_4	Methane
Cl^-	Chloride
CO_2	Carbon dioxide
CO_3^{-2}	Carbonate
COOH	Carboxylic acid
Gly^-	Glycine
H^+	Hydrogen
H_2O	Water
HCl	Hydrochloric acid
K^+	Potassium
Mg^{+2}	Magnesium
N	Nitrogen
Na^+	Sodium
$Na_2B_4O_7$	Sodium borate
NaCl	Sodium chloride
NaOH	Sodium hydroxide
NH_2^-	Amine
NH_3	Ammonia
NH_4^+	Ammonium
O	Oxygen
OH^-	Hydroxide
P	Phosphorus
PO_4^{-3}	Phosphate
Pr^-	Propionate
S	Sulphur
SO_4^{-2}	Sulphate
U	UKZiNe
Va^-	Valerate

Subscripts

exp	Experimental
i	Denotes species/functional group (UKZiNe)
m	Model
N	Number of functions
eq	Equilibrium

Superscripts

n	Number of ions
N	Number of tests
T	Transpose

Units

°C	Degrees Celsius
g	Grams
L	Litres
mg	Milligrams
mL	Millilitres
mM	Millimolar
mmol	Millimoles
mS	millisiemens
M	Molar
N	Normality
ppm	Parts per million
rpm	Revolutions per minute
s	Seconds
µL	Microlitres

Chapter 1 Introduction

1.1. Background

Biological wastewater treatment modelling is used to describe and monitor the behaviour of biological wastewater processes in aerobic and anaerobic systems. The existing models have focused largely on biological processes with a lesser emphasis on predicting the physicochemical reactions accurately.

Physicochemical processes are non-biological processes such as weak acid-base interactions, precipitation processes and redox conversions. (Batstone et al., 2010). Physicochemical reactions play an important role in any aquatic environment including wastewater and drinking water systems. Understanding these reactions and incorporating them in the modelling of anaerobic digestion is essential as they often establish the success or failure of the related biochemical processes. The physicochemical processes which need to be developed further in current models are (i) acid-base reactions, (ii) gas-liquid transfer, (iii) precipitation and (iv) chemical oxidation-reduction reactions; furthermore, it is necessary to characterise the influences of (i) non-ideality, (ii) temperature and (iii) reactions with organic solids (Batstone, et al., 2010).

The outcomes of the study are to develop a more robust model than what is currently available in the literature that allows for a better prediction of pH in anaerobic digesters and thereby reduce the uncertainty of the investigated physicochemical processes and influences that may affect anaerobic digestion modelling.

The improved modelling and prediction of pH and alkalinity in wastewater systems is of particular interest in anaerobic digestion models as the biological reaction kinetics are strongly influenced by the pH of the reaction liquor. The project plans to address the modelling and prediction by investigating two of the areas of interest in the position paper of Batstone et al. (2010), namely the acid-base reactions and the reactions with organic solids.

The characterisation of organic matter in wastewater (i.e. biomass) is of interest as different functional groups in the microorganism's cell wall interact with inorganic species in reaction liquors, possibly affecting the pH. The reactivity of organic solids is well understood, as suggested by Batstone et al. (2010), but there is no modelled characteristic of the biomass that can predict the reactivity and interaction. The project aims to (i) detail an explicit description of the acid-base interactions in wastewater systems thereby providing a more accurate pH prediction and thereafter (ii) determine the influence of organic solids within wastewater treatment systems by quantifying the ionic effects of biomass on the speciation chemistry of the system.

The project does not plan to address (i) biological reactions within wastewater treatment models with specifics to experiments targeting biological activity, (ii) the inorganic matter present in the sludge and the modelling of its behaviour, (iii) the precipitation of components within the wastewater system and their processes.

1.2. Research Objectives

- To develop a model that predicts interactions between dissolved inorganic ions and particulate organic components by:
    - (i) Modifying the Brouckaert et al. (2011) speciation model to include a representative model component to describe the ionic behaviour of particulate organic matter.
    - (ii) Conducting potentiometric titrations with particulate organic matter in suspension
    - (iii) Matching the model-simulated speciation behaviour to the titration data by the model component parameter regression.
- To determine whether biomass has an impact on the pH buffering capacity of wastewater in the operating range of anaerobic digesters by translating of model-simulated titration curves into buffer capacity curves and determining the buffer capacity contribution of the particulate organic matter.

Chapter 2 Literature review

In this chapter a review of the literature concerning the development of an acid-base model for biomass interaction with solution will be described. This includes pH prediction of anaerobic digestion models, cell wall chemistry of micro-organisms, the use of titrimetry for weak acid-base system characterisation and previous work into the development of the ionic description of biomass. Section 2.3 describes glycine and its use in previous research to describe metal-sludge systems. This is of importance as glycine is used in the thesis presented to model the ionic behaviour of biomass.

A review of the ionic speciation model based on the principles of Stumm and Morgan (1996) and Brouckaert et al. (2010) is provided in Section 2.4. A referencing convention has been applied throughout Chapter 2 such that if a reference is present in the body of the text, it is applicable to the entire paragraph.

2.1. Anaerobic digestion

2.1.1. Description of anaerobic digestion

In anaerobic digestion, complex particulate organic matter is broken down into carbohydrates, proteins and lipids in a disintegration step. The carbohydrates, proteins and lipids are further degraded by biochemical processes into mono-saccharides (sugars), amino acids and long chain fatty acids respectively. Acidogenesis or anaerobic oxidisation results in the relatively simple, soluble compounds being converted to short chain fatty acids (SCFAs), alcohols, carbon dioxide, hydrogen and ammonia. Some of the hydrolysis products are also converted to intermediate products which are further converted by acetogenesis to acetate, hydrogen gas and carbon dioxide. Methanogenesis consists of two different processes; these processes use the acetate and hydrogen formed in the previous process to (i) convert acetic acid to methane and carbon dioxide and (ii) convert hydrogen to methane by using carbon dioxide as an electron acceptor. See Figure 2-1 for an illustrated description of the anaerobic digestion processes reversible (Batstone, et al., 2002).

Anaerobic digestion requires multiple groups of organisms to complete the digestion of the organics. Each group of organisms has different metabolic behaviour. The behaviour can either be dynamic (short term changes in metabolic rate without any population change) or transient (long term change accompanied by possible population changes) (McCarty & Mosey, 1991). The organism groups referred to here are acidogens, acetogens, acetoclastic methanogens and hydrogenotrophic methanogens. Each of these organism groups has a specific range of pH for optimal growth. Acidogens operate best at a pH of around 6, while the acetogens, hydrogenotrophic and acetoclastic methanogens operate best at a pH of 7 (Moosbrugger, et al., 1993).

The groups of organisms operate in the following way:

(i) The acidogens allow for the conversion of complex organics to acetic and propionic acid, carbon dioxide and hydrogen.

(ii) Propionic acid is converted to acetic acid and hydrogen by acetogens.

(iii) The acetoclastic methanogens convert acetic acid to carbon dioxide and methane.

(iv) The hydrogenotrophic methanogens convert hydrogen and carbon dioxide to methane and water.

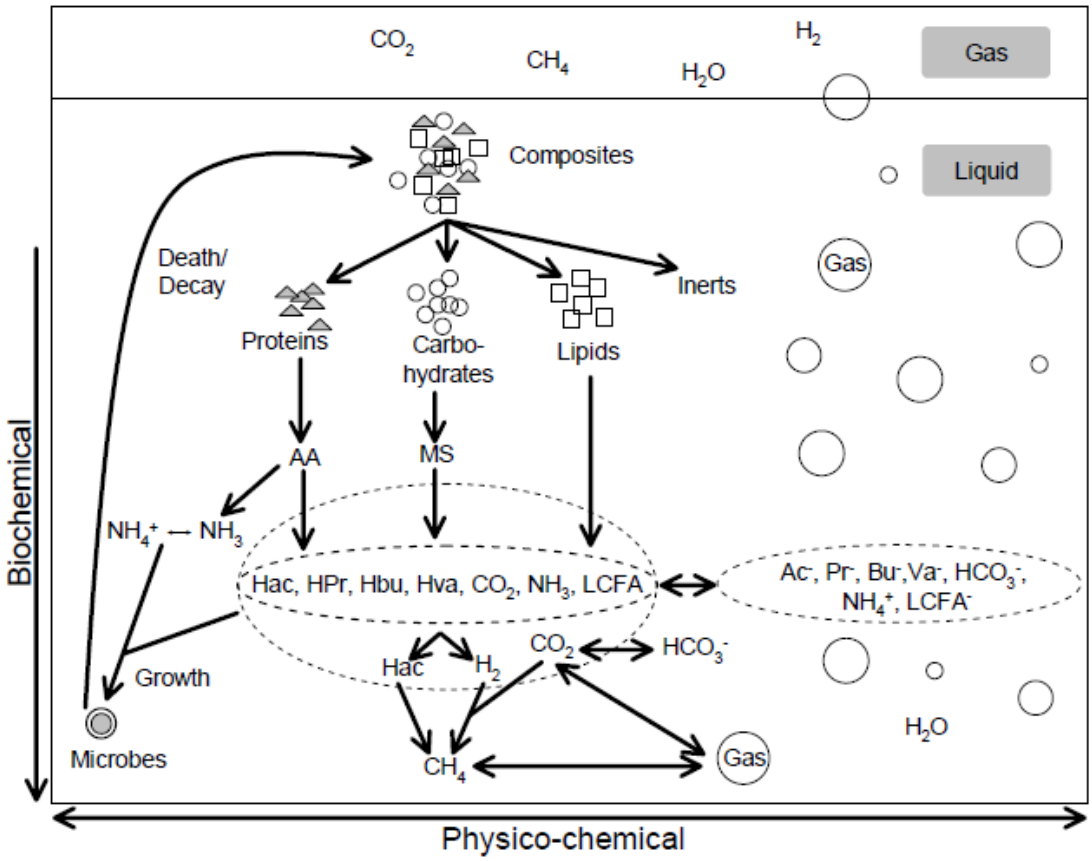

Figure 2-1: Conversion processes in anaerobic digestion. Biochemical reactions are implemented as irreversible, while physicochemical reactions are implemented as reversible (Batstone, et al., 2002)

The conversion processes involved in anaerobic digestion consist of physicochemical (non-biological) and biochemical processes. Figure 2-2 shows the conversion processes that impact anaerobic digestion.

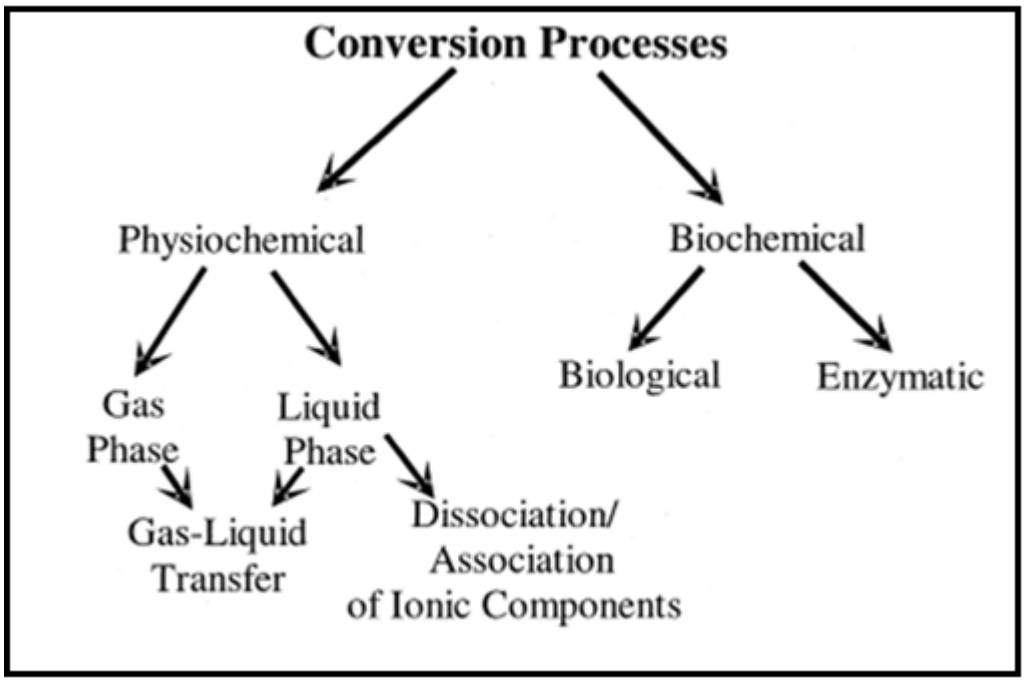

Figure 2-2: Physicochemical and biochemical conversion processes in anaerobic digestion (Batstone, et al., 2002)

Batstone et al. (2010) describe physicochemical processes as physical processes and chemical reactions that commonly occur in biochemical systems without the direct mediation of microbes. Physicochemical processes can either act as an individual treatment, have an impact on biochemical processes or be closely connected to the underlying biochemical process. Physicochemical reactions consist of ion association or dissociation processes and interphase (liquid-gas and liquid-solid) transfers of material. Batstone et al. (2010) have stated that the physicochemical sub-models embedded in the existing standardised biological wastewater treatment models are often rudimentary, empirical, or both. The corrections that need to be made for physicochemical systems are well understood. The solution non-ideality, temperature and impact of complex organic buffers need to be considered to address the limitations in current models.

2.1.2. Components of anaerobic digester sludge

Organic matter can be divided into biodegradable and unbiodegradable organic matter. Figure 2-3 shows that this matter can be further divided into particulate and soluble organic matter. Understanding the characteristics of both the soluble and particulate organics is important as both play an important role in the functioning of the anaerobic digester system. Adsorption of cations to the particulate organics comprising the wastewater sludge is commonly exploited for removing metal ions from water. A combination of the soluble organic matter characteristics (i.e. concentration and acidity constants) and the solution pH govern the total number of free sites available for metals complexation. Wang et al. (1998) explain that the soluble organic matter affects metal uptake by sludge particulates by competing with the particulate matter for metal ions.

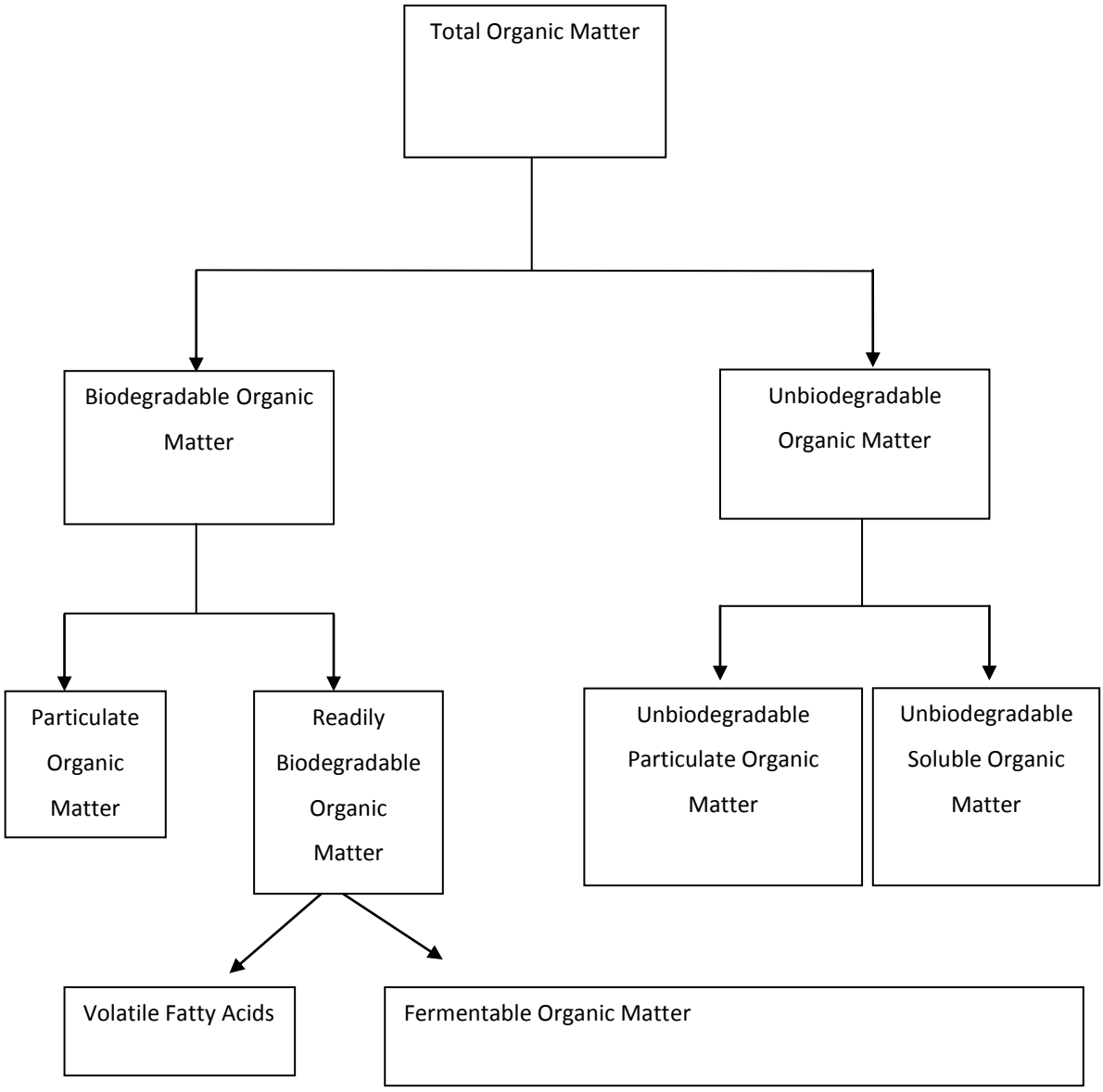

Figure 2-3: Characterisation of organic matter (Sotemann, et al., 2005)

2.1.3. Anaerobic digestion modelling

There have been several attempts at modelling activated sludge systems and anaerobic digestion. These attempts have resulted in the development of the widely accepted activated sludge models ASM series (ASM1, ASM2, ASM2d, ASM3) and the anaerobic digestion model ADM1. The activated sludge models, like ASM1 (Henze, et al., 1987), UCTOLD (Dold, et al., 1980), ASM2 (Henze, et al., 1995) and UCTPHO (Wentzel, 1992) use only COD, N and P mass balances and do not explicitly account for C, H and O balances. Most wastewater treatment systems processes can be

adequately described by COD balances, however, in anaerobic digestion the redistribution of C, H and O needs to be accounted for. This is as a result of (i) COD leaving the system as CH_4 without being destroyed, and (ii) the release and uptake of H^+ in large amounts, as well as the creation and destruction of organic acids that cause consequential changes in pH and solution buffering capacity.

In the ASM1, ASM2, ASM2d and ASM3 models, only the alkalinity state is accounted for (Henze, et al., 2000). In the ADM1 (Batstone, et al., 2002) and the river water quality model, RWQM1 (Reichert, et al., 2001), the actual pH is calculated. The current activated sludge models use a global alkalinity state (S_{ALK}), which is influenced by acid or base producing (or consuming) dynamic processes (Batstone, et al., 2010). The ASM approach assumes that the acids/bases are not weak and so do not contribute significantly to the alkalinity dynamics. The alkalinity state provides an estimate of whether the pH is near neutrality or far below it ((Henze, et al., 2000) as cited by Batstone et al. (2010) but does not predict an actual pH value.

At present none of the IWA models include non-ideal behaviour (i.e. species activity and ion-pairing) in the modelling of activated sludge systems and anaerobic digestion. The UCT models (Musvoto, et al., 2000) as cited by Batstone et al. (2010)) do take into account simplified ion activity correction as well as some ion-pairing behaviour. The disregard of non-ideal behaviour in the current modelling of the systems greatly impacts on the pH prediction as liquors treated in anaerobic digestion are not infinitely dilute and so cannot be assumed to be ideal.

The ADM1 (Batstone, et al., 2002) is one of the primary anaerobic digestion models used currently. The ADM1 model considers the feed to be made up of carbohydrate, protein and lipid fractions. The ADM1 model is composed of three primary steps:

i. Biological processes: acidogenesis, acetogenesis and methanogenesis
ii. Extracellular disintegration
iii. Extracellular hydrolysis

The kinetic model incorporated into the ADM1 accounts for all intracellular reactions, growth and biomass death and decay. The ADM1 (Batstone, et al., 2002) model incorporates algebraic algorithms based on weak acid-base equilibrium chemistry and the continuity of charge balances. These algebraic algorithms attempt to model the environment surrounding the biological processes to predict the pH. The model is structured so that the algebraic algorithms and calculation of pH operate externally to the kinetic model.

The model is limited in situations where many minerals contending for the same species may precipitate simultaneously or sequentially as in 3-phase multiple weak acid-base systems (Musvoto, et al., 2000). Chemical precipitation processes affect the charge balance and so will interfere with the pH

calculation. The chemical precipitation processes may render it important to include chemical precipitation in the model as some anaerobic digestion systems may have large amounts of mineral precipitation in the pipe work leading from the digester or within the actual digester(Barat, et al., 2009).

The UCTADM1 (Sotemann, et al., 2005) is a model similar to the ADM1. Figure 2-4 represents a simplified flow diagram of the approach used in the UCTADM1 modelling of anaerobic digestion. The reaction scheme differs from the typical reaction scheme in the following ways (Sotemann, et al., 2005):

- The separate carbohydrate, protein and lipid hydrolysis has been simplified to a single hydrolysis step where the complex sewage sludge is represented as a generic organic material, $C_xH_yO_zN_a$ (McCarty, 1974).
- The simplification of the single hydrolysis warranted the removal of the separate hydrolysis products whilst still maintaining the atom balance for C, H, O and N. A single end-product was chosen to be the idealised carbohydrate, glucose.

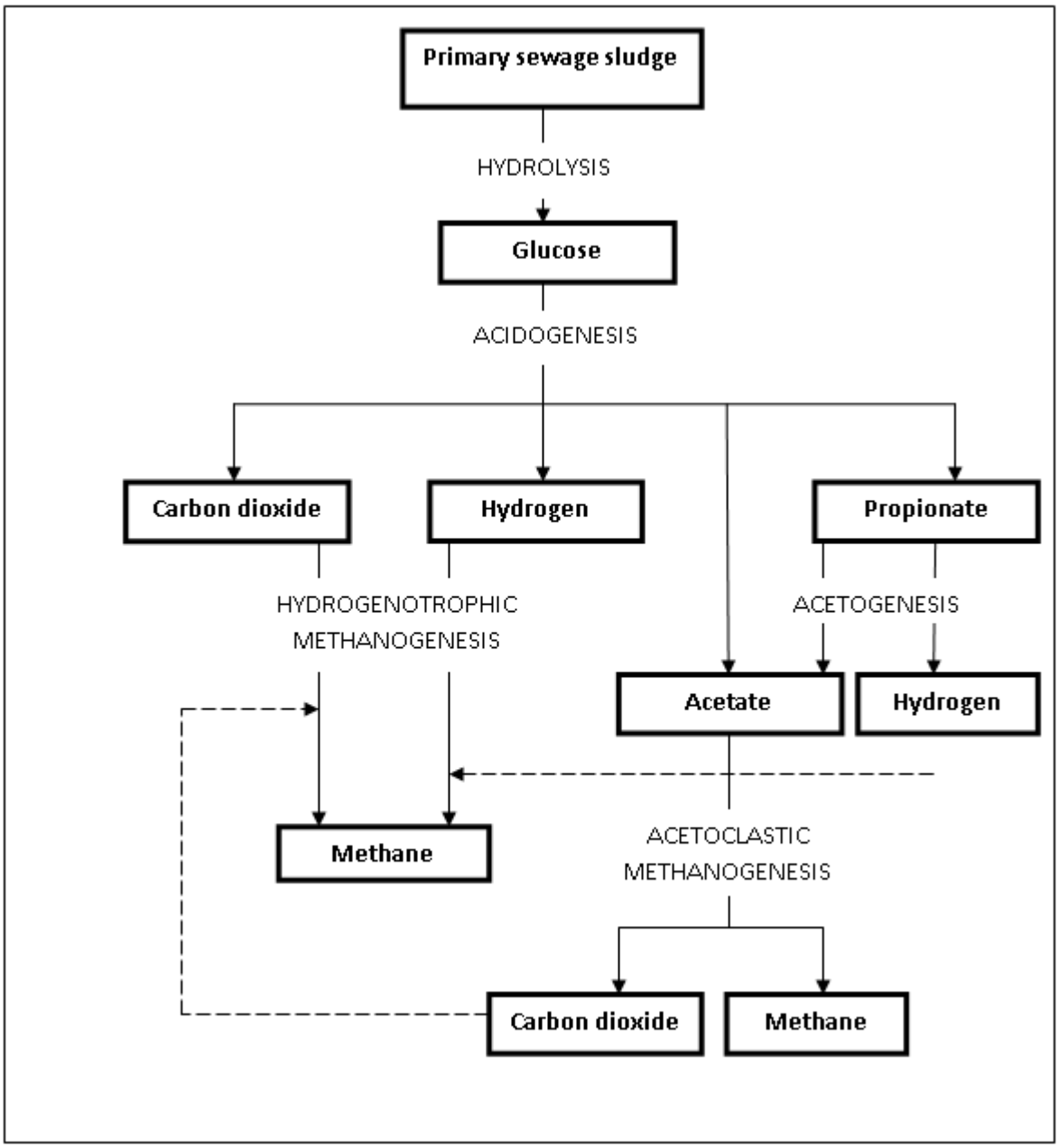

Figure 2-4: Process flow diagram of the different anaerobic digestion processes in the UCTADM1. Adapted from Sotemann et al. (2005).

The UCTADM2 is an extension of the UCTADM1 with some modification made (Brouckaert, et al., 2010). The UCADM2 extends the UCTADM1 in several ways; the principle extension is related to the inclusion of explicit modelling of factors which influence reaction liquor pH and alkalinity. The other extensions include incorporation of components that undergo acid/base or precipitation/dissolution reactions, kinetic reactions of slower processes (e.g. mineral precipitation) as well as an external speciation routine capable of calculating the equilibrium distribution of ionic species and the pH for any given total concentration of ionic components in solution.

The following features in the UCTADM2 should be highlighted (Brouckaert, et al., 2010):

- The wastewater organics composition has been assumed to comprise of the following elements: C, H, O, N and the model has been extended to include phosphorus (P). The compositions vary according to the relative proportions of each of the elements. The notation used to describe the composition is given in the form of $C_xH_yO_zN_aP_b$ where x, y, z, a and b denote the molar carbon, hydrogen, oxygen, nitrogen and phosphorus proportions. The amount of C, H, O, N and P (e.g. number of moles) are conserved. The organic components characterised by this formula are the inert solubles and particulates, biodegradable soluble and particulates, microorganisms, polyhydroxyalkanoates (PHA), endogenous residue, acetate, propionate and glucose each with their own stoichiometric formula.
- Although all of the microorganisms have the same stoichiometry, they are separated into 6 groups according to the reactions that they mediate. In anaerobic reactions 4 of the groups are required and the heterotrophs and phosphate accumulating organisms are represented as they may appear in the reactor feed.
- The minerals struvite, k-struvite and calcium phosphate and their precipitation/dissolution reactions have been accounted for in the UCTADM2.
- The ionic components accounted for are H^+, Na^+, K^+, Mg^{+2}, Ca^{+2}, NH_4^+, Cl^-, Ac^-, Pr^-, CO_3^{-2}, SO_4^{-2} and PO_4^{-3}. These components are represented as total concentrations. Using these total concentrations the external speciation routine calculates concentrations of all related ionic complexes and so the pH, alkalinity and ionic strength can be determined. The pH in the model is related to the free concentration of hydrogen ions.

2.1.4. Importance of pH and acid-base chemistry in anaerobic digestion

The microorganisms involved in anaerobic digestion require an optimum pH range of 6.4 to 7.6 in order to grow and function properly (Anderson & Yang, 1992). Toxicity and inhibition are two important factors which influence biological processes in anaerobic digestion and result when the digester operates outside of the optimum pH range due to the toxic effect of the hydrogen ions (Anderson & Yang, 1992).

Biocidal and biostatic inhibition are two forms of inhibition that can affect biological processes . Biocidal inhibition is described as reactive toxicity that is normally irreversible whereas biostatic inhibition is described as nonreactive toxicity that is normally reversible (Batstone et al., 2010). The pH and weak acid-base pair activity are two factors that can interfere with homeostasis and ultimately result in biostatic inhibition. Biostatic inhibition can have detrimental consequences as it influences the overall kinetics and functioning of the system.

A disruption in cell homeostasis can be a consequence of free acid and base inhibition due to changes in pH. The change in pH is caused by passive transport of the free acid or base across the cell membrane, followed by dissociation (Henderson, 1971). At ion and pH levels outside of the optimum conditions, the micro-organisms have to use energy to maintain homeostasis rather than using it for anabolism; consequently, the biomass yield decreases even though the substrate to product uptake may vary slightly.

Weak acids and bases play an important part in establishing the pH as well as buffering against pH changes in aqueous systems. When a weak acid/base dissociates in solution, the degree to which it dissociates depends on the pH, dissociation constant(s), the total species concentration of the weak acid/base system and the ionic strength of the electrolyte (Loewenthal, et al., 1989)

Acid-base chemistry influences the water quality in aqueous environments indirectly and directly. The direct contribution is by controlling the pH of the solution. The indirect contribution is by controlling the dissolution and precipitation of solids, altering the solubility of gases, aiding many other reactions and influencing the interactions of chemicals with organisms (Batstone, et al., 2010).

In municipal wastewaters carbonate, phosphate and ammonia are important weak acid-base contributors. In anaerobic digestion sulphides and short-chain fatty acids are also substantial weak-acid base contributors. The phosphate, ammonia and sulphide weak acid/base sub-systems are of minor importance in terms of pH buffering in the pH range of 6.6 to 7.4 (Moosbrugger, et al., 1993). However, they need to be determined for several reasons; firstly, to prevent nutrient deficiency or inhibition effects and secondly to accurately determine the total species concentration of the carbonate sub-system when using titrimetric methods. Ammonia, produced as a result of biodegradation reactions, also has a significant effect on the pH as it is a direct contributor to the alkalinity of the solution. A description of the weak-acid base sub-systems and their chemistry is shown in Figure 2-5.

The inhibition effects described above are pH-dependent as the relative amount of free acids or bases, when compared with the ionic component amounts, is strongly dependent on pH (Batstone, et al., 2002). Free acid or base pH inhibition can be detrimental in circumstances where (Batstone, et al., 2002):

i. organisms use substrate-to-product reactions with a low energy yield,
ii. organisms use proton motive forces[1] , for instance propionate and butyrate/valerate- oxidising organisms and

[1] Proton motive force is described as the measure of potential energy stored as a combination of proton and voltage gradients across a cell membrane. The movement of ions across a permeable cell membrane is

iii. methanogenic organisms use hydrogen and acetate as substrates.

Listed below are some compounds that are important in acid/ base inhibition in anaerobic digestion (Batstone, et al., 2002):

i. Free organic acids (in the associated form), namely HAc, HPr, HBr, HVa as well as Hydrogen.
ii. Free ammonia as well as major contributors to the free base in anaerobic digesters.
iii. Hydrogen sulphide.

The list above shows that the free acids (e.g. related organic acids, hydrogen sulphide) result in inhibition at a lower pH as they predominantly exist in the associated form and free bases (e.g. ammonia), existing predominantly in the dissociated form, cause inhibition at a higher pH . The organisms that are most affected by free acid/base inhibition are, in descending order of effect:

Aceticlastic methanogens > hydrogenotrophic methanogens > acetogenic organisms.

The last two are highly dependent on each other and so a decrease in the activity of the hydrogenotrophic methanogens will result in an apparent drop in the activity of organic oxidizing organisms because of the accumulation of hydrogen and formate in the system.

Characterisation and dosing estimations must be considered when working with weak acid-base systems. Characterisation involves estimating the species concentrations for each of the weak acid-base systems. Dosing estimation involves estimating the chemical dosage required to change the pH and species concentration to be within the desired range.

---

dependent on two factors: (i) Diffusion force resulting from a proton concentration gradient and (ii) Electrostatic force resulting from an electrical potential gradient. The proton motive force is derived from the combination of these two factors.

Aqueous phase equilibrium and mass balance equations for the different weak acid-base systems as stated by Stumm & Morgan (1996)

Carbonate system

Reaction 1: $H^+ + HCO_3^- \leftrightarrow H_2CO_3$ Eqn 2-1

Reaction 2: $H^+ + CO_3^{-2} \leftrightarrow HCO_3^-$ Eqn 2-2

Total Carbonate: $C_t = [H_2CO_3] + [HCO_3^-] + [CO_3^{2-}]$ Eqn 2-3

Ammonia system

Reaction 1: $H^+ + NH_3 \leftrightarrow NH_4^+$ Eqn 2-4

Total Ammonia: $N_t = [NH_4^+] + [NH_3]$ Eqn 2-5

Phosphate system

Reaction 1: $H^+ + H_2PO_4^- \leftrightarrow H_3PO_4$ Eqn 2-6

Reaction 2: $H^+ + HPO_4^{-2} \leftrightarrow H_2PO_4^-$ Eqn 2-7

Reaction 3: $H^+ + PO_4^{-3} \leftrightarrow HPO_4^{-2}$ Eqn 2-8

Total Phosphate: $P_t = [H_3PO_4] + [H_2PO_4^-] + [HPO_4^{2-}] + [PO_4^{3-}]$ Eqn 2-9

Short chain fatty acids (represented by acetate only)

Reaction 1: $H^+ + Ac^- \leftrightarrow HAc$ Eqn 2-10

Total SCFA: $A_t = [Ac^-] + [HAc]$ Eqn 2-11

The alkalinity is defined as the proton accepting capacity of the solution of mixed acid/base systems in water relative to a reference state.

Alkalinity of a H_2CO_3* /H_3PO_4/HAc/NH_4^+

$$\text{Alkalinity} = 2[CO_3^{2-}] + [HCO_3^-] + 3[PO_4^{3-}] + 2[HPO_4^{2-}] + [H_2PO_4^-] + [Ac^-] + [NH_3] + [OH^-] - [H^+]$$ Eqn 2-12

Figure 2-5: Aqueous phase equilibrium and mass balance equations for the different weak acid-base systems

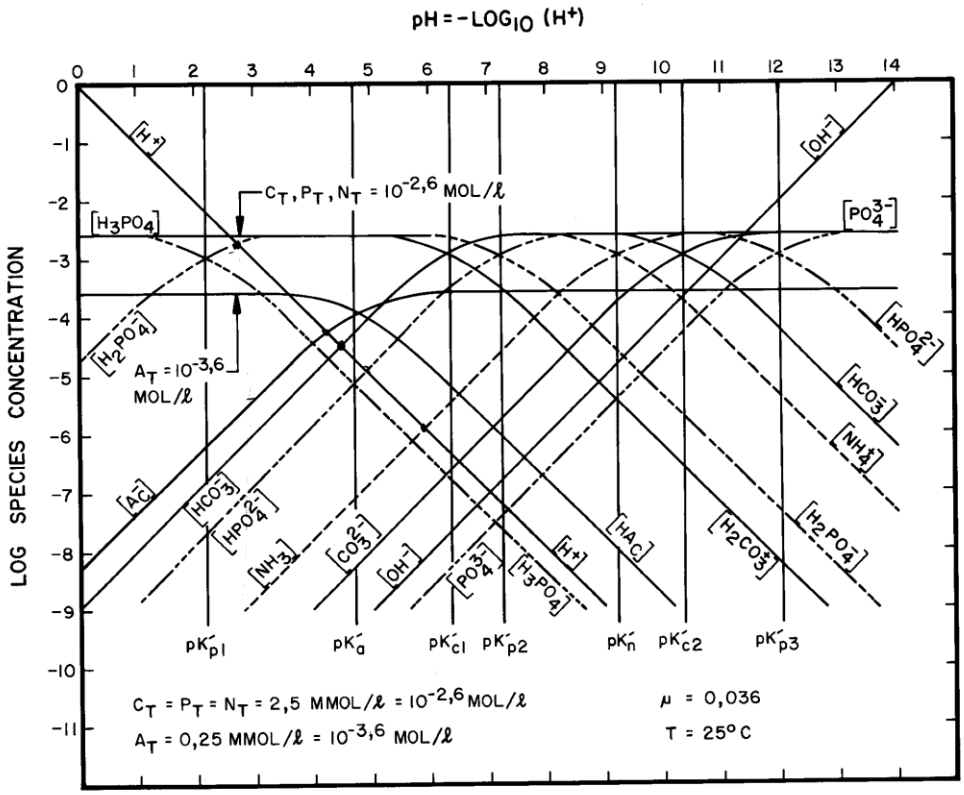

Figure 2-6: Log species-pH diagram for a mixture of carbonate, phosphate, acetate and ammonium systems (Loewenthal, et al., 1989).

Figure 2-6 is a classic log species-pH diagram and shows which species dominate at different pH values for the various weak acid-base sub-systems (Loewenthal, et al., 1989). In speciation modelling a number of influencing factors must be considered when modelling a weak acid-base pair; these are the ion-pairing and other co-ordination reactions with ionic species as well as the pH. The pH range being modelled must be established so as to determine the dominant species present at different pH values. The contributions of the species play an important role in determining which species should be included in the speciation model.

2.2. Cell wall chemistry

Batstone et al. (2010) acknowledge that although organic solids are known to be reactive, their influence on the physicochemical system has not been considered in models to date. It is believed that the redox state, acid-base properties and the chemical speciation of wastewater are affected by the presence and behaviour of microorganisms within the wastewater. Batstone et al. (2010)state that microbes and organic solids may act as acidity buffers, with negatively charged sites at high pH, and neutrally charged sites at neutral and low pH, rendering their importance in current models.

The interactions of ionic species and organic solids can be placed in two categories; firstly, ionic interactions between ions in solution and ionic sites on the exterior of the organic solids and secondly,

biological uptake and assimilation into the interior of active cells. It is believed that the former is the more significant effect (Nelson, et al., 1981). However, Claessens et al. (2004) report that live cells generate a far greater buffering capacity than that associated with its cytoplasm and cell wall.

The microorganism's cell wall is very important in regulating the movement of chemical substances into and out of the cell. It controls the interactions with other microorganisms as well as with its immediate environment. The cell wall structure aids in distinguishing between different bacteria. The cell wall can either be gram-positive or gram-negative (Beveridge, 1999). Gram-positive cell walls provide more acidic functional groups in comparison to gram-negative cell walls, thereby increasing the reactive nature of the cell wall (Beveridge, 1999). According to Voet and Voet (1990) the cell wall is made up of covalently linked polysaccharide and polypeptide chains forming a bag-like structure that completely encloses the cell.

The cell wall has various functional groups allowing for solute and colloidal species available in the surroundings to attach to the binding sites of the cell wall. Processes like ion exchange, complexation, precipitation, crystallization and/or physical forces result in the initial surface binding of proteins, lipids and different polysaccharides (e.g. glucan, mannan, chitin, and chitosan) onto the cell wall (Ruiz-Herrera, 1992; Korn & Northcote, 1960). The functioning of the cell-water interface is potentially influenced by carboxylate, phosphate and amino functional groups (Plette, et al., 1995; Haas, et al., 2001 as cited by Claessens, et al., 2006).

The chemical processes that occur in bacteria exposed to high pH are the deprotonation of functional groups and proton leakage. Macromolecules present in the cell wall contain exposed ionisable functional groups that can protonate or deprotonate depending on their acid dissociation constant and the pH of the medium. Proton leakage is the diffusion of hydrogen ions out of the cell at a high pH due to the presence of a concentration gradient across the cell wall. The charge of the cell wall is dependent on the pH due to protonation and deprotonation of the functional groups present (Claessens, et al., 2004).

The acid-base activity of cell walls is key to understanding metal binding, adhesion of minerals to the cells as well as mineralization or dissolution processes resulting from microbial action. The cell wall's make-up and structure play an important role in the biosorption of metals. The main functional groups in the cell determine the degree to which the bacterial cells and metal ions interact (Stumm & Morgan, 1996). According to Tien and Huang (1991) the amino acid groups are the most active binding sites in the uptake of metal ions by sludge.

The pH value of a solution is an important parameter to take into account when dealing with sludge particulate and organic matter. The pH influence on heavy metal uptake by sludge particulates has been shown by many researchers (Nelson, et al., 1981); (Tien & Huang, 1991); (Sreekrishnan, 1993).

Literature shows that the pH value can affect metal speciation through protonation of both the solid surface sites and the dissolved organic ligand (Fristoe & Nelson, 1983); (Nelson, et al., 1981); (Tien & Huang, 1991) as well as dissolution of organic matter from sludge particulates (Tien, 1987).

Acid-base titrations are a useful method of characterising the various functional groups as the titrations are able to quantify the protonation and deprotonation of the functional groups (Dzombak & Morel, 1990) as cited by Claessens et al. (2006). Acid base titrations aid in: (1) estimating the cationic exchange capacities of biosorbents (Coleman, et al., 1959) as cited by Naja et al. (2005); (2) identifying the acid ionizable functional groups or binding sites where ionic interactions with protons or other toxic metal ions take place (Pagnanelli, et al., 2004) as cited by Naja et al. (2005), and (3) in describing the chemical heterogenic reactivity of organic surfaces (Cox, et al., 1999) as cited by Naja et al.(2005).

In cases where the cells are alive, continuous titration curves may be affected by proton consumption or production related to active cellular processes (e.g. metabolic processes) or cell wall destabilization (Plette, et al., 1995). Forward and reverse potentiometric titrations can be used to quantify different processes occurring by analysing the hysteresis between the two curves. Forward and reverse experiments were used by Sederes and Fien (2011) to quantify the environmental concentrations and characteristics of dissolved organic molecules exuded from bacterial cells. Claessens et al. (2006) state that a combination of chemical analysis and titration curves of isolated cell walls results in a proposed approximate carboxylate, phosphate and amino group ratio of 2 :1 :1 with pK_a values of 4.3, 7.8 and 9.9. Table 2-1 shows a comparison of different studies of the functional groups characteristics, *viz.* the ionic group site concentrations and the pK_a values. Table 2-1 will be useful in comparing and validating the model developed in this study.

Table 2-1: pK_a values and ionic group site concentrations pertaining to the cell wall analysis of different species from various studies

Study	Species	Group 1		Group 2		Group 3		Group 4	
		pK_a (±)	A*	pK_a (±)	A*	pK_a (±)	A *	pK_a (±)	A *
(Yun, 2004)	*Sargassum Polycystum*	3.7 (0.09)	2.57 (0.06)	5.41 (0.31)	0.45 (0.07)	8.77 (0.28)	0.65 (0.11)	/	/
(Fang, et al., 2009)	*B. thuringiensis*	4.16 (0.18)	1.01 (0.48)	7.48 (0.28)	0.72 (0.07)	11.44 (0.63)	2.3 (0.21)	/	/
(Fang, et al., 2009)	*E.coli*	3.3 (0.24)	0.9 (0.05)	6.65 (0.36)	0.76 (0.06)	11.7 (0.9)	2.15 (0.07)	/	/
(Fein, et al., 2005)	*Bacillus subtilis*	3.3	0.75	4.7	0.96	6.8	0.31	8.9	0.75
(Kapetas, et al., 2011)	*Pantoea Agglomerans*	4.34 (0.24)	0.279 (0.041)	5.68 (0.24)	0.288 (0.022)	7.58 (0.19)	0.216 (0.51)	9.79 (0.09)	0.253 (0.086)

* Ionic group site concentration – mmol/g

2.3. Glycine

Artola et al. (1997) compared the behaviour of glycine-copper systems and sludge-metal systems. The work concluded that the behaviour of the two systems were similar, suggesting that the primary functional groups for binding metals in sludge are of the amino acid type. Sharon (1969) states that glycine, glutamic acid and alanine are commonly found in the cell wall. Glycine was chosen as a representative compound of biomass as it is the simplest amino-carboxylic acid. An additional motive for using glycine is because of its well-known behaviour in aqueous environments (i.e. solution thermodynamics) (Artola, et al., 1997).

Glycine (NH_2CH_2COOH) has the structure shown in Figure 2-7:

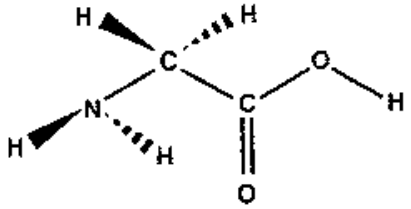

Figure 2-7: Glycine structure (Corliss, 1994)

Glycine Chemistry

The equilibrium reactions are as follows:

a. $H_2Gly^+ = H^+ + HGly$ [deprotonation of the $-COO^-$ group] Equation 2-13

b. $HGly = H^+ + Gly^-$ [deprotonation of the $-NH_2$ group] Equation 2-14

(Kiss et al., 1991; Stumm and Morgan, 1996)

Glycine, when not polymerized into a polypeptide chain, usually favours the zwitterionic state in both solution and solid form (Kiss, et al., 1991). The zwitterion is the $[HGly]^{\pm}$ form. When glycine exists as a zwitterion the amino group is protonated ($-NH_3^+$) whilst the carboxyl group is deprotonated (COO^-).

At a pH value of between 2 and 3 the carboxyl groups undergo protonation and the $[H_2Gly]^+$ complex is formed. The amino group loses a proton between pH values of 9 and 10 to become Gly^-.

2.4. Review of ionic speciation modelling

Most models have focused primarily on the biological processes occurring in the anaerobic digester. The significance of modelling the interactions of biological processes in weak acid -base environments is well understood; however, previous modelling experience has proved to be quite complex due to the effect of pH on the biological processes. Loewenthal et al. (1989) allowed for the inclusion of multiple weak acid-base systems which made it possible to estimate the digester pH and determine and interpret some of the digester control parameters, short chain fatty acids and alkalinity.

Several ionic speciation models exist as stand-alone models. The constraint in using these models in biological-type processes is that these models show little account (if any) for biological activity or interaction with organic solids. Some examples of ionic speciation models include WATEQ4F (Ball and Nordstroom, 1991), PHREEQC (Parkhurst and Appelo, 1999), SpecE8 (Bethke and Yeakel, 2010), EQ3NR (Wolery, 1992), MINTEQA2 (Allison et al., 1991), SOILCHEM (Sposito and Coves, 1988).

The mentioned ionic speciation models are used in every-day applications to screen water quality data by checking system charge balances, computing individual ion activities from analytical data determining aqueous speciation for bioavailability and toxicity as well as computing saturation indices which indicate the tendency of minerals to precipitate or dissolve.

Chemical speciation models by Allison et al. (1991) and Sposito & Mattigod (1979) model the organic ligand complexation of metals (i.e. the binding of metals using organic substances) and aid in determining the influence of ionic organics on the system pH, alkalinity and ionic strength. These

models, in general, involve simple organic acids and most of the geochemical models in application fail to estimate the uncertainty of predicted results.

The principles of ionic speciation and the corresponding calculations are provided in Stumm & Morgan (1996). PHREEQC ionic speciation software can be used as a reference model for comparing and validating the developing equilibrium ionic speciation models.

Speciation refers to the detailed distribution of the total concentrations of components between its ionic species; further explained, as the changing concentration of the different forms of an ion as the solution pH changes.

The speciation model published by Brouckaert et al. (2011) relates the concentrations of 42 ionic species to the total concentrations of 12 components by a set of 12 stoichiometric balances, together with a set of 30 equilibrium relationships.

The components chosen were based on the typical make-up of an anaerobic digester (i.e. carbonate, phosphate, ammonia, acetate, propionate and water weak acid/ base subsystems (Loewenthal, et al., 1994)). Other components such as sodium, potassium, magnesium, calcium, chloride and sulphate are commonly found in municipal wastewaters and, therefore, were also included (Brouckaert, et al., 2015). The components are : H^+, Na^+, K^+, Ca^{++}, Mg^{++}, NH_4^+, Cl^-, Ac^-, Pr^-, $CO_3^=$, $SO_4^=$ and PO_4^{-3}. The ion species are: H^+, Na^+, K^+, Ca^{++}, Mg^{++}, NH_4^+, Cl^-, Ac^-, Pr^-, HCO_3^-, $SO_4^=$, $HPO_4^=$, OH^-, H_2CO_3, $CaCO_3$, $MgCO_3$, $CaHCO_3^+$, $MgHCO_3^+$, $CO_3^=$, $H_2PO_4^-$, $MgPO_4^-$, $CaPO_4^-$, $MgHPO_4$, $CaHPO_4$, HAc, HPr, NH_3, $CaSO_4$, $MgSO_4$, $CaOH^+$, $MgOH^+$, $NH_4SO_4^-$, $NaHPO_4^-$, $NaCO_3^-$, $NaHCO_3$, $MgH_2PO_4^+$, $CaAc^+$, NaAc, $MgAc^+$, $CaPr^+$, $MgPr^+$ and $NaSO_4^-$.

Most of the ionic species, excluding the ionic components, are of no direct interest to the biological model as they do not explicitly participate as reactants or products of the biological processes and also do not directly influence the kinetics of these processes. However, it is necessary to solve for the ionic species in order to obtain an accurate prediction of the pH as these species indirectly affect the pH.

Solution non-ideality becomes important when the solution is away from infinite dilution as the component's activity is lower than its concentration (Batstone, et al., 2010). In the case of Brouckaert et al. (2011), the non-ideality is accounted for by the use of species *activities*. The incorporation of species *activities* act as a correction for solution non-ideality to allow for better prediction of physicochemical systems. The equilibrium relationships are described in terms of species activities, which are related to their concentrations by *activity coefficients* (see Equation 2-15). The Davies equation (Stumm and Morgan, 1996) has been used in modelling the activity coefficients (Brouckaert et al., 2011). The Davies equation makes a simplification for the activity coefficients as it calculates

one activity for each of the monovalent, divalent and trivalent ions at each ionic strength and does not consider variations between different ions with the same valence state (see Figure 2-8).

$$a_i = \gamma_i \, c_i \qquad \text{Equation 2-15}$$

where a_i: activity; γ_i : activity coefiicient (function of ionic strength); c_i : concentration

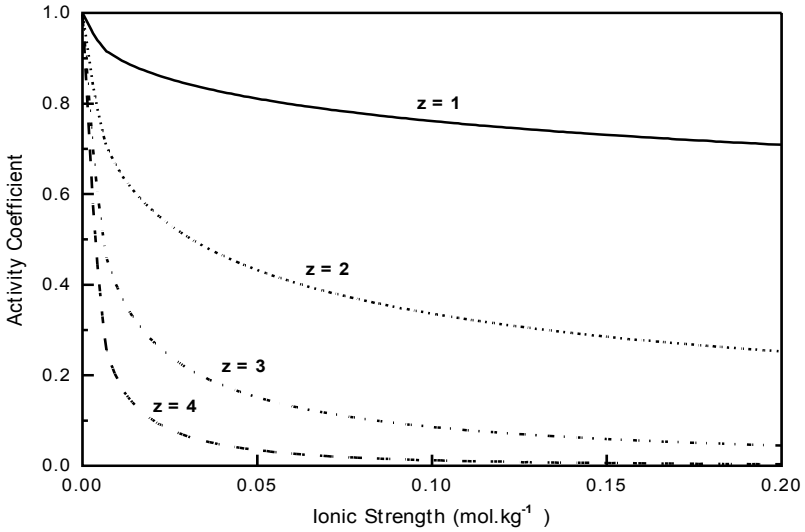

Figure 2-8: Activity coefficients of charged species predicted by the Davies equation

The speciation algorithm in Brouckaert et al. (2011) searches iteratively for a set of species concentrations which (i) satisfy all the equilibrium relationships with known equilibrium constants (Brouckaert, et al., 2010) and (ii) add up to the total known component concentrations at the same time. The species composition then allows for characteristics like the pH and alkalinity to be calculated.

Brouckaert et al. (2010) make the statement that most laboratory analyses do determine total concentrations, but the total H^+ and total $CO_3^{=}$ are important exceptions that are usually represented indirectly by pH and alkalinity measurements. Measuring the concentrations of all ions present in the sample is usually impractical and too time-consuming. This results in the ionic strength not being known and therefore the charge balance not being met due to missing analytical information. Knowledge of the ionic strength is vital in predicting the ionic activity coefficients which are used in the speciation calculations. Theoretically, the ionic strength determination requires the complete ionic composition to be known, but is reasonably accurately correlated with electrical conductivity (Loewenthal et al., 1989 as cited by Brouckaert et al., 2010).

Conductivity is frequently used to give an overall indication of the concentration of ionic solutes in a solution. Temperature is extremely important when dealing with conductivity. A correction for the temperature has been taken into account in the Brouckaert et al. (2011) model.

This correction is of the form (Talbot et al., 1990 as cited by Brouckaert, 1995).

$$\kappa(T) = \kappa(20^{O}C)\left[\frac{\mu(20^{O}C)}{\mu(T)}\right]^{0.896} \quad \text{Equation 2-16}$$

where

κ: conductivity ; μ: viscosity

It is important to take the speciation of ions into account when dealing with conductivity as the conductivity is the overall outcome of the ionic mobility in solution and the ionic charge.

The speciation model developed by Brouckaert et al. (2011) uses the expressions:

$$\kappa = \kappa^{o} - NI^{n} \quad \text{Equation 2-17}$$

$$I = \frac{1}{2}\sum z_i^2 c_i \quad \text{Equation 2-18}$$

where κ^{o}: limiting solution conductivity; N: correction factor; I: Ionic strength; n: number of ions; z: charge; c: concentration

The distribution of ions and the limiting equivalent conductivities of the original ions is used to calculate the limiting specific solution conductivity (Brouckaert, 1995):

$$\kappa^{o} = \sum c_i |z_i| \lambda_i^{o} \quad \text{Equation 2-19}$$

where λ_i^{o}: limiting solution activity

Chapter 3 Materials and methods

It has been identified that there is a gap in current modelling descriptions with regard to physicochemical processes and their influence on the overall prediction of pH and buffering of reaction liquors. Batstone et al. (2010) address the need for inclusion of solution non-ideality, the impact of complex organic buffers and temperature within existing embedded physicochemical models. The work of Artola et al. (1997) suggests that modelling a glycine-like component would be a fair representation of reactive organic solids.

Therefore, the objectives of this study are to develop a mathematical description of the pH buffering capacity of anaerobic sludge either by representing its ionic behaviour by that of glycine, or some other chemical description, and to determine the overall impact of the organic solids on the digester liquor's buffering capacity.

Hypothesis

It is proposed that:

i. Glycine can be used as a representative model component to describe the ionic behaviour of biomass
ii. Alternatively, if the above is not supported by the results, then biomass can be described by a formulated model component at equilibrium
iii. Alternatively, if the above is not supported by the results, then biomass can be described by a formulated model component with both equilibrium and kinetic considerations.

3.1. Experimental plan

It is assumed that the ionic speciation behaviour of biomass can be observed by a potentiometric titration between high and low pH values (or vice versa) and that a model that can describe this can also describe the ionic behaviour of the biomass in an active biological system. Therefore, the experiments performed involved titrations of different preparations of biomass and chemical reagents with acid or base and thereafter simulating the experiment with a *titration model*.

The experimental plan aimed at testing the 3 hypotheses by following the program below:

1. Formulate a mathematical description of the ionic speciation behaviour of biomass relating to the hypothesis being tested.
2. If required, modify the titration model that includes the built-in ionic speciation model developed by Broackaert et al. (2011) to incorporate the mathematical description of the ionic speciation behaviour described in (1).

3. Design and execute an experiment to generate data against which the model prediction can be tested.
4. Fit the titration model to the generated experimental data by parameter adjustment

The sections that follow include:

- The titration model (Section 3.2). The formulation of the mathematical descriptions pertaining to each of the 3 hypotheses can be found in the respective chapters (Chapters 4, 5 and 6)
- The titration experiment (Section 3.3). A generic review is outlined in this section; the details relevant to each experiment are described in the respective chapters (Chapters 4, 5 and 6)
- The parameter estimation used in establishing the parameters in the ionic speciation model (Section 3.4).
- The experimental errors and uncertainties (Section 3.5).
- The delimitations of the study as a whole (Section 3.6).

3.2. The model

The titration model built in this study describes the titration of a preparation of biomass with acid or alkaline titrant. The titration model makes use of a built-in speciation model developed by Broackert et al. (2011) and modifies the model to include a model component that describes the ionic behaviour of biomass. The overall objective is to identify a biomass model component in terms of molar concentration per mass of biomass and one or more pK_a values of the model component such that the model simulated titration output (pH value after addition of a fixed amount of titrant) matches the equivalent value measured experimentally. It uses known inputs (volume of initial solution, volumes of acid or alkaline solution added and concentration of titrant) and regressed parameters (initial ionic component concentrations in the biomass sample) to deliver the outputs of pH, buffer capacity and species concentrations after a known volume of acid or alkaline titrant is added. A mass balance algorithm (refer to Section 2.4) within the model is used to calculate the total component concentration after each titrant volume addition (corresponding to a data point from a real titration experiment) using the component amount from the previous step and the amount added with the titrant.

The model uses literature constants for equilibrium reactions (Brouckaert, et al., 2010) and initial sample component concentrations as the primary model parameters. The generated component concentration vector for each point on the titration curve is fed to the built-in ionic speciation algorithm developed by Brouckaert et al. (2011), (Section 2.4), that calculates the species concentrations, pH value and buffer capacity. For the testing of each hypothesis, the mass balance

algorithm and built-in ionic speciation model were modified to include the mathematical description to be tested.

The first hypothesis was tested by modelling a glycine-like component where the characteristics of the functional groups such as number of ionic groups, ionic group site concentration ratios[2] and pK_a values were based on those of glycine. The user-provided inputs into the modelling of phase 1 (hypothesis 1) were the initial sample component concentrations, the initial sample volume, the titrant concentration as well as the amount of titrant added. The speciation constants for the glycine species were sourced from literature (Kiss, et al., 1991).

The alternative hypotheses were tested in phases 2 and 3 by including an ionic description of the component's functional group characteristics different to that of glycine, as described in the model developed for testing the first hypothesis. The models used to test the alternate hypotheses build on the formulated model component, named UKZiNe, by (i) identifying the functional groups of the component, (ii) regressing for the functional group site concentration ratios and total alkalinity and (iii) regressing for the pK_a values of the identified functional groups as seen in phase 3 (hypothesis 3). Phase 2 (hypothesis 2) involved manual fitting of pK_a values for the individual functional groups.

The buffer intensity was thereafter calculated by numerical differentiation, using a central difference formula for both the experimental and model data:

$$\frac{dY(i)}{dX(i)} = \frac{2\,(Y(i+1)-Y(i-1))}{X(i+1)-X(i-1)} \qquad \text{Equation 3-1}$$

The model makes the following assumptions:

i. The solution is in ionic equilibrium for testing the first and second hypotheses. For testing the third hypothesis, it is assumed that mass transfer exists between the UKZiNe and the bulk solution. The only ions considered to undergo mass transfer are hydrogen ions.
ii. Biological reactions and carbon dioxide exchange between the solution and atmosphere are assumed to be negligible when testing the first and second hypotheses. The model used to test the third hypothesis accounts for carbon dioxide exchange between the solution and atmosphere.

[2] Ionic group site concentration ratios: The ratio of the site concentrations of the ionic groups to one another (carboxylate: phosphate: amino)

iii. The lag in pH probe reading after a volume of titrant has been added was assumed to be negligible when testing the first and second hypotheses. The third hypothesis accounts for a significant pH probe response delay.

iv. Literature values are assumed to be valid for dissociation constants for all components (Brouckaert, et al., 2010), in the built-in ionic speciation model, except UKZiNe and therefore are treated as known model constants.

v. There are no significant precipitation or dissolution effects during the experiment.

vi. The biomass does not change with respect to functional group characteristics between different samples.

3.3. The experiment

This section describes a generic review of the materials and methodology used in the experiments for each of the phases. The Methods section, Section 3.3.3, describes the principles of the test used; a full description of the experimental methodology relevant to each phase can be found in the respective chapters (Chapters 4, 5 and 6).

3.3.1. Materials

This section reviews the materials used in the experimental methodology. The reagents used were supplied from ACE (Associated Chemical Enterprises) and were AR grade. The review details the following :

- The acid and alkaline titrants used in titrating the experimental sample sets
- The synthetic anaerobic digestion liquor used as a representative background solution for experimentation
- The glycine used in the first phase of the study
- The yeast and anaerobic sludge used as organic matter

3.3.1.1. Titrants

It is necessary to titrate with both acid and base to cover the entire pH range under investigation as most anaerobic digestion samples have starting pH values between 6 and 8.

Aliquots of standardised 0.1 or 0.5 M hydrochloric acid and 0.1 or 0.5 M sodium hydroxide were used to titrate the sample solutions. The hydrochloric acid was standardised with 0.1 M disodium borate tetrahydrate and the sodium hydroxide was standardised relative to the hydrochloric acid. The titrants were standardised at least weekly and with every addition of new reagent to the reagent bottle. Refer to Section 3.3.3. for the full standardisation procedure.

3.3.1.2. Synthetic anaerobic digestion liquor

The components making up the synthetic liquor composition were chosen based on the composition of primary sludge or waste activated sludge anaerobic digestion liquor (Ikumi et al., 2010) as according to Table 3-1. Precipitation was not considered in the experiments and hence calcium chloride dihydrate and magnesium chloride hexahydrate were not used.

Table 3-1: Primary sludge/waste activated sludge anaerobic digestion liquor composition(Ikumi, 2010)

Reagent used	Concentration (mmol/L)
Ammonium chloride	12.69
Disodium hydrogen orthophosphate	14.70
Sodium hydrogen carbonate	12.78
Magnesium chloride hexahydrate	1.03
Calcium chloride dihydrate	0.67
Sodium acetate	0.20

Table 3-2 shows the final prepared solution compositions that make up the mixed salt background solution for the experimental titrations.

Table 3-2: Solution compositions containing varying phosphate and carbonate concentrations

Concentration of (mmol/L):	Disodium hydrogen orthophosphate	Sodium hydrogen carbonate	Ammonium chloride	Sodium acetate
Solution 1	4.06	12.77	10.43	0.20
Solution 2	3.91	12.01	/	/
Solution 3	1.60	5.04	/	/

3.3.1.3. Glycine

Titration experiments were performed on solutions of 0.004 M , 0.008 M and 0.016 M glycine.

3.3.1.4. Organic Matter

The biomass was stored in an air-tight container and was purged with nitrogen gas to remove oxygen from its surroundings. The container was stored at 4 °C to ensure minimal biological activity and degradation of the sludge. The various types of biomass investigated were:

(i) Washed compressed baker's yeast: 2.28 – 8.69 g TS/L
Baker's yeast in cake form was bought from a local baker. It is important to note that the history of the different batches of yeast (prior to purchase) was unknown.

(ii) Anaerobic digester sludge from municipal waste :0.96 - 3.85 g TS/L

3.3.2. Equipment

- Radiometer TIM860/TIM870[3] autotitrator and software. The unit and software allow for the experimental processing parameters to be set. These include:
    i. Burette speed
    There is one 25 mL burette installed on the TIM 860 and two burettes installed on the TIM 870 (25 mL, 10 mL burettes). The speed of titrant addition in the burette can be set between 0.001 mL/min – 3 times the nominal burette volume (mL/min). The burette speed was set between 0.001 – 0.5 mL/min for the experiments conducted.
    ii. Magnetic stirrer installed
    The stirrer bar can be set to a mixing speed between 100 and 1100 rpm to achieve a homogeneous mixture. Caution must be taken when setting over 450 rpm that a vortex is not formed in the sample. The stirrer was set between 250 – 950 rpm for the experiments conducted.
    iii. Method
    The user can specify a method such as pH end point, continuous, monotonic and dynamic inflection point. The experiments used the pH end point method with a pH end point of 3 for acidimetric titrations.
- Hanna HI1131 pH probe

[3] The TIM860 was used in phases 1 & 2 due to software malfunction on the TIM870 that was originally responsible for the titrations. Following the resolution of the TIM870 software malfunction, the TIM870 was used for the phase 3 of testing.

- Radiometer temperature probe T201
- Boeco Micropipette (10 mL)
- Hermle Z323 centrifuge
  This was used to centrifuge the washed samples to separate soluble and particulate organic matter.
- OHAUS Adventurer balance PA214

3.3.3. Methods

The methods described in this section involve the procedure followed to complete an experiment. The procedure involves (i) sample preparation and (ii) sample titration.

3.3.3.1. Sample preparation

The samples were prepared for titration by weighing the required components of the mixture into a titration vessel. The components refer to a water phase, mixed salt background solution stock reagents, glycine and biomass where required.

The inclusion of biomass in the sample required a pre-treatment before mixing into the background solution. Following a similar methodology to Claessens et al. (2006), the biomass (sludge or yeast) was prepared for titration by a series of centrifugation and washing steps. The particulate organic matter remaining was centrifuged twice at 10 000 rpm for 10 mins. The samples were washed with distilled water or NaCl solution (refer to Chapters 5 and 6 for specific washing solution) before centrifugation to ensure the removal of any soluble inorganic and organic material on the surface of the biomass. The total solids and fixed solids of the prepared particulate organic matter were measured according to Standard Methods (AWWA, 1989). The total solids is a measure of the moisture-free solids per unit of sample. The fixed solids is a measure of the inorganic solids remaining after volatilisation of any volatile solids per unit volume/mass of sample. The total and fixed solids measurements are used as a measure of the composition of the biomass used in the titrated sample.

Following the addition of the components into the titration vessel, the solution was mixed using a magnetic stirrer to ensure that the solids were homogenously suspended in the background solution.

3.3.3.2. Sample titration

Titrimetric methods were developed to determine the acid-base titration characteristics of glycine, baker's yeast and anaerobic digester sludge in a water phase as well as in a background synthetic solution analogous to anaerobic digestion liquor using an autotitrator. Ongoing software malfunctioning resulted in the use of only one burette for most of the experimental work. The sodium hydroxide solution was dosed using a pipette and in later

experiments was titrated into the sample. The sodium hydroxide was dosed to reach the pH endpoint specified for the experiment. The samples were subsequently titrated with acid to a pH endpoint to develop an acidimetric titration curve of volume of acid added versus pH and time.The titrations were conducted in an uncontrolled environment with respect to gaseous exchange with the solution and temperature control of the solution and atmosphere.

The model parameter regression and titration curve fitting used between 3 to 7 experimental titrations each consisting typically of 70 to 500 data points dependent on the titrant concentration, solution compostion and titrant rate of addition.

3.3.3.3. Experiment sequence and procedure

(i) The pH probe was calibrated and the titrants standardised

(ii) Each of the burettes was flushed – this was done to remove any air bubbles throughout the piping and nozzles

(iii) The sample was weighed into the sample container
   (a) The sample was tared on the scale
   (b) The solids were first mixed before they were added to the sample container
   (c) The required background solution was added to the sample container by weighing into the sample container

(iv) The magnetic stirrer was added and the sample was stirred for approximately 1 min at the specified speed before starting the titration experiment

(v) The pH was measured

(vi) The base was titrated into the sample, while stirring, to rise the pH to the specified value and the amount was recorded

(vii) The acid was titrated into the sample, while stirring, to drop the pH to a value of 3.The experiment was repeated

3.4. Parameter estimation

As mentioned in the description of the model, the overall objective of the study is to identify a biomass model component in terms of molar concentration per mass of biomass and one or more pK_a values of the model component such that the model simulated titration output (pH value after addition of a fixed amount of titrant) matches the equivalent value measured experimentally. The matching of the simulated and experimental values on the titration curve is accomplished by the parameter estimation whereby the parameters are estimated through regression to achieve the lowest objective

function value, calculated from the difference between the experimental and simulated titration curves.

The algorithm determining the equilibrium speciation solves a set of highly non-linear algebraic equations. As the model outputs are highly dependent on the parameter values to be regressed for, the model outputs will also be non-linear. This introduces some complexity to the parameter estimation.

Model non-linearity, data scarcity and non-Gaussian error distribution as well as determining the "best" parameter values contribute to the common difficulties experienced in parameter estimation (Marsili-Libelli et al., 2003). The recurring theme apparent from relevant literature is the concept of seeking a "valid" set of parameters in terms of residuals rather than searching a "true" model (Marsili-Libelli et al., 2003).

The parameter estimation was conducted using an initial value approach with:

$$y = f(p) \qquad \text{Equation 3-2}$$

where p is the set of parameters to be regressed; in the case of phase 2 it is the site concentrations of UKZiNe and the alkalinity and in phase 3 it is the UKZiNe site concentrations, the alkalinity, the CO_2 rate and mass transfer time constant.

Parameter estimation consists of finding the minimum objective function. In this study MATLAB was used to find the minimum objective function using the equation below:

$$\varphi(\boldsymbol{p}) = \sum_{i=1}^{N}(y_{i,exp} - \boldsymbol{y}_{i,m}(p))^2 \qquad \text{Equation 3-3}$$

where φ is the objective function, p is the parameter vector, i is the point along the titration curve, N is the total number of data points, $y_{i,e}$ is the experimental pH value at each point, $y_{i,m}$ (p) is the calculated simulated pH value using the estimated parameters.

3.4.1. Parameter estimation sensitivity analysis

Once the data is modelled and the parameter estimates are obtained it is valuable to perform a sensitivity analysis. Sensitivity analysis has been used extensively in determining the uncertainty in the output of a model. Sensitivity analysis can be defined as how the uncertainty in the model output can be attributed to different sources of uncertainty in the model input (Saltelli et al., 2008); in this case, primarily the parameter values.

The Jacobian matrix (J) can be defined as a matrix of changes to the model output values for perturbations In the model parameter values.

$$J = \frac{\partial(f_1, f_2, \ldots\ldots f_n)}{\partial(p_1, p_2, \ldots\ldots p_n)}$$ Equation 3-4

The Jacobian matrix is used to calculate the co-variance to determine the correlation and dependency of the parameters on one another as explained by the following equation:

$$cov = (\sum_{i=1}^{N} (J^T) Q_i (J))^{-1}$$ Equation 3-5

The experimental portion of the uncertainty analysis is summarised in the Fisher information matrix (FIM) by combining the sensitivity functions, $\delta \boldsymbol{f} / \delta \boldsymbol{p}$, and the measurement error, $\boldsymbol{Q_i}$ (Peterson et al., 2001). The FIM is described as a summary of the amount of information in the data relative to the quantities of interest.

$$FIM = 1/cov$$ Equation 3-6

Part of the *fmincon* algorithm in MATLAB calculates the Jacobian matrix (Equation 3-4) which is used in the computation of the confidence intervals and other sensitivity analysis calculations. The confidence intervals give an indication of the quality of the estimates and a measure of uncertainty to these ascertained values.

The confidence intervals outputted from the sensitivity analysis information delivers a range which is found by varying one parameter along the x or y-axis plane while holding all other parameters constant. The confidence regions, however, are a multi-dimensional set as the parameters do not exist in a 1 or 2 dimensional plane, but rather a 5 dimensional plane in the case of the equilibrium model and a 7 dimensional plane in the non-equilibrium model (if only 1 set of experimental data is used for regression purposes). The 5 and 7 dimensions refer to the 5 or 7 parameters that are regressed.

For a linear model, the objective function is quadratic in the parameters, and the confidence region is a multidimensional ellipsoid. It can be described analytically by a parameter covariance matrix. For non-linear models, the confidence region is no longer ellipsoidal, and generally cannot be determined analytically. However, it is often approximated by linearizing the model around the optimum point. The approximation can be improved numerically by searching along the directions of the eigenvectors of the linearized parameter covariance matrix to find edges of the actual confidence regions. This technique delivers different sets of parameter values that, in combination, will deliver a model output within a specified confidence level.

Figures 3-1 and 3-2 show eigenvector diagrams produced from the parameter uncertainty analysis. The remainder of the eigenvector diagrams for phase 2 and 3 can be found in appendix 3. The red solid line represents the 95 % confidence level for the objective function. The blue solid line

represents the objective function value which is determined as the model searches backwards and forwards along the distance of the eigenvector from the optimum to the points where the confidence limit is reached. Figure 3-1 is an example of when linearization would be a good approximation as there is good symmetry across the distance of the eigenvector and the best parameter values are positioned in the centre of their confidence region. Figure 3-2 is an example of where the use of linearization is not a good approximation. Asymmetry across the distance of the eigenvector can be observed in Figure 3-2 as a result of the interaction between the model structure and the experimental data.

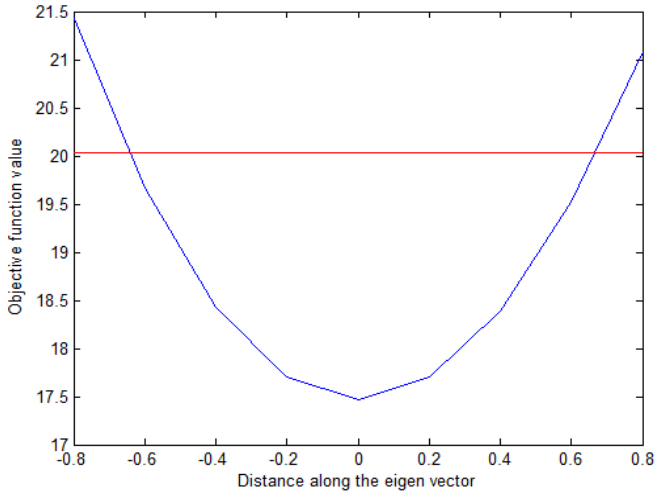

Figure 3-1: Eigenvector diagram in phase 2

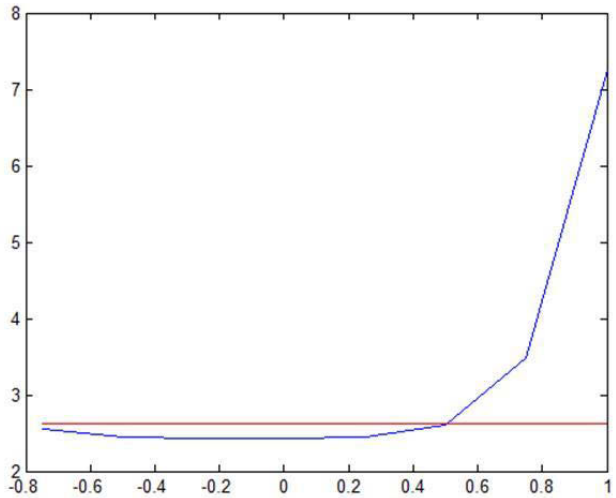

Figure 3-2: Eigenvector diagram in phase 3

Non-linear sensitivity analysis is complex and depends on many complex assumptions; therefore, many researchers assume that the system response to perturbations in model parameter values is approximately linear over a small perturbation range and that linear theory can give a reasonable prediction of the uncertainty of the estimated parameters. Linear theory for non-linear systems has been used to conduct model sensitivity analyses by many researchers in response to the complexity of non-linear sensitivity analysis; Examples include Ennola et al. (1998), Tang et al. (2001) and Tang & Wang (2002).

3.5. Experimental errors and uncertainties

The following section describes the uncertainties in the experimental results due to material standardisation, methodological error or equipment measurement tolerances.

3.5.1. Repeatability

Each of the titrations used in establishing the model component were repeated 2-3 times and replicate titration curves obtained were compared to assess the degree and causes of variation between experiments.

3.5.2. Calibrations

The pH probe was calibrated daily and again after a set of 5 sample titrations using buffers with pH value 4,7 and 10. The pH calibration range was chosen due to the broad pH range tested during the titrations.

3.5.3. Titrant standardisation

The hydrochloric acid was standardised using a 0.1 M borax (disodium borate tetrahydrate) solution as follows:

- A 0.1 M borax solution was prepared by drying a mass of $Na_2B_4O_7,10H_2O$ in the oven for 24 hours, weighing 19.07 g of the dried $Na_2B_4O_7,10H_2O$ and diluting to 1000 ml with distilled water to make up a 1 L solution.
- An aliquot of 20 ml of the 0.1 M borax solution was pipetted into a sample beaker.
- The sample was acidimetrically titrated with HCl to an end point pH of 5.1, following the Radiometer suggestions on method parameters for the autotitrator.
- The volume of titrant dispensed was recorded and the titrant concentration was calculated by using the formula :

  $c_1V_1 = c_2V_2$ Equation 3-7

  where c = concentration; V = volume

The sodium hydroxide was standardised relative to the standardised hydrochloric acid by:

- An aliquot of 20 ml of the standardised HCl solution was dosed into a sample beaker.
- The sample was titrated with NaOH to an end point pH of 7, following the Radiometer suggestions on method parameters for the autotitrator.
- The volume of titrant dispensed was recorded and the titrant concentration was calculated by using Equation 3.7.

3.5.4. pH probe response time

The pH probe response time was initially investigated by monitoring the pH response upon changing from the one buffer to the next (4,7,10). The response time, τ, was calculated by fitting Equation 3-8 to the data obtained:

$$\frac{dpH}{dt} = 1 - e^{-\frac{t}{\tau}} \qquad \text{Equation 3-8}$$

An additional set of experiments using a phosphate solution was conducted to determine the response time. The experimental method involved measuring an aliquot of 0.0041 M phosphate solution and dosing the solution with incremental doses of 0.2 mL, of 0.5 M acid up to a cumulative total of 0.8 mL and measuring the response of the solution to a change in pH value. The time constant, τ, was calculated by fitting an exponential curve of the form shown in Equation 3-8 to the experimental change in pH after a dose of hydrochloric acid. The phosphate solution tests were used as they imitate a titration-type experiment which agrees with the procedure being investigated in this project. The pH probe response time was evaluated as 1.4±0.8 s. This was evaluated by taking the average of the τ-values for the phosphate experiments. The experiments and evaluations of Equation 3-8 can be seen in Appendix 1 in Table A 1-2.

3.5.5. Titrimetric methods

Three titrimetric methods were considered for titrating the samples:

(i) The first method involved having two beakers with equal volumes of the same sample solution. The titration would involve titrating one beaker from the starting solution pH to the upper pH limit using an alkaline titrant and titrating the other beaker to the lower pH limit using acid.

(ii) The second method involved having one sample solution and titrating down to the lower pH limit first using acid and then titrating to the upper pH limit using an alkaline titrant.

(iii) The third method involved having one sample solution and initially pre-dosing with base to the upper pH limit and then titrating down to the lower pH limit using acid.

The third method was chosen as the best option. The first and second methods were discarded; the first involved the unnecessary use of extra reagents and some uncertainty in the sample volume measurement and the second was discarded because at low pH values the equilibrium position favours carbon dioxide evolution but the evolution is slow in comparison to the dissociation/association reactions, therefore, resulting in reduced carbonate species in the upward-titration.

3.5.6. Measuring instrument errors

- The sample solution was weighed into a beaker

Table 3-3: OHAUS PA214 balance specifications (OHAUS, 2004)

Capacity (g)	Readability (mg)	Repeatability (mg)	Linearity (mg)	Sensitivity drift (ppm/^{o}C)[4]
200	0.1	0.1	± 0.3	4.0

- Volume of titrant added

Table 3-4: Burette specification according to ISO 8655-3 (Radiometer Analytical SAS, 2008)

Burette volume (mL)	Maximum permissible systematic errors		Maximum permissible random errors	
	± %	± µL[5]	± % [6]	± µL[7]
25	0.2	50	0.07	17.5

- pH probe

[4] The amount by which the scale's measurement sensitivity varies as ambient conditions change

[5] Expressed as the deviation of the mean of a tenfold measurement from the nominal volume

[6] Expresses as the coefficient of variation of a tenfold measurement

[7] Expressed as the repeatability standard deviation of a tenfold measurement

Table 3-5: HI1131 specifications

Resolution (pH)	Response time (s)[8] (4.01,7,10.01 buffers)	Sensitivity (%)
0.001	≤39.4	>95

- Temperature probe has an error of 0.1 ^{o}C

3.5.7. Experimental errors

- The experiments were not conducted under a controlled temperature and humidity environment and hence ambient temperature varied from 19 to 25.7 ^{o}C.

- A delayed response between titrant dispensing and the change in pH as a result of mixing also contributes to the error in pH change

- A presence of carbonate in the sample solution due to cell respiration or absorption of CO_2 will possibly result in an incorrect starting pH value.

- Different batches of yeast were used for the experiments at different stages within the project. The history of the yeast before purchase was unknown and so can contribute to model component establishment errors.

- It will be shown in Chapter 4 that representing sludge ionic interactions as glycine-equivalents did not represent the behaviour of biomass well. When anaerobic sludge was used to continue the model component establishment, it was found that there was a large and variable amount of dissolved inorganic solids that influenced the behaviour of the titration and masked the effect of the biomass interactions. Baker's yeast was selected as a source of biomass for developing a model of biomass ionic interactions. Baker's yeast was chosen as a suitable option due to its (1) common availability and (2) industrial preparation. The industrial preparation would render it a "cleaner" form of biomass composition and the amount of non-yeast solids which could potentially negatively impact the analytical data.

[8] The average time taken (across the 3 buffer solutions) or the pH electrode to settle on a constant pH

3.6. Delimitations of the study

The following aspects were considered as delimitations of the study:

- The soluble organic matter was not considered in the study.
- The glycine concentration range considered was calculated to give a similar pH buffering capacity to that observed during titration of an anaerobic sludge sample as per Batstone et al. (2010).
- The biomass concentration range considered was only reflective of concentrations of biomass in anaerobic digesters.
- The background solution mixed salt concentrations considered were only reflective of a typical wastewater background solution.
- The background solution did not consider any precipitating ions.
- The experimental methodology only considered potentiometric titrations as a form of investigating and characterising the ionic nature and buffering capacity of solutions containing biomass with and without a background solution of inorganic mixed salts.
- The conductivity of the experimental titration solutions was not investigated due to equipment capability.

Chapter 4 Phase 1: The use of glycine to establish a model component

The glycine system was used for establishing and verifying the ionic speciation model against experimental titration data. It was also used as a first phase for model component establishment following the suggestion of Artola et al. (1997). As mentioned in the literature review, the aqueous chemistry of glycine is well known and it has similar weak acid-base groups to biomass (amine, carboxylic group) which made it a favourable choice for modelling biomass. It was hypothesized that glycine had similar titration characteristics to biomass and so glycine equivalents could be used to model biomass interactions.

4.1. Experimental design

The section to follow describes the validation of the built-in ionic speciation model developed by Brouckaert et al. (Brouckaert, et al., 2011) and the generation of the model description for glycine used to describe ionic interactions with biomass as well as a detailed review of the experiments conducted.

4.1.1. Formulating the model

The first objective of phase 1 was to validate that the built-in ionic speciation returned the same results as other available software. The second objective was to include glycine as a model component of biomass and validate its use as an ionic description of biomass. An explanation of the principles used in modelling the system and the details surrounding the parameter regression can be found in section 3.2.

Oreskes et al. (1994) and Tsang (1991) state that a model can be validated if (i) the computer code is verified by ensuring that the composition of the algorithms and its answers are mathematically correct and (ii) the model predictions are comparable with the experimental measurements and the field observations in natural systems to a certain extent within a specific range of conditions.

In this study, the built-in ionic speciation model was validated against a commercially available software using a solution of known concentrations. The solution and concentrations were representative of a mixed salt background solution to be used in the experimentation to follow.

The built-in ionic speciation model developed by Brouackert et al. (2011) was extended, in the research presented, to include 13 ionic *components* for the mass balance with the Gly^- forming the

additional component. The ionic components in the mass balance are distributed among 50 ionic *species,* where the extensions to the *species* are Gly^-, HGly, H_2Gly^+, $MgGly^+$, $CaGly^+$ and $CaHGly^{++}$. The equations considered in the ionic speciation model are the following:

$H_2Gly^+ \rightarrow H^+ + HGly$ Equation 2-13

$HGly \rightarrow H^+ + Gly^-$ Equation 2-14

$MgGly^+ \rightarrow Mg^{2+} + Gly^-$ Equation 4-1

$CaGly^+ \rightarrow Ca^{2+} + Gly^-$ Equation 4-2

$CaHGly \rightarrow Ca^{2+} + HGly$ Equation 4-3

The model uses glycine's actual pK_a values (without any regression) which describe the corresponding amine and carboxyl groups (Kiss, et al., 1991). The amine dissociation constant is slightly higher than that for the ammonium ion (9.778 vs 9.244 at 25 ^oC) and the carboxyl group dissociation constant is substantially lower than that of acetic acid (2.35 vs 4.757 at 25 ^oC) (Brouckaert, et al., 2010).

The ionic group site concentrations obtained by regression were 13.146 mmol/g VS for both the carboxyl and amide groups as the site concentrations were proportioned in a 1:1 ratio for the two functional groups. A review of the mass balance used in the ionic speciation model can be found in Appendix 5.

4.1.2. Formulating the experiments

The objective of the experiments was to generate titration curves containing glycine and different curves containing sludge and see whether the ionic behaviour of the two solutions was similar during a titration.

Acid-base titrations of the following solutions were performed:

a. Pure glycine solutions of 3.8, 7.5 and 15 mmol glycine/L concentration were titrated.
b. Glycine solutions of 3.8, 7.5 and 15 mmol glycine/L concentration were titrated. The glycine solutions were augmented with a mixed salt background solution corresponding with Table 3-2 solution 2.
c. Washed anaerobic sludge suspensions of 0.5, 1.0, 2.0 g TS/L were titrated. The sludge was washed with distilled water as conducted by Naja et al. (2005) in removing culture medium residues.

The glycine concentrations chosen for experimentation were comparable to biomass concentrations in anaerobic digestion liquor. The glycine concentrations chosen corresponded with the alkalinity required to titrate anaerobic sludge as per Batstone et al. (2010).

The pH range tested in the experimental titrations was from a pH of 3 to 11. The sample was prepared by weighing all components into the titration vessel. An aliquot of approximately 130 mL sample solution was dosed with 0.24 M NaOH using a micropipette to a pH between 10 and 11. The sample solution was acidimetrically titrated with 0.5 M HCl. The sample was agitated throughout the titration using a magnetic stirrer set at 450 rpm to ensure uniform concentration in the sample. The pH and temperature were monitored simultaneously throughout the experiment. The details of the equipment and philosophy behind the test can be found in Section 3.3.

4.2. Results

The section below describes the built-in ionic speciation model validation using PHREEQC software as well as the ionic speciation modelling of glycine. The results show the comparisons of the experimental titrations and simulated results using glycine as well as the overall comparison of glycine to washed anaerobic digester sludge.

4.2.1. Speciation model validation

The preliminary formulation of the ionic speciation model was validated by comparing the model predictions to the PHREEQC predictions of pH for different concentrations of mixed salt solutions. The mixed salts considered were calcium, magnesium, ammonia, carbonate, phosphate and acetate with the respective range of concentrations between 0.67-1.04 mM, 1.03-1.61 mM, 10.41-16.27 mM, 12.78-15.98 mM, 4.79-7.49 mM and 0.20-0.30 mM. Both the PHREEQC software and the model gave very comparable results for all trials as seen in Figure 4-1. A small difference in titration simulations can be seen in the lower pH region (pH 2-3). This can be explained by two theories, (i) the ionic speciation model does not consider all species in the very low pH region (e.g. sulphuric acid) and (ii) the activity coefficient models used by PHREEQC and the ionic speciation model are different.

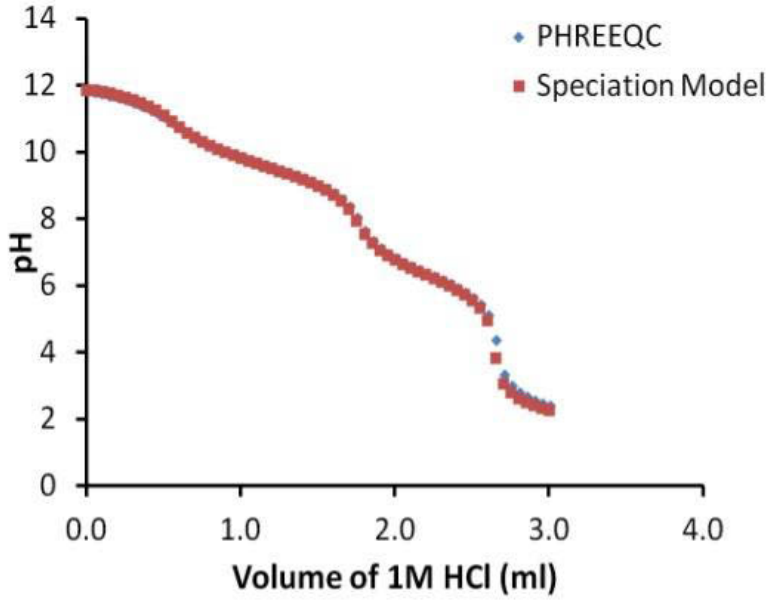

Figure 4-1: Comparison between PHREEQC and the speciation model used in this project

4.2.2. Ionic speciation modeling using glycine

Figure 4-2 shows the experimental data (points) for acidimetric titration of solutions containing increasing concentrations of glycine in a background solution containing phosphate and carbonate (Table 3-2, solution 2) compared to the model simulation (solid line).

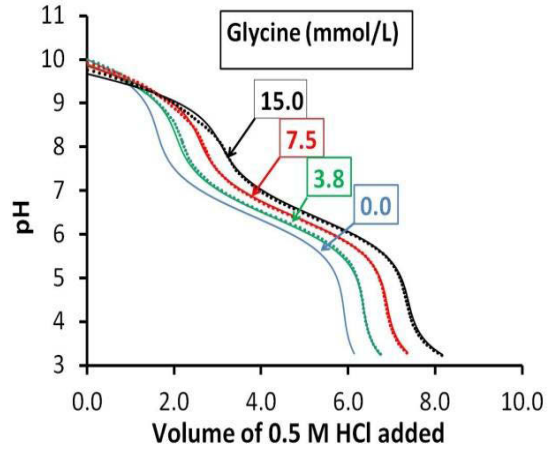

Figure 4-2: Experimental data (points) and model simulation (lines) from acidimetric titrations for solutions containing increasing concentrations of glycine in a background solution of 3.91 mmol/L disodium hydrogen orthophosphate and 12.01 mmol/L sodium hydrogen carbonate

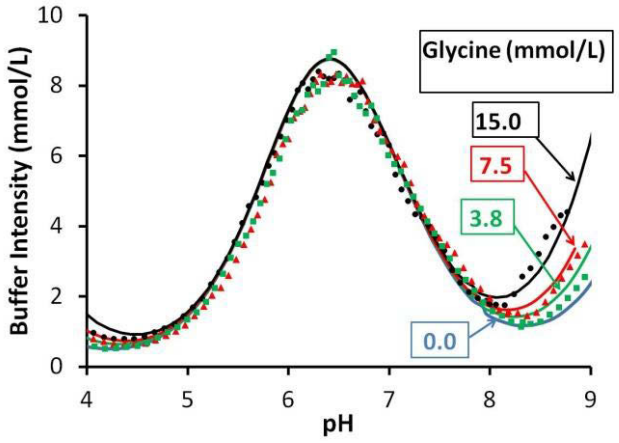

Figure 4-3: Calculated Buffer intensity for increasing concentrations of glycine from data shown in Figure 4-2

Figure 4-2 shows good agreement between the model curves, generated by the ionic speciation model, and the experimental titration data points for the different glycine concentrations. The model titration curves were generated by using the assumptions specified in Section 3.2 without any need for parameter regression to get the fit between the model and data points.

Figure 4-2 was converted into buffer intensity curves, as shown in Figure 4-3, by using numerical differentiation of the titration data points and model curves. The buffer intensity is here defined as the derivative $d([HCl])/d(pH)$ where HCl represents the moles of acid per liter of solution. Figure 4-3 shows the good fit of the buffer intensity data (points) and the model curves (solid line) generated using the ionic speciation model in the area of interest between pH 6 and 8 as this is the optimal pH range for bacteria to grow and function properly in anaerobic digestion (Anderson and Yang, 1992a) .

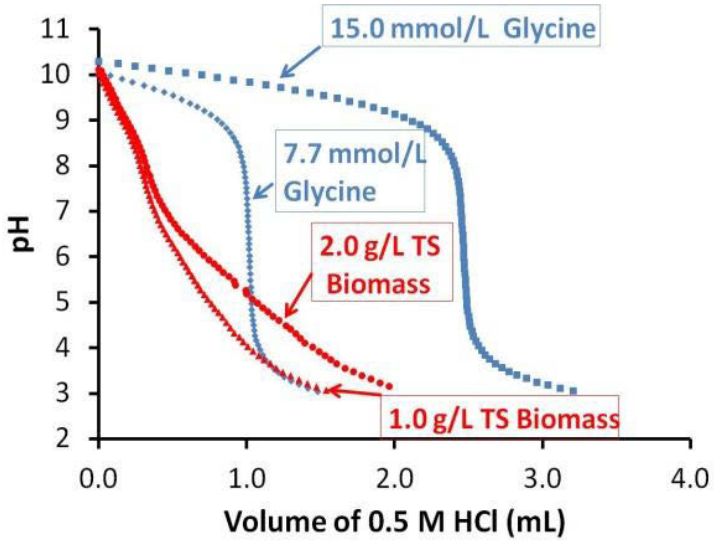

Figure 4-4: Comparison of titration data between experiments using glycine solution and washed anaerobic sludge (biomass) in a solution of NaOH

Figure 4-4 shows the titration data for glycine solutions (blue experimental data points) and washed anaerobic sludge/biomass (red experimental data points) in a solution of NaOH. This graph shows the behaviour of the two systems when acidimetrically titrated with HCl. The regions of the pH scale that show high and low buffer capacity clearly do not match, and the inflection points (acid equivalence points) are also not at the same pH values as seen on the graph. The biomass inflection points can be clearly observed in the plot of buffer intensity in Figure 5-16.These differences in the two systems' characteristics verify that glycine is not a good model component to describe organic solids, and in particular, washed anaerobic sludge.

It was considered possible that precipitates in the anaerobic digestion sludge may have contributed to the measured buffer capacity (further discussed later on). The total solid (TS) and ash content of the washed sludge were measured at 0.24 g/g and 0.12 g/g respectively.

4.3. Discussion

The ionic speciation model, as described in Section 3.2, was used to generate the model titration curves in the results section by using the known starting concentrations from the experiments.

The model assumed all of the reactions to be at equilibrium with reactions being reversible. CO_2 exchange between the atmosphere and the solution was not accounted for and the chemical impurities from chemicals used in the titrations were assumed to have no negative impacts on the titration data. The statements can be validated as true as the ionic speciation model used did not require any parameter regression to fit the model predictions to the experimental titration data.

The results show that the extension of the ionic speciation model to include glycine species was successful from the good agreement of the experimental and model simulated curves of the pure glycine system.

4.3.1. Comparison between glycine and sludge

The experimental titrations of glycine and washed anaerobic sludge were compared; it was found that general titration characteristics did not agree between the washed anaerobic sludge and the glycine.
The comparison yielded the following differences:

- The number of functional groups: The glycine titration curves show two clear inflection points indicating the presence of two functional groups known to be the carboxylic acid and amine functional groups (only one of the functional groups is visible as a buffer intensity peak in Figure 4-3 due to the pH range shown). The biomass titration curves

show possibly 3 to 4 inflection points on the span of the titration curve with the two sets of inflection points being above and below a pH value of 7.

- The type of functional group can be determined by its dissociation constant which can be verified by the position of the inflection point on the pH range of the titration curve. From literature (Claessens, et al., 2006) it is known that the cell wall is composed of carboxylate, amine and phosphate functional groups. In the case of the glycine system, the carboxylate functional group accounts for the inflection point in the lower pH and the amine group in the higher pH range.
- The concentration of each of the functional groups which is a reflection of the shape of the titration curve at the inflection point and the volume of titrant added up to the particular inflection point.

These differences suggest that glycine cannot be used to represent biomass as hypothesised. This conclusion can possibly be explained by two reasons: (i) the fact that the Gibbs free energy for each of the functional groups of glycine, in the zwitterionic form (Section 2.3) , is different to the non-zwitterionic form of glycine. The difference in the Gibbs free energy results in pK_a values that are different to those of ammonia and carboxylic acid. (ii) Glycine has a much simpler structure in comparison to the complex nature of the protein likely to be present on the surface of biomass.

4.3.2. Washed anaerobic sludge as a model component for biomass

The measured total solids and ash content of 0.24 g/g and 0.12 g/g respectively, show that the washed anaerobic sludge had a very high ash content (50 % of the total solids content). The species making up the ash content are likely to contribute to the ionic behavior of the solution in a manner that cannot be reproducibly described by ionic functional groups of biomass. As mentioned in Section 3.3.3.1, the biomass was washed to remove any soluble inorganic and organic material on the surface of the biomass. It is possible that because the sludge was washed, the remaining ash content was likely to be due to slowly dissolving precipitated constituents which might have dissolved at a slow rate (non-equilibrium reaction) during the titration. This is because anything that was readily soluble would have been washed away.

4.4. Conclusions

The results in this chapter suggested that the chemistry of glycine was not an appropriate representation of the ionic behavior of organic sludge (pK_as were different and the number of functional groups were different).

However, the high ash concentration of the sludge makes it impossible to identify which characteristics of the measured titration curve are attributed to the organic constituents of the biomass

surface and which are from the sludge ash. The organic constituents attributed to the sludge ash are preferred to be considered as part of the background solution.

Therefore, it is recommended that a “cleaner” source of biomass be selected to investigate the ionic nature of the sludge.

Chapter 5 Phase 2: UKZiNe at equilibrium conditions

Following the conclusion of Chapter 4, a "cleaner" source of biomass was required to investigate the ionic nature of sludge. Baker's yeast was chosen as a suitable source to continue the study of building the overall model component structure.

The objectives of the study were to develop a model that predicts ionic interactions between dissolved inorganic ions and particulate organic components and thereafter determine whether the biomass has an impact on the overall pH buffering capacity of wastewater within the anaerobic digester operating range. Phase 2 of the study planned to address the research objectives by using the hypothesis that biomass can be described by a formulated model component, UKZiNe, at equilibrium. The UKZiNe establishment in hypothesis 2 involved modelling the yeast biomass at equilibrium conditions. Equilibrium conditions were assumed as it was assumed that ions do not transfer across the membrane in sufficient quantities to influence the cell solution chemistry outside the cell. The only mechanism considered was ion association and dissociation with functional groups on the external surface of the cell membrane.

5.1. Experimental design

The following section describes the formulation of the model component, UKZiNe, at equilibrium conditions as well as the experimental methods used in generating the titration curves using baker's yeast particulate organic matter.

5.1.1. Formulating the model

From Chapter 4, anaerobic sludge appeared to have 4 inflection points; two above pH 7 and two below. It was assumed that these could be described by modified phosphate, amine and carboxyl groups, with the phosphate and amine describing the above pH 7 inflection points and the carboxyl groups describing the below pH 7 inflection points.

The built-in ionic speciation model, developed by Brouckaert et al. (2011), was extended to include 16 ionic *components* for the mass balance where the extension includes U1-COO^-, U2-COO^-, U3-PO_4^{2-}, U4-NH_3^+. The ionic *components* for the mass balance are distributed among 52 ionic *species*, where the extensions are to the species U1-COO^-, U2-COO^-, U3-PO_4^{2-}, U4-NH_3^+, U1-COOH, U2-COOH, U3-PO_4^-, U4-NH_2.

Model component functional group reactions:

$U1\text{-}COO^- + H^+ \rightarrow U1\text{-}COOH$ Equation 5-1

$U2\text{-}COO^- + H^+ \rightarrow U2\text{-}COOH$ Equation 5-2

$U3\text{-}PO_4^{2-} + H^+ \rightarrow U3\text{-}PO_4^-$ Equation 5-3

$U4\text{-}NH_3^+ \rightarrow U4\text{-}NH_2 + H^+$ Equation 5-4

An explanation of the principles used in modelling the system and the details surrounding the parameter regression can be found in Section 3.2. A review of the modifications to the ionic speciation model can be found in Appendix 5.

A block diagram of the modelling methodology can be seen in Figure 5-1. The ionic interactions of the biomass were modelled using a model component *UKZiNe,* made up of ammonia, phosphate and carboxylic acids. The model component was built by first establishing the pK_as of UKZiNe. This was determined by manual curve-fitting of the model using various experimental curves and using the glycine system pK_as as starting estimates for the amine and one carboxyl functional group. The establishment of the site concentrations was performed by fitting the model to the experimental titration while regressing for the functional groups site concentrations (with the pK_as remaining fixed). A sample set of 7 experimental titrations were used in the regression of the model component, UKZiNe. The regression was seen to be highly interactive with changes in the site concentrations and alkalinity impacting on one another. The model pH could then be determined per titrant volume added by using the adapted built in speciation model developed by Brouckaert et al. (2011).

Following the model parameter regression, the confidence intervals were obtained for the parameter set and the combination of the model parameters was applied to other experimental titrations.

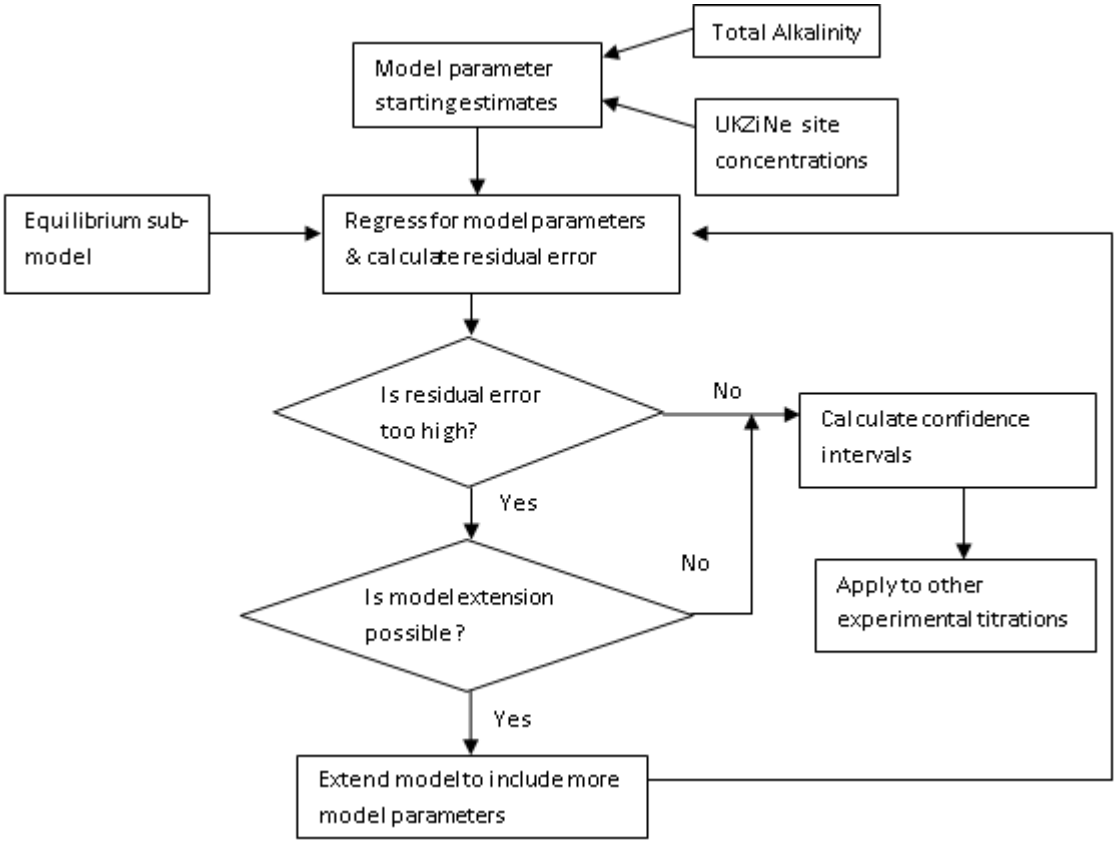

Figure 5-1: Methodology of parameter regression, model extension and application to experimental titrations

5.1.2. Formulating the experiment

The objective of the experiments was to generate titration curves containing baker's yeast to be used in the parameter regression of the model component UKZiNe and to investigate the buffering capacity in the operating region of an anaerobic digester.

Acid-base titrations of the following solutions were performed:

(i) Yeast suspensions of 1.12, 2.29, 4.45 and 8.69 g TS/L concentration were titrated. These suspensions were made up by mixing the particulate organic matter with distilled water.

(ii) Yeast suspensions of 1.12, 2.29, 4.45 and 8.69 g TS/L concentration were titrated. These suspensions were made up by mixing particulate organic matter with a mixed salt background solution corresponding with Table 3-2, solution 2.

As per Section 3.3.3.1, the particulate organic matter was washed to remove any culture medium residues. The washing medium used was distilled water as conducted by Naja et al. (2005).

The pH range tested in the titrations was from 3 to ±11. An aliquot of approximately 130 mL sample solution was dosed with 0.5 M NaOH using a micropipette to a pH between 10 and 11 and the sample solution was acidimetrically titrated with 0.5 M HCl. The sample was agitated throughout the titration

by using a magnetic stirrer set at 950 rpm to ensure uniform concentration in the sample. The pH and temperature were monitored simultaneously throughout the experiment. The details of the equipment and philosophy behind the test can be found in Section 3.3.

5.2. Results

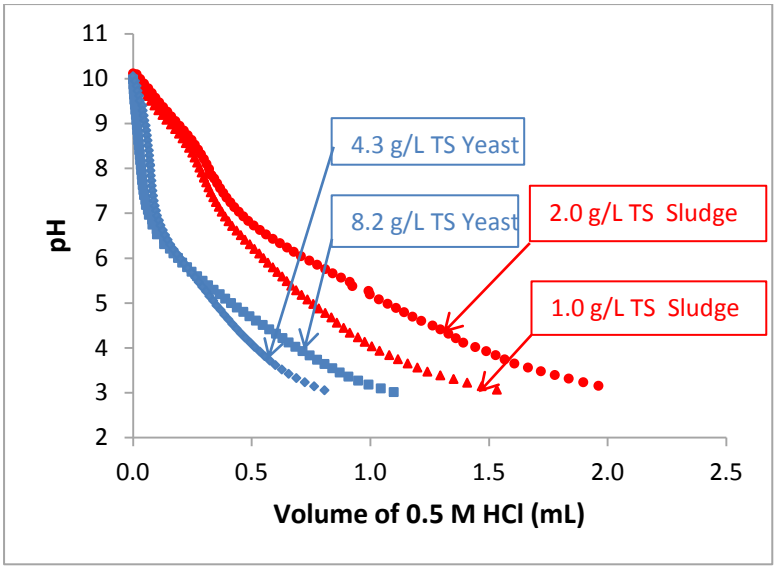

Figure 5-2: Comparison of titration data between experiments using yeast suspensions and washed anaerobic sludge in a solution of NaOH

Figure 5-2 shows the titration data for yeast suspensions (blue experimental data points) and washed anaerobic sludge/biomass (red experimental data points) in a solution of NaOH. This graph shows the behaviour of the two systems when acidimetrically titrated with HCl. Upon comparison of the two systems curves it can be observed that the shape of the curves are similar, however, an increased concentration of yeast is required to meet the same acid demand by the washed anaerobic sludge. The study was continued with yeast biomass to model the ionic behaviour of particulare organic matter.

Figures 5-3 to 5-6 show the agreement between the yeast biomass experimental titrations (data points) and the model curves (solid line) regressed to determine the UKZiNe site concentrations for the 4 functional groups.

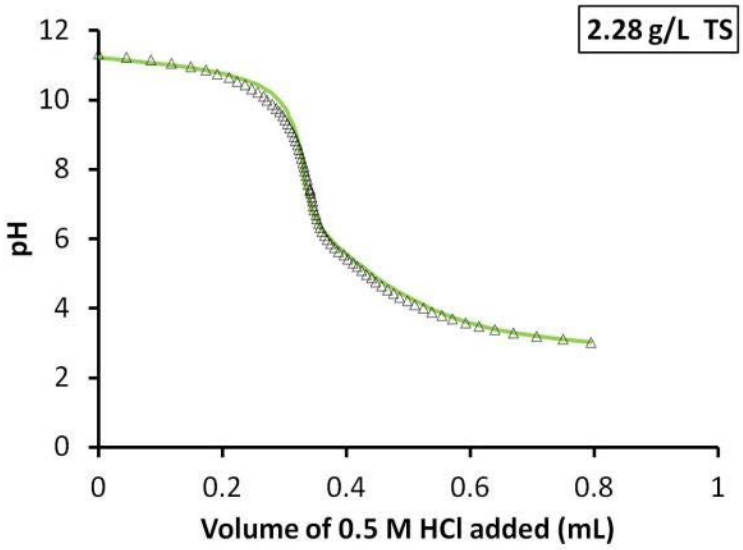

Figure 5-3: Establishment of UKZiNe parameters by fitting the model (solid line) to experimental titration (points) of yeast biomass (2.28 g/L TS) in a NaOH solution

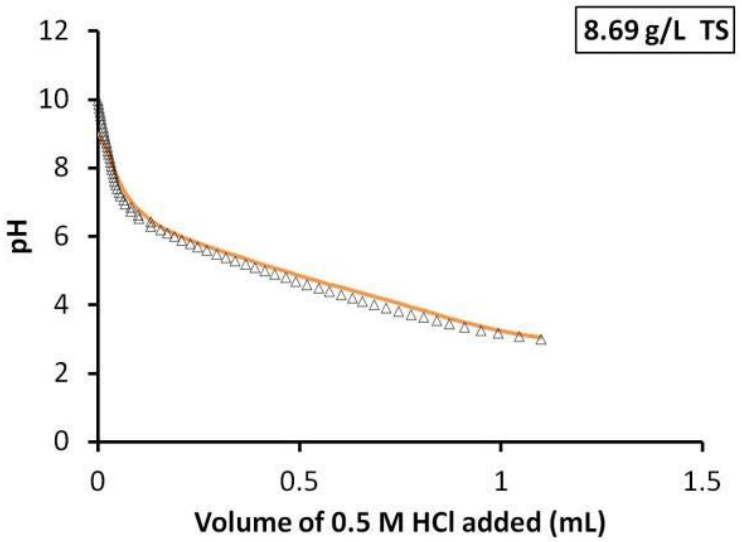

Figure 5-4: Establishment of UKZiNe parameters by fitting the model (solid line) to experimental titration (points) of yeast biomass (8.69 g/L TS) in a NaOH solution

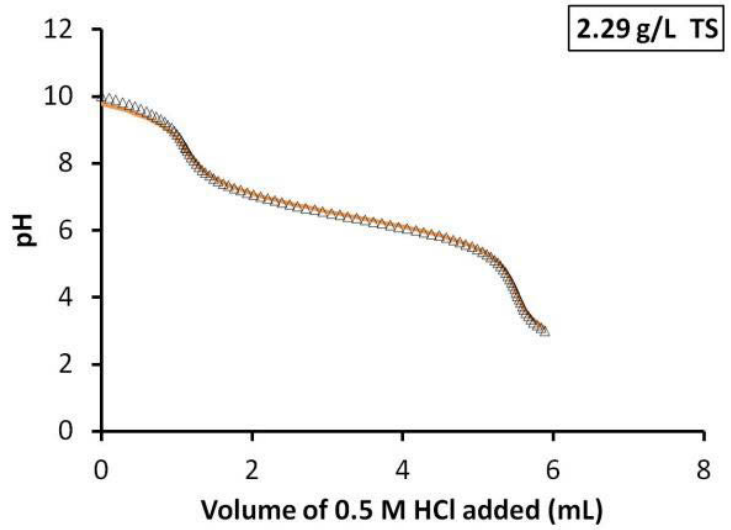

Figure 5-5: Establishment of UKZiNe parameters by fitting the model (solid line) to experimental titration(points) of a yeast suspension (2.29 g/L TS in a background of 12.5 mmol/L $CO_3^{=}$ and 4 mmol/L PO_4^{-3})

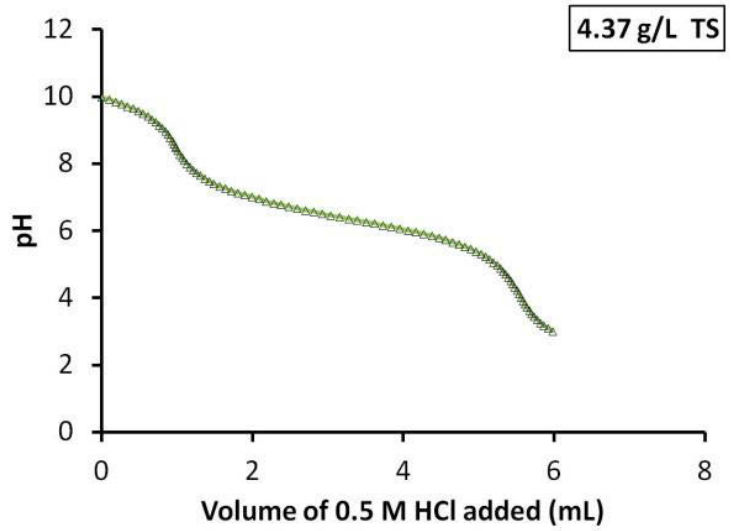

Figure 5-6: Establishment of UKZiNe parameters by fitting the model (solid line) to experimental titration (points) of a yeast suspension (4.37 g/L TS in a background of 12.5 mmol/L $CO_3^{=}$ and 4 mmol/L PO_4^{-3})

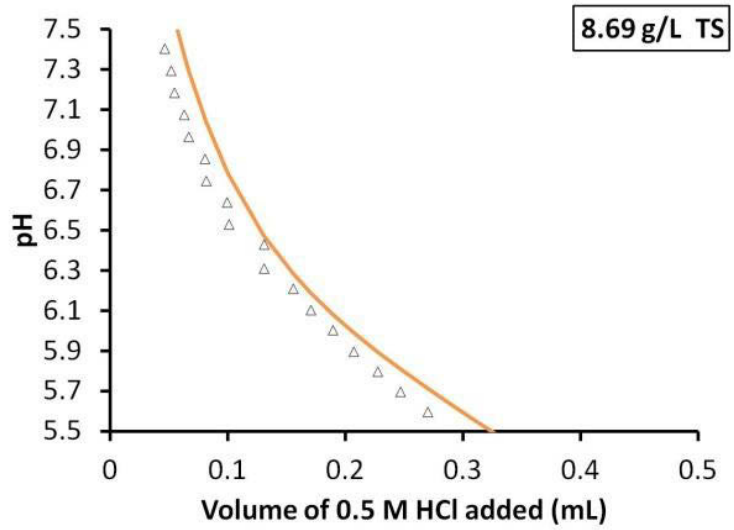

Figure 5-7: Figure 5-4 magnified to show a smaller axis range

These curves were regressed assuming ionic equilibrium at each point for yeast biomass concentrations ranging from 1.12 to 8.69 g TS/L for a sample set of 7 experimental titrations. The figures above show results for the experiments tested with a solution of sodium hydroxide as well as with a background solution of carbonate and phosphate to imitate salt concentrations found in wastewater.

It was considered possible that precipitates in the anaerobic digestion sludge may have contributed to the measured buffer capacity (further discussed later on). The total solid (TS) and ash content of the washed baker's yeast were measured as 0.28 g/g and 0.01 g/g respectively for the washing with distilled water.

The fit shown in Figures 5-3 to 5-6 was achieved by introducing two anionic groups (assumed to be carboxylic acids) with pK_a values at 25 °C of 4.35 and 5.65, which can be compared to 4.757 for acetic acid, in addition to the phosphate and amine groups with pK_a values at 25 °C as 7.198 and 9.244 (Brouckaert, et al., 2010). The UKZiNe site concentrations were regressed to give a best fit value and confidence interval on the regressed parameter (presented as best fit value (minimum of confidence region – maximum of confidence region)).

Table 5-1: Functional group site concentrations and pK_a values for phase 2

	Site Concentration (mmol/g VS)	**pK_a Value**
Carboxyl group 1	0.202 (0.113 - 0.294)	4.35
Carboxyl group 2	0.165 (0.105 – 0.219)	5.65
Phosphate group	0.026 (0 – 0.055)	7.198

Amine group	0.043(0.024 - 0.062)	-9.244

The phosphate group site concentration, as shown in Table 5-1, is not significant which suggests the possible removal of the group from the model.

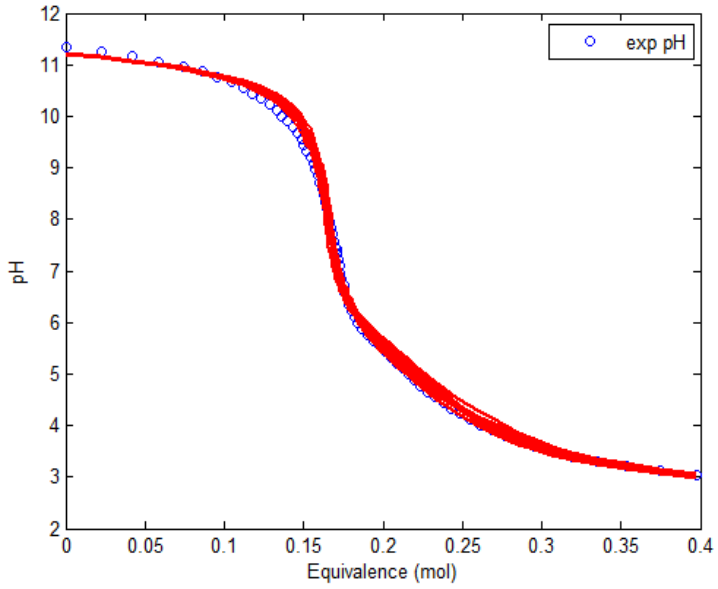

Figure 5-8: Uncertainty range of simulations showing experimental data (blue points) with simulations plotted in red (solid line) for a 2.28 g/L TS yeast suspension

The details of the uncertainty analysis for the parameter regression for the constituents of UKZiNe is presented in Appendix 3. The eigenvector graphs for the uncertainty analysis show good symmetry across each of the regressed parameters. The objective values for each of the searches across the eigenvectors can be seen in Appendix 3 with the corresponding titration curves for each of the parameter uncertainty sets shown in Figures A 3-11 to A 3-17 (e.g. the curve for Figure 5-3 is presented here in Figure 5-8). The variation in titration curve for the figures mentioned can be seen to be negligible, producing no major differences in shape or characteristics of the curve, highlighting that there would be no major difference in calculated pH buffering capacity across the pH range for any value of the parameter within the calculated confidence ranges. The parameter correlation table can also be viewed in the uncertainty analysis (Appendix 3, Table A 3-1). The parameter correlation gives a good indication of the dependency of the parameters on each other. The parameter correlation for phase 2 shows that the carboxyl group site concentrations are highly correlated and, therefore, dependent on one another. The coefficient is negative indicating that the dependency is inversed, as one parameter increases the other decreases.

5.2.1. Biomass in a NaOH solution

Figures 5-9 to 5-11 show 3 increasing concentrations of biomass (i.e. 2.28, 4.52 and 8.69 g/L TS) in a solution of NaOH.

In the plots, the red data points show the buffer intensity as calculated from the titration curves of solutions of background salts and biomass. The black points are by subtraction of the background solution buffer intensity from the overall buffer intensity (solution of background solution and biomass). The lines are the model predictions of the buffer capacity assuming ionic equilibrium at each pH value and the best fit parameter values of functional group pK_a value and concentration for biomass solution (UKZiNe - black line), for the solution alone (NaOH - blue line) and the mixed solution (red line). Since buffer capacity is a stoichiometric property of the solution components, the solution and biomass solution buffer capacities should add to give the mixed solution buffer capacity.

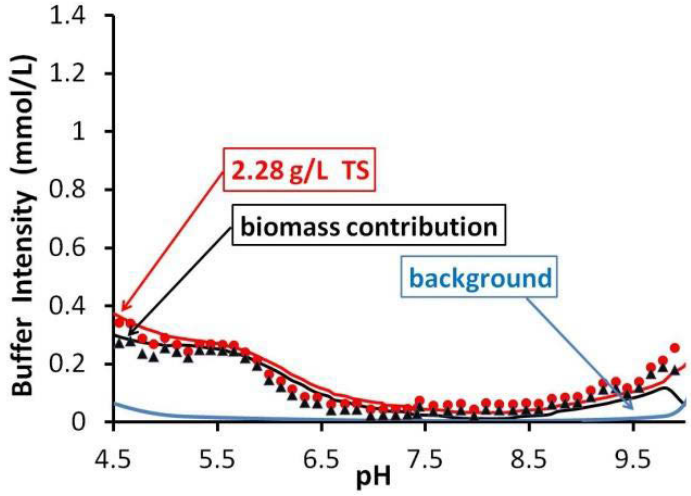

Figure 5-9: Buffer intensity of 2.28 g/L TS yeast biomass in a NaOH solution showing contribution of biomass and solution to overall buffer capacity

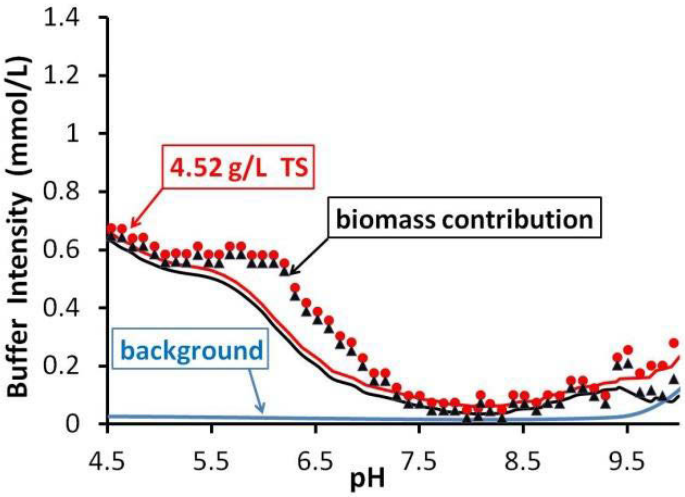

Figure 5-10: Buffer intensity of 4.52 g/L TS yeast biomass in a NaOH solution showing contribution of biomass and solution to overall buffer capacity.

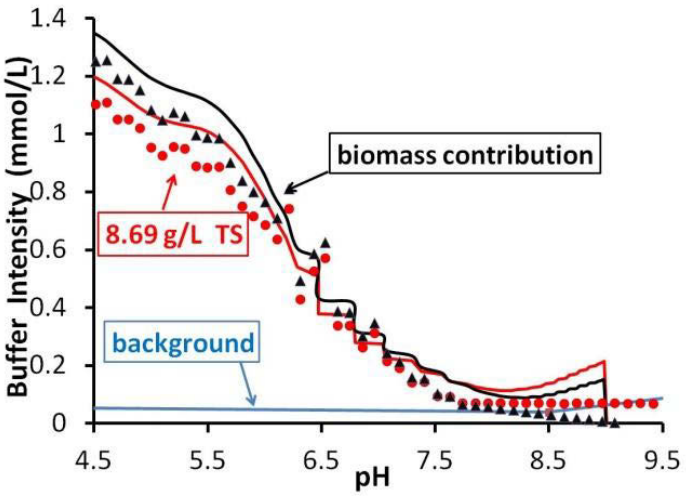

Figure 5-11: Buffer intensity of 8.69 g/L TS yeast biomass in a NaOH solution showing contribution of biomass and solution to overall buffer capacity

The NaOH solution was used to see the contribution of the biomass as clearly as possible, as H_2O contributes virtually no buffer intensity in the pH range of 5-10.

Figure 5-10 shows a discrepancy between the experimental data points and model simulations; this is a translation of the titration curve as seen in Appendix 2, Figure A 2-2, where the model simulation underpredicts the pH in the region of pH 3 - 6.5. Figure 5-11 shows the model simulation exhibiting *steps* in buffer capacity between pH 6 - 7.5. The stepping phenomenon is a numerical construction which probably has origins in the slight lag of the pH probe. The magnitude of the pH change is the same in the region irrespective of the volume added resulting in the stepping. This can be shown by Figure 5-7 which is the titration curve of Figure 5-11 buffer capacity plot.

It can be observed from Figure 5-9 that for lower yeast biomass concentrations (i.e. 2.28 g/L TS) the contribution of biomass to the buffering capacity is negligible in the region of interest (pH 6-8) with a maximum of 0.15 mmol/L. However, Figures 5-10 and 5-11 show that higher concentrations of biomass (4.52 and 8.69 g/L TS) deliver an increased buffering capacity in comparison.

5.2.2. Biomass in a mixed salt background solution

Figures 5-12 to 5-15 show the buffering capacity of 4 titrations with the overall solution, biomass contribution and background buffer intensities plotted with experimental values depicted as data points and the model simulation as a solid line. The buffer capacity graphs were constructed in the same manner as described in Section 5.2.1.

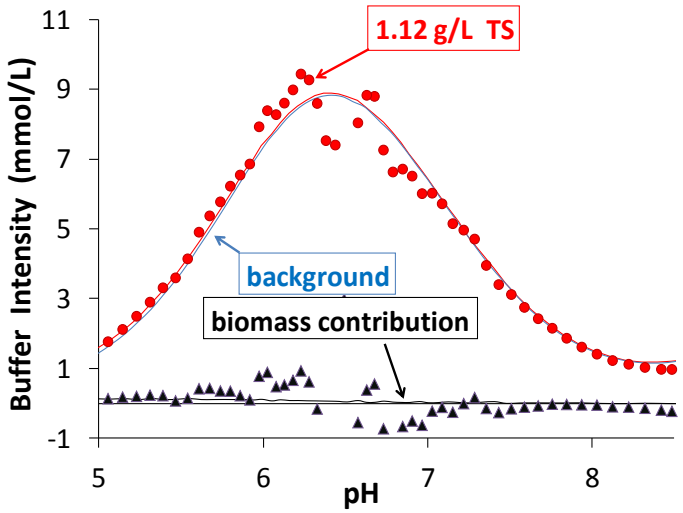

Figure 5-12: Buffer intensity of a 1.12 g/L TS yeast suspension (Background solution of 12.5 mmol/L $CO_3^{=}$ and 4 mmol/L PO_4^{-3})

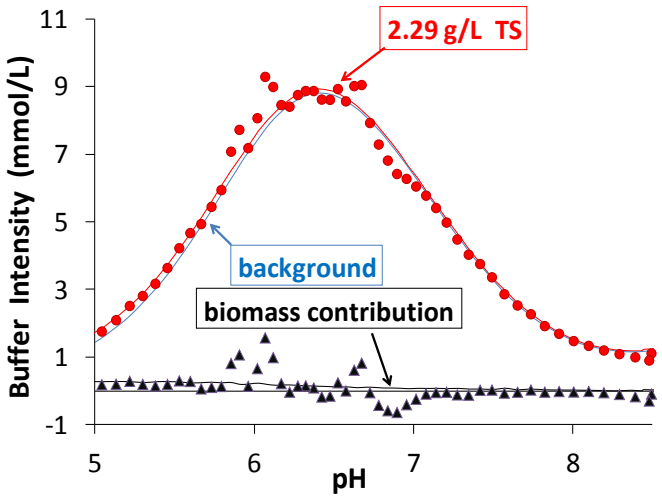

Figure 5-13: Buffer intensity of a 2.29 g/L TS yeast suspension (Background solution of 12.5 mmol/L $CO_3^{=}$ and 4 mmol/L PO_4^{-3})

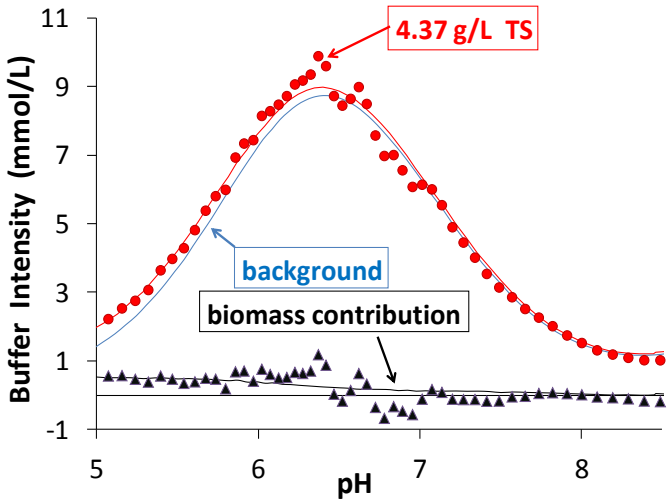

Figure 5-24: Buffer intensity of a 4.37 g/L TS yeast suspension (Background solution of 12.5 mmol/L $CO_3^{=}$ and 4 mmol/L PO_4^{-3})

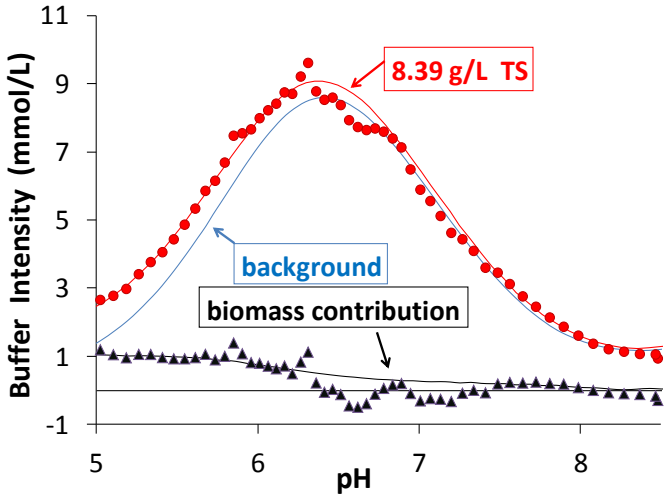

Figure 5-15: Buffer intensity of a 8.39 g/L TS yeast suspension (Background solution of 12.5 mmol/L $CO_3^{=}$ and 4 mmol/L PO_4^{-3})

These titrations have an included background solution of carbonate and phosphate with concentrations similar to typical wastewater streams (Ikumi, 2010). The background solution was used to determine the effect of the biomass in relation to the mixed salt background that would be present in reality. The background solution offers its own buffering capacity which can be seen to be quite high in relation to the buffering capacity of H_2O.

The biomass contribution in Figures 5-12 and 5-13 can be seen to be virtually negligible for both the model and the experimental data points across the pH range. In Figures 5-14 and 5-15 there is a more noticeable effect of higher biomass concentration on the buffering capacity from pH 5 to pH 7; however, this effect is small in comparison to that of the overall solution buffering capacity.

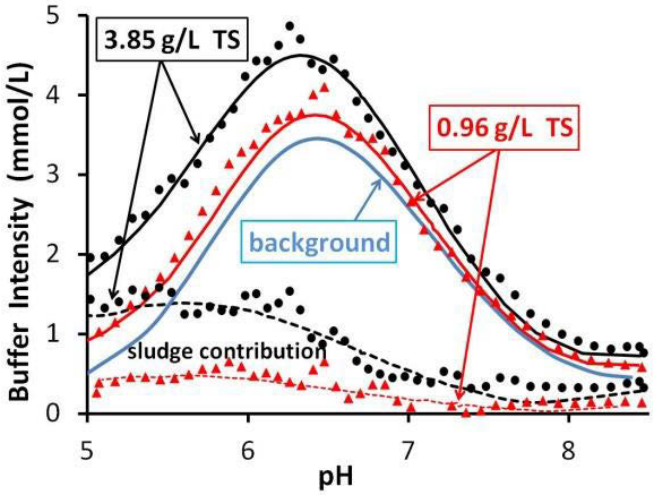

Figure 5-16: Buffer intensity results for washed anaerobic sludge in 5 mmol/L $CO_3^{=}$ and 1.6 mmol/L PO_4^{-3}

Figure 5-16 shows preliminary work in the study where washed anaerobic sludge was titrated as per the experimental procedure. Biomass was added to a carbonate and phosphate background solution to deliver sample concentrations of 0.96 g/L TS and 3.85g/L TS. The respective contributions of the sludge (inorganic and/or organic) were unknown and this should be investigated and accounted for in future research. The experimental data simulation was conducted by performing a manual regression of data. The characteristics of the sludge were established using the same pK_a values as determined to describe UKZiNe above for the yeast suspension regressions but the site concentrations were determined as 0.17 mmol/g VS for the two carboxylic groups, 0.076 mmol/g VS for the amine and 0.021 mmol/g VS for the phosphate group.

A simulated portion of carbonate had to be added to the UKZiNe model formulation to achieve the fit between the model and experimental data. It seems significant that the inorganic fraction of the total solids was about 50 % for the sludge, but only 5 % for the yeast; although further investigation is needed to confirm this, it seems likely that carbonate might have been released from precipitates in the anaerobic sludge during the titration. It can be seen that the sludge contribution to buffer intensity in the pH 6.5 to 8.5 range is significant (Figure 5-16); it has been hypothesised that this originates from inorganic carbonate precipitates rather than biomass.

5.3. Discussion

The alternate hypothesis (named hypothesis 2) stated that the ionic behaviour of biomass could be described by functional ionic groups in equilibrium with the solution. The equilibrium model did not take into account any possible mass transfer or dynamic effects. It was assumed that the effect of these contributions in this modelling phase would be negligible in their effect on the pH buffering capacity of suspensions of biomass. This assumption was made because the mass transfer time constant for ionic species to move between the bulk solution and the surface of the biomass and other

possible delays are small and were assumed to be virtually insignificant when compared with the characteristic reaction time of the biologically mediated processes in the digester. During the titration experiments, it was further assumed that biologically mediated reactions were negligible as the yeast was stored at very low temperatures during storage inhibiting activity and because there was no organic substrate for biological functioning.

The equilibrium modelling phase used baker's yeast biomass as an experimental micro-organism after unsuccessfully attempting to describe the ionic behaviour of anaerobic sludge with the glycine system. The yeast biomass was chosen as this form of biomass was assumed to be free of unknown inorganic ions that may complicate the experiments and have fewer unknowns in terms of history and make-up than typical wastewater sludge.

It was identified that the exterior of an active (or recently deactivated) micro-organism is far more chemically complex than can be described in terms of a single free amino acid only. A range of other molecules with different functional groups and different energies of protonation and deprotonation will be present. Cell exterior characteristics may be expected to differ between genera depending on factors such as whether a micro-organism is gram-positive or –negative, on extrapolymeric substance (EPS) production and composition, the existence of a capsule around the cell and the range of extra- and intra-cellular activities that the cell undertakes (Seders & Fien, 2011).

Thus it is reasonable to propose a model of the cell wall exterior that is defined in terms of common functional groups. A similar approach was employed by the authors presented in the literature survey in Table 2-1 where between 3 to 4 functional groups were used to model the behaviour of bacteria binding proton and metal ions.

Upon comparison of the functional group's site concentrations in Table 2-1 to each other and to the results for the equilibrium yeast experiments, it was concluded that there is high variability between the studies and in comparison to literature. This statement can be confirmed by Claessens et al. (2006) as the study of acid-base activity of live bacteria showed large variability in acid base activity. The variability may be as a result of (i) cell wall property variations and the initial metabolic state as a result of cell preparation, (ii) pH-dependent variations in cell viability and metabolic activity and (iii) intrinsic differences in cell wall and metabolism among different species.

The pK_a values of the functional groups determined in this study are comparable with the research conducted by Kapetas et al. (2011). Kapetas et al. (2011) determined the pK_a values to be 4.34, 5.68, 7.58 and 9.79. The error (i.e. difference in pK_a values) between the pK_a measurements from this study phase and the literature values of Kapetas et al. (2011) is 0.23, 0.53, 5.30 and 5.91 % respectively. The study conducted by Kapetas et al. (2011) investigated the kinetics of biomass titrations and their

effect on the establishment of functional group site characteristics as well as the equilibration time of the titrations. It was shown that the total site concentrations varied for different titration speeds, suspected to be due to the presence of exudates. The exudates produced by the bacteria in the study have an impact on overall buffering capacity to the titration curve as the exudates react with the titrating acid or base consuming the titrant that should be attributed to the cell surface. This is prevalent at high pHs where maximum hysteresis in reversibility titrations was observed (refer to Chapter 6 and Figure 6-3 to observe the hysteresis and how the model addressed it).

It is not certain whether the buffering capacity of the yeast behaves in the same way as the anaerobic sludge biomass. Possible investigations of the yeast include analyzing the particulate and soluble organic matter by titration and comparing with the anaerobic sludge. As seen from the results section, the model predicted for the washed anaerobic sludge is comparable with the yeast biomass as the functional group's site concentrations fall within the uncertainty range (apart from the amine group); the ionic site concentrations for the the 2 carboxylate, phosphate and amine groups respectively are 0.17, 0.17, 0.021 and 0.076 mmol/g VS for the washed anaerobic sludge versus 0.202 (0.113 - 0.294), 0.165 (0.105 – 0.219), 0.026 (0 - 0.055), 0.043 (0.024 -0.062) mmol/g VS for the yeast biomass. The amine group in the washed anaerobic sludge is elevated in comparison to the yeast biomass. It is speculated that this elevation may be as a result of (i) the compensation for metabolic activity of the biomass or (ii) due to the inorganics present from the biomass or (iii) because the biomass surface is ionically different due to the fact that baker's yeast are a type of fungae whereas anaerobic sludge consists predominantly of bacteria and archae. Further work is required to confirm the speculation.

5.4. Conclusions

UKZiNe, a developed model component, was used to represent and investigate the ionic nature of biomass. The model component was composed of 4 functional groups; 2 carboxyl groups, 1 phosphate group and 1 amine group. The simulated titration curve was found to fit the experimental titrations well for lower concentrations of biomass and the buffering capacity of the biomass increased with the increase in biomass concentration. This was, however, viewed as negligible when comparing to the overall solution buffering capacity.

The comparison of the regressed values for the anaerobic sludge and the yeast biomass showed some difference in the amine functional group characteristics. The speculated causes of biomass metabolic activity as well as the presence of inorganics in the biomass call for the following aspects to be included in an alternate hypothesis where carbon dioxide evolution, mass transfer kinetics and a different biomass washing method for the removal of inorganics from the surface of the biomass are investigated. The apparent stepping in the titration curve as well as the underprediction of pH value in

the model relative to experimental data also validates an investigation into the experimental methodology and biomass model description.

Chapter 6 Phase 3: UKZiNe including partial equilibrium conditions and dynamic effects

The alternate hypothesis (named hypothesis 3) postulated that a rate limiting process (e.g. reaction kinetics or mass transfer) is significant and therefore a non-equilibrium rate process must be incorporated in the model to accurately describe the experimental data.

In the previous section an equilibrium model was compared to experimental titrations of a background solution containing biomass; the model incorporated a constructed component, UKZiNe, to represent the functional groups of the outer surface of biomass that may be involved in ionic association or dissociation reactions during the titration. The model fitted the data well for the experimental conditions, which included a rapid titration with strong agitation. Under these conditions, transport of ionic components into and out of the biomass was assumed to have much longer characteristic times than those of mixing and titrant addition, therefore the influence of these processes on the experiment was assumed to be negligible. The good agreement between the model and experimental data supported this assumption. However, during operation of a biological reactor the rate of change of pH should be significantly slower than in a titration, and therefore the transport of ionic components between the interior and exterior of the cells making up the biomass could be significant. Therefore, this chapter uses baker's yeast to continue the model component development with the inclusion of non-equilibrium conditions and rate processes.

The metabolic activity of live cells is described in Claessens et al. (2006). It is stated that the acid-base activity of live cells cannot be solely described by protonation and deprotonation reactions, but that the hysteresis of acid-base titration curves is indicative of irreversible reactions like cellular metabolism (Kapetas et al. 2011). Claessens et al. (2006) showed the importance of carbon dioxide evolution at high pH values (above pH 7) as base neutralisation was apparent during pH stat experiments and a measurable quantity of succinate, an intermediate product of aerobic respiration, was present in the solutions.

The non-equilibrium conditions included the rate of carbon dioxide exchange from the yeast metabolic activity, the delayed pH response time as well as adsorption of ions from the solution to the biomass and vice versa.

6.1. Experimental design

6.1.1. Formulating the model

The built-in ionic speciation model and model component functional group reactions are as per Section 5.1.1. An explanation of the principles used in modelling the system and the details surrounding the parameter regression can be found in Section 3.2. A review of the modifications to the ionic speciation model can be found in Appendix 5.

At the start of the non-equilibrium modelling, both the mass transfer kinetics (Equations 6-2, 6-4 and 6-5), pH probe response delay (Equation 6-6) and the carbon dioxide exchange (Equations 6-3, 6-4 and 6-5) from the biomass to the solution were considered. A mass transfer kinetics integrated sub-model was built into the primary physicochemical model to determine whether the adsorption kinetics were significant or not. The system was modelled at the interface of the cell and the bulk solution as shown in Figure 6-1. Initially, the interface between the cell wall and solution was governed by the biomass reaction kinetics, assumed to be due to the slow transfer of ions to and from the biomass. The model was simplified to only allow hydrogen ions to move across the membrane.

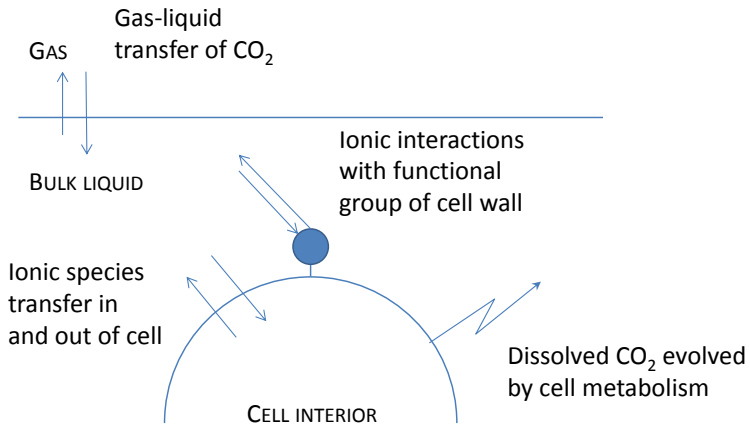

Figure 6-1: Theoretical construction of the non-equilibrium model. The model has been constructed to consider the interfaces between the cell interior and the bulk liquid

This was built into the model by including the following reactions:

- The concentration of the hydrogenated UKZiNe component at equilibrium was illustrated as the following:

  $[UK\text{-}H]_{eq} = [U1\text{-}COOH] + [U2\text{-}COOH] + [U3\text{-}PO_4^{-}] - [U4\text{-}NH_2]$ Equation 6-1

- The kinetic model was incorporated by augmenting the hydrogenated UKZiNe concentration with a mass transfer coefficient, k_a. [UK-H] is calculated independent of time.

  $$\frac{d(c[UK-H])}{dt} = -k_a * ([UK-H]_{eq} - [UK-H])$$ Equation 6-2

- The initial CO_2 in the solution was augmented by accounting for it in the initial carbonate concentration:

  $$[CO_3^{-2}]_{Total} = [HCO_3^-]_{Initial\ in\ solution} + [CO_2]_{Initial}$$ Equation 6-3

- The exchange rate of CO_2 between the bulk solution and the cell membrane, k_{CO_3}, was accounted for by the following reactions:

  $$[H]_t = [H]_{t=0} + 2[UKZiNe]_{Initial} k_{CO_3}\ t_t$$ Equation 6-4[9]

  $$[CO_3]_t = [CO_3]_{t=0} + [UKZiNe]_{Initial} k_{CO_3}\ t_t$$ Equation 6-5

- The pH probe lag was taken into consideration by accounting for the time lag in an integrated model according to the following:

  $$\frac{dpH_{actual}}{dt} = \frac{(pH_{simulated,t} - pH_{actual,t})}{Time\ constant}$$ Equation 6-6

The regression of model parameters for the mass transfer integrated model was found to be slow due to the numerical integrator getting stuck on local minima and not delivering the lowest objective function in the parameter regression. This was resolved but the model regression was still very slow on settling on the lowest objective function. The initial results, whereby the sample set was regressed considering both proton transfer to the biomass and the carbon dioxide exchange rate, proved to be very interactive and the certainty of which variable was constituting the change was questionable. The regression results provided a time constant that was between 0.003 and 0.05 seconds. This time constant, when compared with the operating time of the anaerobic digester, was small; as the time constant could not be confirmed by experimental data, it was decided to continue the regressions considering only the the initial CO_2 in solution, pH probe response delay and carbon dioxide exchange rate. The pH probe response delay time constant was measured to be 1.4 ±0.8s by the phosphate solution titration experiments carried out as described in Section 3.5.4.

[9] t refers to the time step, t, of the titration

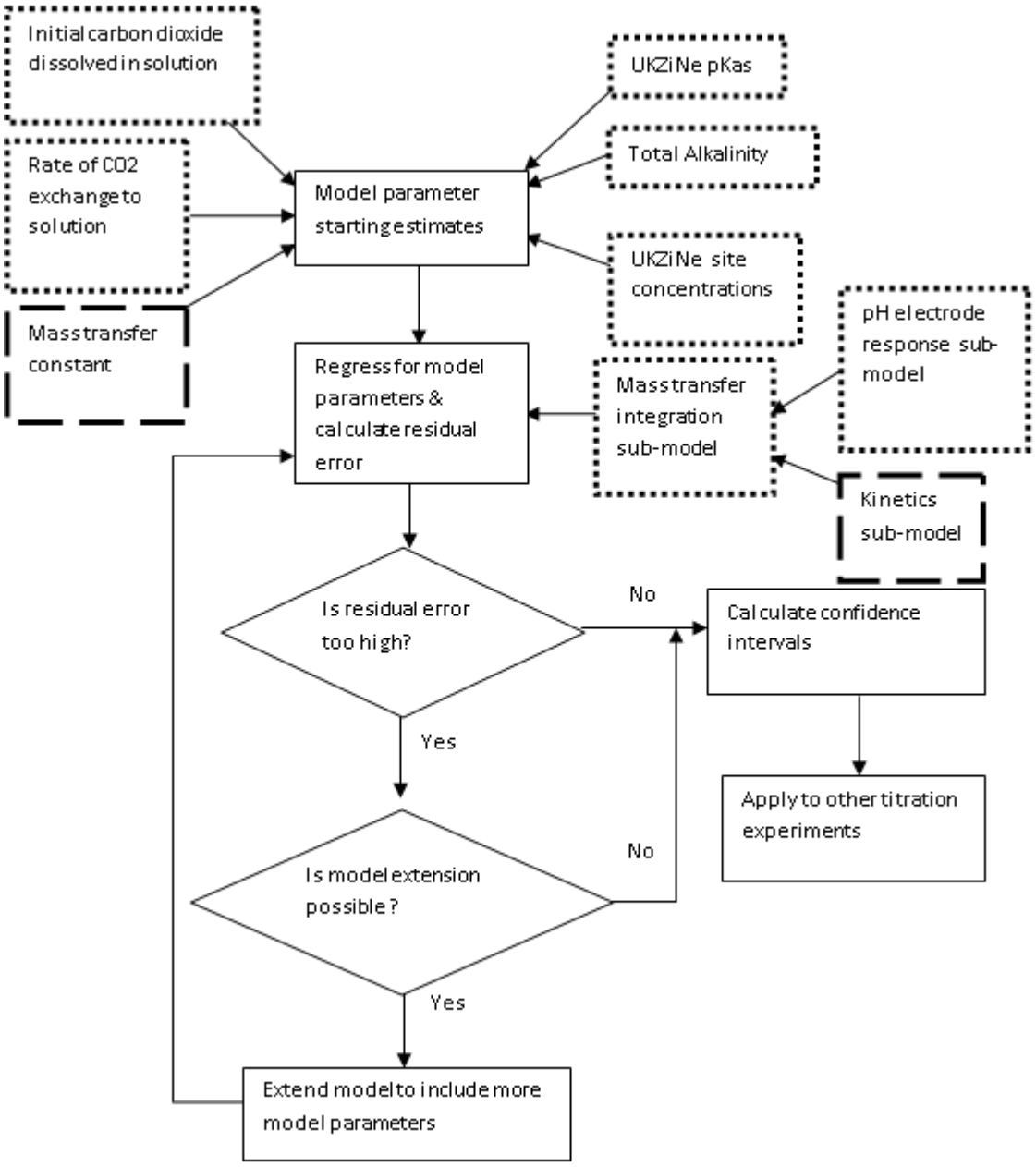

Figure 6-2: Methodology of parameter regression, model extension and application to experimental titrations

Figure 6-2 shows the different stages of the model component development. As stated before, initially all model parameters were considered (dotted and dashed outline boxes). The second phase removed the dashed outline boxes and only considered the dotted outline boxes in the parameter regression. Following the model parameter regression, the confidence intervals were obtained for the parameter set and the combination of the model parameters was applied to other experimental titrations.

6.1.2. Formulating the experiment

The objective of the experiments was to (i) Adjust the experimental procedure to validate the hypothesis that the conditions in the solution were significantly different to those calculated assuming equilibrium and (ii) generate titration curves containing baker's yeast to be used in the parameter regression of the model component UKZiNe and to investigate the buffering capacity in the operating region of an anaerobic digester. Acid-base titrations of the following solutions were performed:

(i) Yeast suspensions of 6.39 (6.34 – 6.44)[10] g TS/L concentration were titrated. The suspensions were made up by mixing particulate organic matter with a 151 mM NaCl background solution.

As per Section 3.3.3.1., the particulate organic matter was washed to remove any culture medium residues. The washing medium was changed from distilled water to a 151 mM NaCl solution, which corresponds to an assumed internal ion concentration of bacterial cells as per Appendix 1, Table A 1-1. The 151 mM NaCl concentration corresponds to the addition of the cation salt concentrations in Table A 1-1 (i.e. potassium + sodium). The washing method was changed to prevent possible cytolysis to the hypotonic surrounding solution.

The pH range used in the titrations was from 3 to ± 9. An aliquot of approximately 80 mL sample solution was titrated with 0.1009M NaOH to an approximate pH value of 9 with a burette speed of 0.5 mL/min and for the hysteresis comparison of alkaline and acidimetric titrations a burette speed of 0.05 mL/min was used. The sample solution was acidimetrically titrated with 0.1 M HCl using titration speeds of 0.05 mL/min and 0.1 mL/min. The sample was agitated throughout the titration using a magnetic stirrer set at 450 rpm to ensure uniform concentration in the sample. The pH and temperature were monitored simultaneously throughout the experiment. The details of the equipment and philosophy behind the test can be found in Section 3.3.

6.2. Results

The results for this part of the study are divided into two parts: (1) observations confirming the significance of non-equilibrium effects (Sections 6.2.1 to 6.2.4) and (2) experiments to characterise and quantify those effects (Sections 6.2.5 to 6.2.7).

[10] The representation shown is the average concentration of yeast suspension used (minimum yeast concentration – maximum yeast concentration)

6.2.1. Hysteresis between acid and base titrations of the same solution

Figure 6-3 shows the hysteresis between the acidimetric and alkaline titrations which led to the justification of the alternate hypothesis that non-equilibrium rate limiting processes were present. The hysteresis concept was as a result of an experimental discovery during the experimental phase of the project and led to the investigation of the discrepancy between the acidimetric and alkaline titration curves. Figure 6-3 clearly shows that the acidimetric and alkaline titration curves are not a mirror-image of one another and that there is a clear discrepancy between the titration curves in the operating region of anaerobic digester (pH 6 -8).

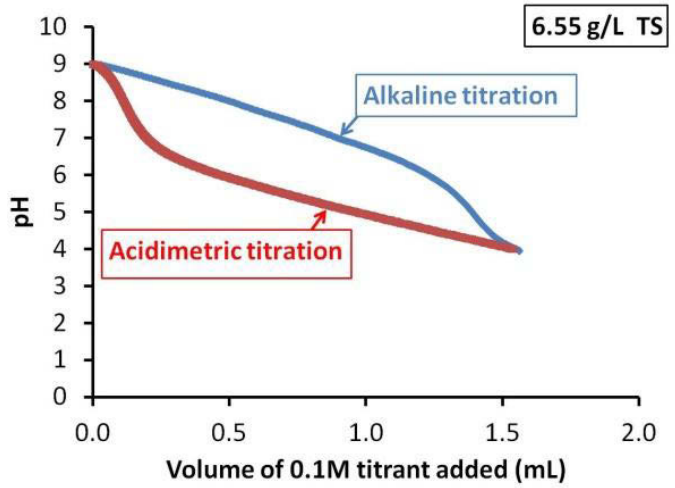

Figure 6-3: Hysteresis between experimental acidimetric and alkaline titrations at a speed of 0.05 mL/min (measured data points shown)

A steady addition of CO_2 would cause the pH to exhibit the behaviour shown in Figure 6-3 qualitatively.

6.2.2. Effect of temperature on amount of titrant required

Figure 6-4 shows a series of titrations of yeast biomass suspensions with an alkaline titrant, whereby a sample (average concentration of 6.7 g/L TS) was titrated with NaOH at different temperatures.

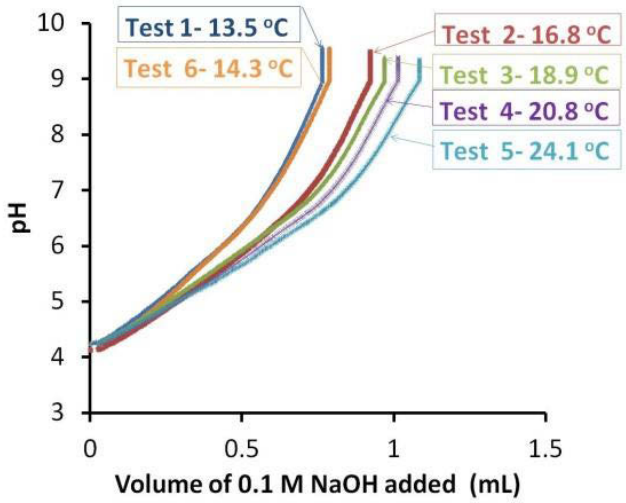

Figure 6-4: Experimental titration with NaOH of biomass suspensions at different temperatures (measured data points shown). The increased alkaline demand is attributed to increasing metabolic activity with increasing temperature

These experiments were originally designed to be a preliminary assessment of the reproducibility of the titrations. It was discovered that differences in the titrations were observed at different temperatures. The different temperatures ranged from 13.5 ^{o}C to 24.1 ^{o}C due to an uncontrolled sample temperature. It must be noted that the order of experiment execution was not increasing with increasing temperature, but it can be observed that the systematic increase in alkaline titrant demand for the same solution at increasing temperatures. This effect was ascribed to metabolic behaviour of the cells whereby at lower temperatures the cell activity is less, with lower associated CO_2 evolution and so the titration consumes less alkaline titrant to reach the setpoint pH.

6.2.3. pH drift independent of titrant addition

Figures 6-5 and 6-7 show a pH drift effect observed in a titration which had previously been titrated with 0.1 M NaOH. Figures 6-6 and 6-8 show the pH value decreasing although no titrant was added during the time interval shown. At the end of the time period shown, additional NaOH titrant was added to the solutions to bring the solution back up to a pH value of 9. The pH versus titrant volume plots for the additional titration are shown in Figures 6-6 and 6-8. It is important to note that the same sample is shown in Figures 6-5 to 6-8, however, as each of the titrations was conducted the sample was further diluted. The significance of the results is that the suspension required no addition of an acidic medium for the solution to decrease in pH over time, indicating that there is a phenomena that needs to be investigated and its contribution described in the model.

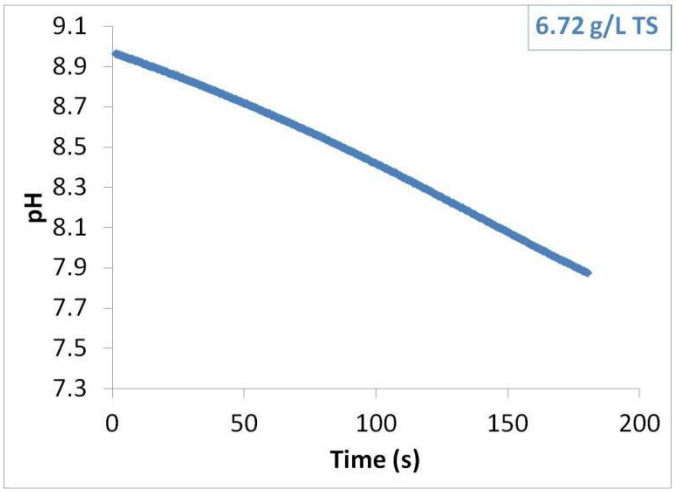

Figure 6-5: pH decrease after a 6.72 g TS/L yeast sample was titrated with 1.706 mL of 0.1 M NaOH

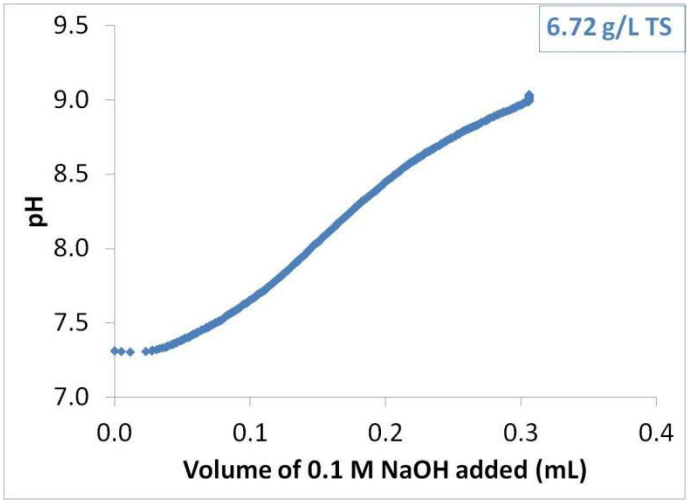

Figure 6-6: NaOH titration required to bring a 6.72 g TS/L yeast sample back to a pH of 9

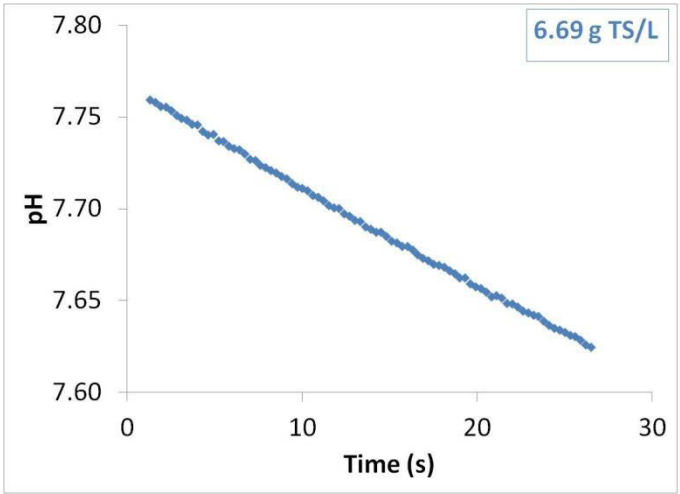

Figure 6-7: pH decrease after a 6.69 g TS/L yeast sample was titrated with 0.306 mL of 0.1 M NaOH

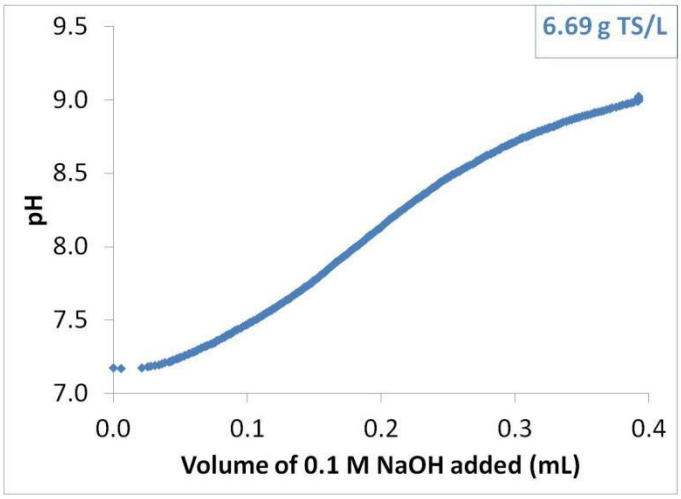

Figure 6-8: NaOH titration required to bring a 6.69 g TS/L yeast sample back to a pH of 9

6.2.4. Effect of titrant addition speed

Figures 6-9 and 6-10 show 2 sets of experiments conducted with the same methodology, as explained in Section 6.1.2., but with different titration speeds to determine if mass transfer effects play a role in the titration.

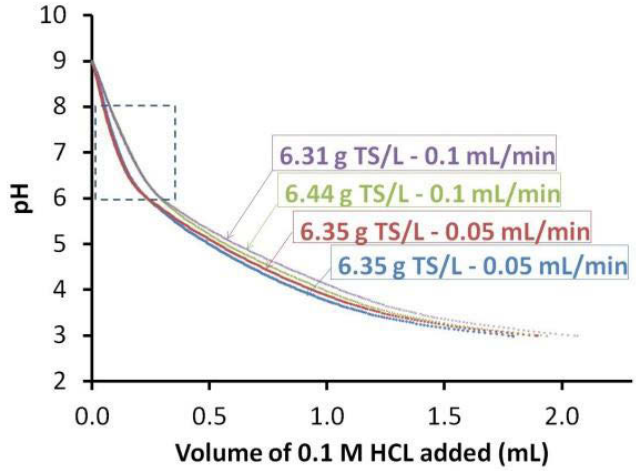

Figure 6-9: Acidimetric titration curves for two different titration speeds (i.e. 0.1 mL/min – 6.31 and 6.44 g TS/L and 0.05 mL/min – 6.35 and 6.35 g TS/L)

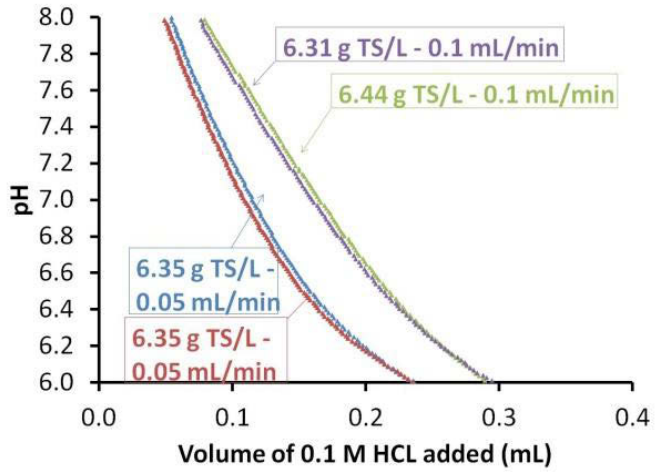

Figure 6-10: Magnified region of Figure 6-9 in the pH range of interest in an anaerobic digester

Figure 6-9 shows that there is marked difference between the faster (0.1 mL/min) and the slower (0.05 mL/min) acidimetric titration curves across the pH range from 9 to 3 with the lower rate of acid dosing producing a much steeper pH/acid dose gradient than with the more rapid rate of acid dosing. This is probably indicative of two phenomenon (i) the pH probe lag and (ii) the carbon dioxide production. It can be explained by the fact that the 0.1 mL/min titration speed consumes more HCl than the 0.05 mL/min titration speed to reach the same pH endpoint of 3.

6.2.5. UKZiNe characteristics when non-equilibrium effects are considered

Using the formulation of UKZiNe obtained in the previous chapter, the model has an amount of UKZiNe in proportion to the mass of biomass and a mass transfer process as stated in Section 6.1.1 The experiments consisted of 6.31 , 6.44, 6.35 and 6.35 g/L TS respectively in a background solution of 151mM NaCl titrated with HCl from a pH of 9.5 to 3. The total solid (TS) and ash content of the washed baker's yeast were measured as 0.26 g/g with a standard deviation of 0.002 and 0.06 g/g with a standard deviation of 0.003 respectively.

As described by Claessens et al. (2006), cells convert their sugar reserves into pyruvate by glycolysis during respiration. The breakdown of the pyruvate produces succinate and releases carbon dioxide. The carbon dioxide gas produced as a result of respiration will dissolve into the solution and form aqueous carbon dioxide;

$$CO_{2,g} \quad \leftrightarrow \quad CO_{2,aq} \qquad \text{Equation 6-7}$$

The aqueous carbon dioxide will react with the free water and produce carbonic acid

$$CO_{2,aq} \quad + \quad H_2O \quad \leftrightarrow H_2CO_3 \qquad \text{Equation 6-8}$$

The carbonic acid will dissociate and form carbonate ions and free hydrogen which will in turn reduce the pH of the solution as per Equations 2-1. and 2-2.

The yeast cells used in the experiments were alive and as a result it is possible that gaseous CO_2 may be produced during respiration. At higher pH values, CO_2 evolution results in a decrease in the pH value.

The model was fitted to the experimental points by adjusting the initial CO_2 in the solution, the functional group site concentrations and pK_a values and the rate of CO_2 respiration. The adjustment to the mentioned parameters was done by making the parameters fit by regression. The regression considered 4 sample sets of yeast biomass titration experiments in a solution of NaOH.

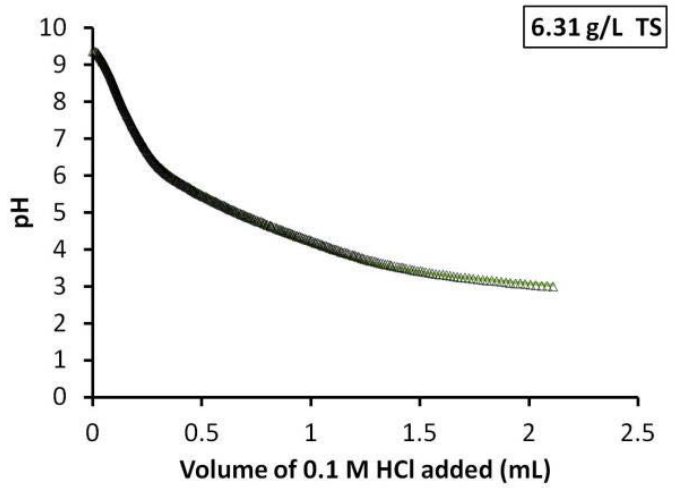

Figure 6-11: Establishment of UKZiNe parameters by fitting the model (solid line) to experimental titration (points) of yeast biomass in a NaOH solution (experimental titration speed of 0.1 mL/min)

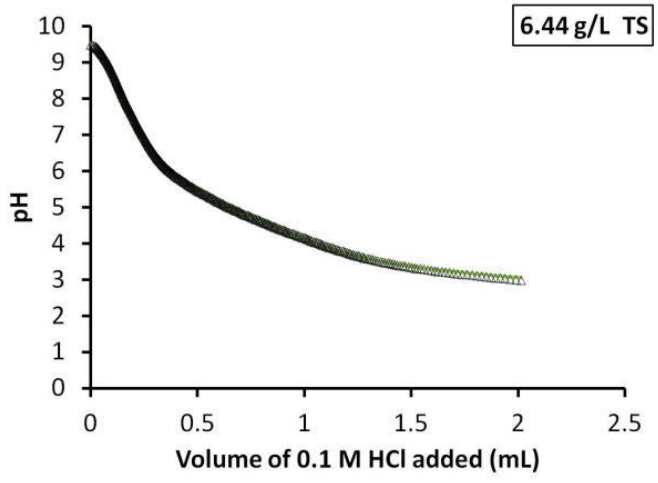

Figure 6-12: Establishment of UKZiNe parameters by fitting the model (solid line) to experimental titration (points) of yeast biomass in a NaOH solution (experimental titration speed of 0.1 mL/min)

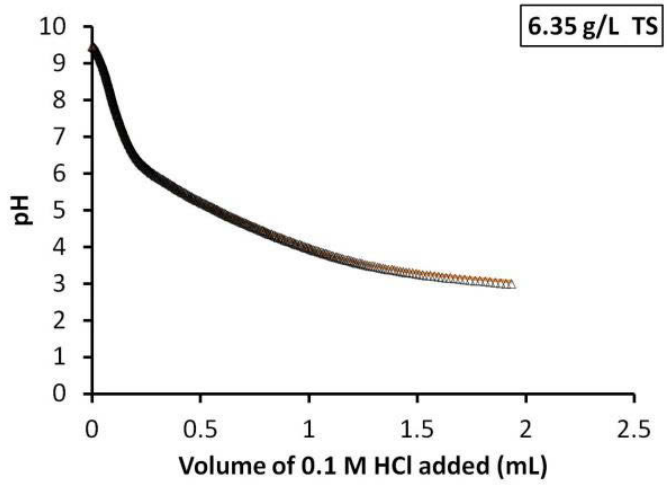

Figure 6-13: Establishment of UKZiNe parameters by fitting the model (solid line) to experimental titration (points) of yeast biomass in a NaOH solution (experimental titration speed of 0.05 mL/min)

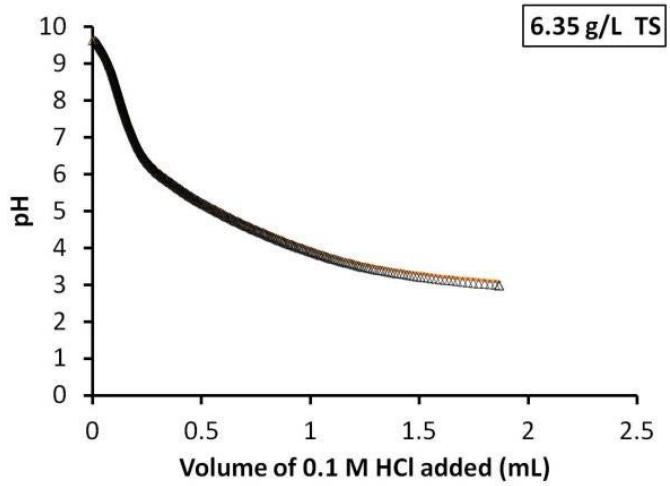

Figure 6-14: Establishment of UKZiNe parameters by fitting the model (solid line) to experimental titration (points) of yeast biomass in a NaOH solution (experimental titration speed of 0.05 mL/min)

Figures 6-11 to 6-14 show the agreement between the yeast biomass experimental titrations (data points) and the model curves (solid line) regressed to determine the UKZiNe characteristics with non-equilibrium conditions in phase 2 but also considered the effects of the rate of carbon dioxide exchange with the headspace.

The fit shown in Figures 6-11 to 6-14 was achieved by considering the same functional groups as biomass to the solution and the contribution of the carbon dioxide dissolved in solution at the start of the experiment. Table 6-1 shows the site concentrations and pK_a values that were simultaneously regressed. The UKZiNe site concentrations and pK_a values were regressed to give a best fit value and confidence interval on the regressed parameter.

Table 6-1: Regressed functional group site concentration and pK_a values for phase 3 (presented as best fit value (minimum of confidence region – maximum of confidence region))

	Site Concentration (mmol/g VS)	**pK_a Value**
Carboxyl group 1	0.111 (0 - 0.130)	4.586 (4.163 – 4.683)
Carboxyl group 2	0.035 (0.016 – 0.130)	5.339 (3.278 – 5.607)
Phosphate group	0.041 (0.036 – 0.045)	7.698 (7.627 – 7.835)
Amine group	0.390 (0.235 – 1.986)	-10.646 (-12.858 - -10.462)

Table 6-2: Functional group site concentrations and pK_a values for phase 2

	Site Concentration (mmol/g VS)	**pK_a Value**
Carboxyl group 1	0.202 (0.113 - 0.294)	4.35
Carboxyl group 2	0.165 (0.105 – 0.219)	5.65
Phosphate group	0.026 (0 – 0.055)	7.198
Amine group	0.043(0.024 - 0.062)	-9.244

A comparison of Tables 5-1 and 6-1 show that there are differences in the functional group site concentrations. The main differences are the carboxyl groups and amine group site concentrations. The differences in phase 2 and 3's regressed carboxyl group site concentrations can possibly be explained by the inclusion of the carbon dioxide terms (CO_2 exchange rate and initial CO_2 in solution) in phase 3. The difference in the amine group site concentrations may be because the pH change per volume titrant added was highest around the amine group equivalence point and therefore was most strongly affected by the pH probe lag and gas transfer effects. The amine group equivalence point shows the most deviation when comparing phase 2 and 3. The carboxyl group 1 site concentration, as shown in Table 6-1, is not significant which suggests the possible removal of the group from the model.

The uncertainty analysis for the parameter regression for phase 3 can be seen in Appendix 3. The parameter correlation for phase 3 shows that there are very strong interactions in the estimation of the parameters. Strong correlations were expected between the carboxyl groups. The trend from the previous chapter's results remained unchanged as the coefficient was again negative indicating that as the one parameter increases the other decreases. Strong interactions can also be observed for the

carboxyl group pK_a values. An interesting observation was the interaction of the carboxyl group site concentrations with the carboxyl group pK_a values. The first carboxyl group site concentration showed a linear dependency on the pK_a values while the second carboxylic acid group showed an inverse relationship. The other parameters showing very strong interactions were the amine group site concentration with the pK_a for the amine group and the correlation between the initial carbonate in solution for the different sample sets. An observation that was noted in the analysis of the parameter correlations was that the CO_2 exchange rate was independent of the carboxyl site concentrations and the carboxyl pK_a values. The objective function value for each of the searches across the eigenvectors can be seen in Appendix 3 with the corresponding titration curves for each of the parameter uncertainty sets shown in Figures 3-35 to 3-38. The variation in titration curve for the Figures mentioned can be seen to be negligible apart from one parameter set which produced substantially different characteristics in titration curve which is also verified by the large objective function seen in Appendix 3.

6.2.6. Non-equilibrium model parameter values

The exchange rate of CO_2 was set as a fixed variable across all of the sample sets whereas the initial concentration of dissolved CO_2 at the start of the experiment was unknown and therefore determined by regression. The regressed and simulated CO_2 concentration in the titration vessels was not in equilibrium with the atmosphere, either because it was evolving through microbial activity, or because the background solution had a higher or lower value than what was in equilibrium with the atmosphere and so there would be spontaneous CO_2 evolution or dissolution. Hence, the amount of CO_2 dissolved at the start of each titration was essentially unknown. The regression results delivered an exchange rate of 1.96×10^{-7} ($(1.475 \text{ to } 2.519) \times 10^{-7}$) mol s g^{-1} TS. The initial number of moles of dissolved CO_2 in each of the titration sets was estimated at values between 0 and 0.00033 moles. The CO_2 evolution increases the uncertainties around the UKZiNe carboxyl groups and makes it difficult to detect the UKZiNe buffer around pH 7.

6.2.7. Buffer intensity calculations

Figures 6-15 to 6-18 show the buffer intensity curves calculated from the data as in Figures 6-11 to 6-14. The buffer intensity curves plot the overall solution, biomass contribution and background buffer intensities. The buffer intensity plots were developed using the same principles as described in Section 5.2.1. In these plots, however, the background solution considers not only the H_2O background buffer intensity but also considers the variations of the CO_2 initially dissolved in solution and added or removed by gas exchange from biomass to solution.

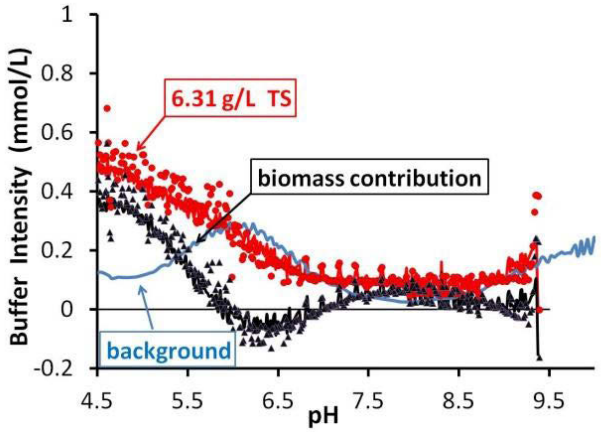

Figure 6-15: Buffer intensity of yeast biomass in a NaOH solution (experimental titration speed of 0.1 mL/min)

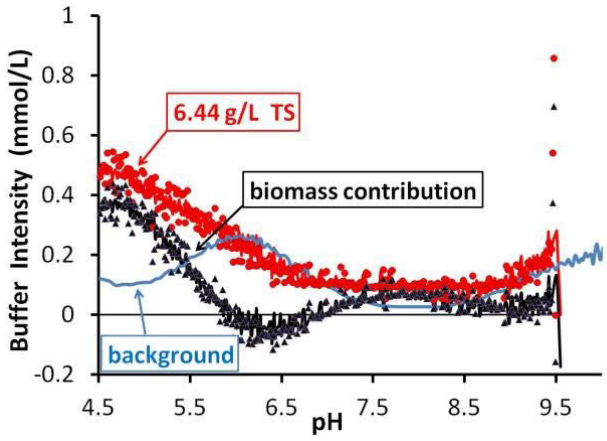

Figure 6-16: Buffer intensity of yeast biomass in a NaOH solution (experimental titration speed of 0.1 mL/min)

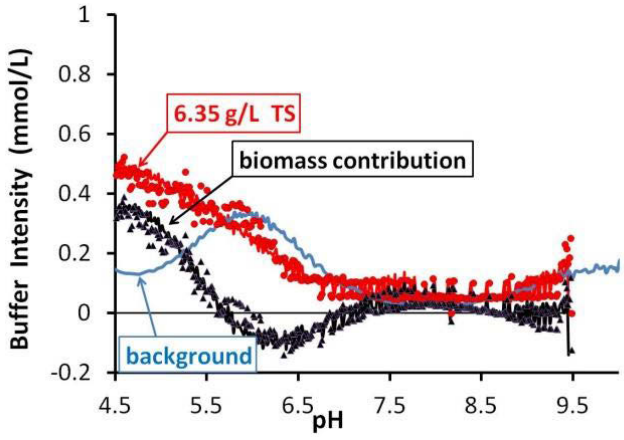

Figure 6-17: Buffer intensity of yeast biomass in a NaOH solution (experimental titration speed of 0.05 mL/min)

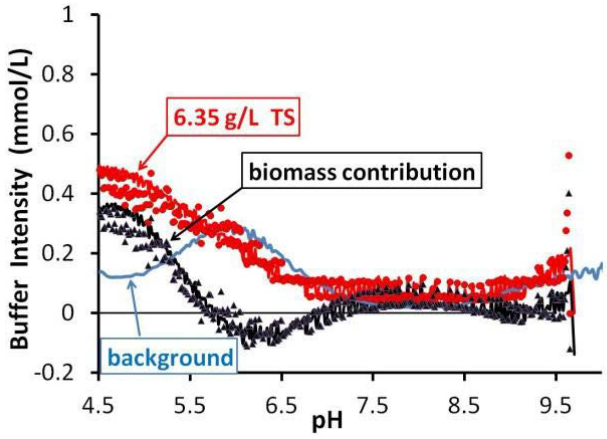

Figure 6-18: Buffer intensity of yeast biomass in a NaOH solution (experimental titration speed of 0.05 mL/min)

The biomass contribution shown in Figures 6-15 to 6-18 is as a result of the subtraction of the modelled contribution to buffer intensity of the background solution from the overall solution. The negative biomass contribution is not realistic and results from subtracting experimentally derived values from the model values, where the calculated background solution buffer intensity includes the non-equilibrium changing dissolved CO_2 concentration. All four figures imply that the buffer intensity of the biomass contribution is so small in the region of interest (pH 6-8) that it is masked by the CO_2 evolution.

6.3. Discussion

In this chapter, the significance of non-equilibrium conditions was considered. A comparison of sequential titrations of the same solution with alkaline and acid titrant showed a hysteresis between the forward and reverse titrations using yeast cell biomass. The results indicated that there were features of the titration experiments that could not be well described by the model when ionic equilibrium was assumed.

The impact of non-equilibrium conditions would be the following:

- The distribution of substances between solid and aqueous phase would be affected
- The reactivity of surfaces in processes such as precipitation, dissolution of minerals, adsorption and redox processes would be affected.

This could potentially lead to an overall inaccurate description of the pH and ultimately the buffer intensity contribution of the biomass.

Figure 6-9 shows that the titrant addition rate influences the observed amount of acid required to achieve a pH range. There is a substantial difference between acid demand for the same solution with different titrant addition rates for acidimetric titrations in the operating range of the anaerobic digester

with a greater acid demand per unit pH value change for the faster addition rate. The difference between the two curves can also be explained by two possible phenomena: (i) carbon dioxide evolution and/or (ii) mass transfer resistance.

The described phenomena can be further confirmed by Figures 6-5 to 6-8 in the results section where the graphs show that the pH tends to decrease spontaneously during titration with an alkaline titrant. The cause was identified as metabolic activity whereby the cells are respiring and releasing carbon dioxide into the solution. This hypothesis was also in agreement with Figure 6-4 where significant metabolic activity was also identified. The CO_2 rate of exchange was therefore taken into consideration in the model by making the rate a function of the mass of yeast present in the sample as well as the time of the titration (refer to Equations 6-4 and 6-5).

The history of the yeast cells was unknown before experimental research was conducted. The original pH value measured in a solution of biomass freshly suspended in a background salt solution was between 3.9 and 4.5, indicating that H^+ ions must be added to the solution by the fresh biomass. This was incorporated into the model by including an amount of carbonate in the initial suspension composition, such that the calculated pH value before commencing titration matched the value observed experimentally.

The above phenomenon of CO_2 evolution was modelled by assuming a fixed exchange rate between the gaseous and liquid form. The rate was described by the concentration of yeast in solution per time step of the titration.

The simulated and experimental curves showed a good fit with little deviation between the model and the data. The buffering capacity plots show that the buffering capacity in the pH region of interest is negligible for the concentrations of biomass tested. If there is sufficient interest, it is recommended that further investigation is required to determine whether higher concentrations of biomass produce the same result.

6.4. Conclusions

In the previous chapter, UKZiNe, a model component, was developed to represent the ionic nature of biomass. In this chapter, the influence of non-equilibrium conditions in terms of the ionic speciation were considered in attempting to model the behavior of biomass in background solutions during potentiometric titrations using UKZiNe. The model component was composed of 4 functional groups; 2 carboxyl groups, 1 phosphate group and 1 amine group. The ionic speciation model initially considered mass transfer kinetics, pH probe response delay, CO_2 exchange between the biomass and solution as well as the initial concentration of carbon dioxide in the solution. The mass transfer time constant was found to be small when compared with an anaerobic digester's operating time and not a

major contributor to the overall fit of the simulation to the experiment. The non-equilibrium conditions used in the model component development thereafter were the pH probe response delay, carbon dioxide exchange between the biomass and solution as well as the initial concentration of carbon dioxide in the solution. The incorporation of the non-equilibrium effects in the simulation resulted in significant changes to the regressed pK_a and site concentrations of UKZiNe amine group.

The buffering capacity, considering non-equilibrium conditions, did not produce vastly differing results in phase 3 as compared to phase 2, in that the buffering capacity in the operating region of an anaerobic digester was again seen to be negligible compared to an overall mixed salt background solution buffering capacity.

Chapter 7 Overall Discussion

The objective of the study was to investigate the influence of biomass on ionic speciation in a biological system and to determine if the inclusion of an ionic description of the biomass in the modelling of the system would allow an improved prediction of the solution pH.

The study postulated 3 hypotheses to describe the ionic nature of biomass, (i) the use of glycine equivalence of the biomass surface, (i) the use of a model component, UKZiNe at equilibrium conditions and (iii) the use of a model component, UKZiNe, accounting for non-equilibrium conditions.

Biomass, in the form of particulate organic matter, was used as the medium to model and investigate buffering capacity. Soluble organic matter and its effects on the model component description and buffering capacity were not taken into account.

Figure 7-1 shows the investigation of the hypotheses and what decisions were taken at each of the steps in the study to validate the hypotheses. Phase 1 considered the use of glycine as a biomass descriptor. This hypothesis (hypothesis 1) was not supported as the glycine titration characteristics were not comparable with the anaerobic sludge titration characteristics. The poor comparison was due to differences in inflection points, which was indicative of the functional group site concentrations and pK_a values. The sludge was seen to have a high concentration of inorganic matter assumed to be carbonate. The methodology did not include a validation of this assumption.

Following the rejection of hypothesis 1, the investigation considered developing a model to describe the observed ionic behaviour of the biomass. As the inorganics concentration, as measured by the fixed solids concentration of the anaerobic sludge used in the first phase of this work was high , the development of the model component was based on a "cleaner" form of biomass, namely baker's yeast.

The alternate hypothesis (hypothesis 2) considered a description of biomass, UKZiNe assuming ionic equilibrium during each experimental titration. The model component development resulted in two additional functional groups being accounted for over and above those used in the investigation in phase 1, i.e. the phosphate group and second carboxyl group. The experimental methodology considered two types of titrations, titrations using a mixed salt background solution with biomass and titrations using a NaOH solution with biomass as shown in Figure 7-1. The UKZiNe model description, considering equilibrium conditions, fitted the experimental titrations well. The experimental and simulated titrations were translated into buffer capacity plots. The plots showed that the biomass buffering capacity contribution increased with increasing biomass concentration but was seen to be negligible in the pH area of interest (pH 6-8) when compared with the mixed salt

background solution. The amine functional group site concentration differed when comparing the UKZiNe regressed value to the preliminary work conducted on manually regressing the anaerobic sludge functional group site concentrations and pK_a values. The apparent stepping effect observed and under-prediction of the simulated titration curve relative to the experimental data also justified the need for a more thorough investigation into the experimental methodology and the UKZiNe description. An investigation into the third hypothesis was further justified when significant hysteresis between the acidimetric and alkaline titrations was observed.

The second alternate hypothesis (hypothesis 3) considered non-equilibrium conditions with respect to ionic speciation when determining the biomass model parameters. The description considered mass transfer kinetics, pH probe delay as well as the carbon dioxide contributions, i.e. initial CO_2 in solution and the exchange rate of CO_2, as seen in Figure 7-1. The experimental methodology was also adjusted to (i) change the biomass washing procedure and background sample solution from using distilled water to using NaCl to reduce the chances of cytolysis; (ii) decrease the titrant concentration from 0.5M to 0.1M in order to increase the volume of titrant titrated and hence allow for greater precision; (iii) decrease the upper pH endpoint from a pH value of 11 to a value of 9. At first a pH range of 3 to 11 was used according to the method of Wang & Huang (1998). The concern was that the biomass cell wall structure may change at very high pH values, interfering with the buffering measurements above a pH of 10 as indicated by Fein et al. (2005); (iv) The speed of internal mixing was decreased from 950 rpm to 450 rpm to prevent vortex formation in the beaker which would disturb the pH measurements.

Initially a mass transfer kinetics integrated model accounting for a regressed mass transfer constant was used in the description of biomass. The inclusion of the sub-model resulted in a highly interactive model in terms of parameter estimation. The carbon dioxide transfer and electrode response were found to be adequate and it was not necessary to add proton-transfer resistance into the model. The overriding assumption is that the carbon dioxide exchange played a role in changing the UKZiNe description. It is recommended to continue further experimentation under N_2 purging to strip CO2 from solution, thereby eliminate the effects of CO_2 exchange between the solution and the atmosphere to reduce the uncertainty in the experiments. The non-equilibrium ionic conditions model resulted in a good fit between experimental and simulated titration curves and the biomass contribution was still predicted to be negligible in the pH range of interest.

The functional group site concentrations and pK_a values of phase 3 were compared with the results from phase 2. It can be observed that only the lower carboxyl group manually tuned pK_a value for phase 2 was within the uncertainty range of phase 3 while the second carboxyl group, phosphate group and amine group pK_a values were similar but did not fall within the uncertainty range for phase 3. Phase 3 delivered a considerably higher amine group pKa value with a wide range which may be a

result of the interactive nature of the model parameters in the pH range. The carboxylic group site concentrations were much lower than estimated in phase 2 and this may be as a result of the carbonate contribution from the CO_2 exchange rate and initial CO_2 in solution. The phosphate functional group delivered a concentration comparable with phase 2 but the amine group contributed a concentration almost 10 times the concentration in comparison to phase 2 and with a wide range. It should be noted that the quantitative description of biomass developed in this study applies to the samples and the conditions under which it was measured. These factors should be experimentally validated before being used in any other system.

The biomass contribution to the overall buffer capacity was found to be negligible in the normal operating region of an anaerobic digester, irrespective of whether equilibrium or non-equilibrium ionic speciation condition were assumed, when compared with the overall mixed salt buffering capacity. The kinetic aspects of the model are only important for the titration experiments and associated parameter estimation when the solution pH value is changing rapidly; the buffer intensity calculations indicate that these effects have no practical relevance in the modelling of an anaerobic digestion process, where pH changes should happen over a much smaller range of values, over a much longer time period. The study showed that increasing biomass concentrations showed increasing biomass buffering capacity contribution. The biomass buffering capacity contribution becomes noticeable in the lower pH regions (below pH 6) especially at the higher biomass concentrations tested. The biomass buffering capacity contribution at the lower pH regions may become important when modelling digester failure. If further work is conducted on this study, it is recommended that the work be continued to investigate and validate that the biomass buffering capacity remains negligible when modelling membrane reactors operating at much higher biomass concentrations than those tested.

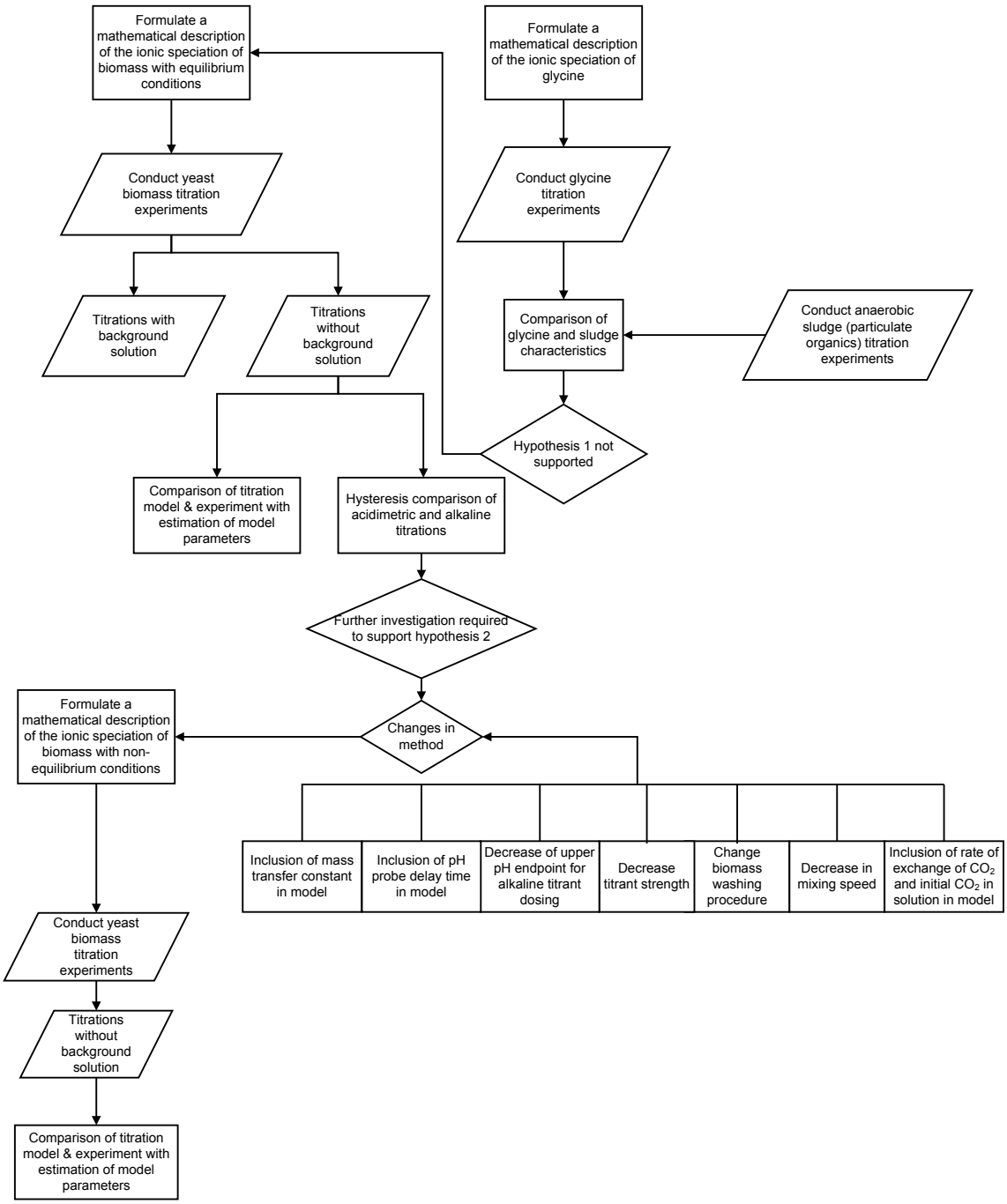

Figure 7-1: Flow diagram to show investigation methods involved in the study

Chapter 8 Conclusions and Recommendations

8.1. Conclusions

Quantitative descriptions of the ionic behaviour of biomass were developed by performing titrimetric experiments on samples of biomass or sludge suspended in salt solutions or distilled water and simulating the titrations using a model of the biomass in a combined mass balance – speciation model of the system.

It was found that glycine could not be used as a representative for characterising biomass pH buffer intensity as the glycine buffer contribution showed significantly different characteristics to those of washed anaerobic sludge, particularly in the pH ranges below 6.5 and above 8.5.

The speciation modelling showed that while assumption of equilibrium (hypothesis 2) and non-equilibrium (hypothesis 3) conditions produced different descriptions of the yeast biomass, the contribution of the biomass to the overall buffer capacity was predicted to be negligible in the range of operation of an anaerobic digester, irrespective of the assumptions made regarding ionic equilibrium.

8.1.1. Recommendations

If there is sufficient interest to continue the study, further research should investigate (i) the impact of soluble organic matter to the overall buffering capacity, (ii) the impact of higher biomass concentrations than those tested to the overall buffering capacity and (iii) the impact of organic solids on the P_{CO2} and alkalinity.

If further research is continued, the experimental methodology should be amended to include the following:

i. Temperature effects of the titration media were not controlled due to equipment limitations. Experimental titrations should be conducted in a controlled temperature and humidity environment to ensure that microbial activity can be eliminated as a factor for consideration in the titrations. Alternatively, experimental titrations can be conducted on dead cells to avoid the complexities of microbiological activity.
ii. The titrations should be conducted under N_2 purging to eliminate the effects of CO_2 exchange as conducted by Fang et al. (2009).

References

Allison, J. D., Brown, D. S. & Novo-Gradac, K. J., 1991. *MINTEQA2/PRODEFA2, A Geochemical Assessment Model for Environmental Systems: Version 3.0 User's Manual.* Washington DC: United States Environmental Protection Agency, Office of Research and Development.

Anderson, G. K. & Yang, G., 1992. Determination of bicarbonate and total volatile aid concentration in anaerobic digesters using a simple titration. *Water Environment Research,* Volume 64, pp. 53-59.

Artola, A., Balaguer, M. D. & Rigola, M., 1997. Heavy Metal Binding to Anaerobic Sludge. *Water Research,* 31(5), pp. 997-1004.

Ball, J. W. & Nordstroom, D. K., 1991. *User's manual for WATEQ4, with revised thermodynamic data base and test cases for calculataing speciation of major, trace and redox elements in natural waters.* Menlo Park: U.s. Geological Survey.

Barat, R., Bouzas, A., Marti, N., Ferrer, J., Seco, A., 2009. Precipitation assessment in wastewater treatment plants operated for biological nutrient removal: A case study in Murcia, Spain. *Journal of Environmental Management,* Volume 90, pp. 850-857.

Batstone, D. J., Keller, J., Angelidaki, I., Kalyuzhnyi, S. V., Pavlostathis, S. G., Rozzi, A., Sanders, W. T., Siegrist, H., Vavilin, V. A.,2002. The IWA Anaerobic Digestion Model No 1 (ADM1). *Water Science and Technology,* 45(10), pp. 65-73.

Batstone, D. J., Keller, J., Angelidaki, I., Kalyuzhnyi, S. V., Pavlostathis, S. G., Rozzi, A., Sanders, W. T., Siegrist, H., Vavilin, V. A., 2010. *Towards a Generalized Physicochemical Framework: WWTmod Workshop Position Paper.* New Orleans.

Bethke, C. M. & Yeakel, S., 2010. *The Geochemist's workbench - GWB Essentials Guide.* Chicago: Hydrogeology program.

Beveridge, T. J., 1999. Structures of gram-negative cell walls and their derived membrane vesicles. *Journal of Bacteriology,* 181(16), pp. 4725-4733.

Brouckaert, B. M., 1995. *Prediction of Conductivity from Equilibrium Ionic Speciation,* Durban: University of Natal.

Brouckaert, C. A., Brouckaert, B. M. & Ekama, G., 2015. *INTEGRATION OF COMPLETE ELEMENTAL MASS BALANCED.*

Brouckaert, C. J., Ikumi, D. S. & Ekama, G. A., 2010. *A 3-phase anaerobic digestion model,* Durban: University of KwaZulu-Natal.

Brouckaert, C. J., Ikumi, D. S. & Ekama, G. A., 2011. *Modelling of struvite precipitation in anaerobic digestion: part 2,* Durban: University of KwaZulu-Natal.

Chen, Y., Cheng, J. J. & Creamer, K. S., 2008. Inhibition of anerobic digestion process:A review. *Bioresoure Technology,* Volume 99, pp. 4044-4064.

Claessens, J., van Lith, Y., Laverman, A. & van Cappellen, P., 2004. What do acid-base titrations of live bacteria tell us? A preliminary assessment. *Aquatic Sciences,* 66(1), pp. 19-26.

Claessens, J., van Lith, Y., Laverman, A. & van Cappellen, P., 2006. Acid-base activity of live bacteria: Implications for quantifying cell wall charge. *Geochimica et Cosmochimica Acta,* Volume 70, pp. 267-276.

Coleman, N. T., Weed, S. B. & McCracken, R. J., 1959. Cation exchange capacity and exchangeable cations in Piedmont soils in North Carolina. *Soil Sc. Soc. Am. Proc,* Volume 23, pp. 146-149.

Corliss, W. R., 1994. *Science Frontiers.* [Online]
Available at: http://www.science-frontiers.com/sf095/sf095b08.htm
[Accessed 17 March 2015].

Cox, J. S., Smith, D. S., Warren, L. A. & Ferris, F. G., 1999. Characterising heterogenous bacterial surface functional groups using discrete affinity spectra for proton binding. *Environmental Science & Technology,* Volume 33, pp. 4514-4521.

Dold, P. L., Ekama, A, G. & Marais, G., 1980. A general model for the activaited sludge process. *Progress Water Technology,* Volume 12, pp. 47-77.

Dzombak, D. A. & Morel, F. M., 1990. *Surface Complexation Modeling: Hydrous Ferric Oxide.* New York: Wley-Interscience.

El-Mamouni, R., Guiot, S. R., Mercier, P., Safi, B., Samson, R., 1995. Limiting impact on granules activity on the multiplate anaerobic reactor (MPAR) treating whey permeate. *Biprocess Engineering,* pp. 47-53.

Ennola, K., Sarvala, J. & Devai, G., 1998. Modelling zooplankton population dynamics with the extended Kalman filtering technique. *Ecological Modelling,* Volume 110, pp. 135-149.

Fang, L., Cai, P., Chen, W., Hong, Z., Huang, Q., 2009. Impact of cell wall structure on the behavior of bacterial cells in the binding of copper and cadmium. *Colloids and Surfaces A: Physicochemical and Engineering Aspects,* 347(1-3), pp. 50-55.

Fein, J. B., Boily, J. F., Yee, N., Gorman Lewis, D.; Turner, B. F., 2005. Potentiometric titrations of Bacillus subtilis to low pH and a comparison of modeling approaches. *Geochimica et Cosmochimica Acta,* 17(7), pp. 1123-1132.

Fristoe, B. R. & Nelson, P. O., 1983. Equilibrium Chemical Modeling of Heavy-Metals in Activated Sludge. *Water Research ,* 17(7), pp. 771-778.

Haas, J. R., DiChristina, T. J. & Wade, R., 2001. Thermodynamics of U(VI) sorption onto Shewanella putrefaciens. *Chemical Geology,* 180(1), pp. 33-54.

Henderson, P. J., 1971. Ion Transport by energy-conserving biological membranes. *Annual Review of Microbiology,* Volume 25, pp. 393-428.

Henze, M., Gujer, W., Mino, T., Matsuo, T., Wentze, M. C., Marais, G., 1987. *Activated-Sludge Model No. 1,* London: IAWPRC.

Henze, M., Gujer, W., Mino, T., van Loosdrecht, M., 1995. *Activated Sludge Model No. 2,* London: IAWQ.

Henze, M., Gujer, W., Mino, T. & van Loosdrecht, M., 2000. *Activated Sludge Models ASM1, ASM2, ASM2d and ASM3,* London: IWA Publishing.

Ikumi, D. S., 2010. *Research Report:Three phase plant-wide mathematical modelling with the inclusin of Phosphorus (P) and the anaerobic and aerobic digestion of P rich sludge,* Cape Town: University of Cape Town.

Kapetas, L., Ngwenya, B. T., Macdonald, A. M. & Elphick, S. C., 2011. Kinetics of bacterial potentiometric titrations: The effect of equilibration time on buffering capacity of Pantoea agglomerans suspensions. *Journal of Colloid and Interface Science,* 359(2), pp. 481-486.

Keenan, P. J., Isa, J. & Switzenbaum, M. S., 1993. Inorganic solids devolopment in a pilot-cale anaerobic reactor treating municipal solid-waste landfill leachate. *Water Environment Research,* 65(2), pp. 181-188.

Kiss, T., Sovago, I. & Gergely, A., 1991. Critical Survey of Stability Constants of Complexes of Glycine. *Pure & Applied Chemistry,* Volume 63, p. 597.

Korn, E. D. & Northcote, D. H., 1960. Physical and chemical properties of polysaccharides and glycoprteins of the yeast-cell wall. *Biochemical Jornal,* Volume 75, pp. 12-17.

Lodish, H. F., 1999. *Molecular cell biology.* New York: New York, Scientific American Books.

Loewenthal, R. E., Ekama, G. & Marais, G. V. R., 1989. Mixed weak acid/base systems Part I: Mixture characterisation. *Water SA,* 15(1), pp. 3-24.

Loewenthal, R. E., Kornmuller, U. R. C. & van Heerden, E. P., 1994. Modelling struvite precipitation in anaerobic treatment systems. *Water Science and Technology,* 30(12), pp. 107-116.

Marsili-Libelli, S., Guerrizio, S. & Checchi, N., 2003. Confidence regions of estimated parameters for ecological systems. *Confidence regions of estimated parameters for ecological systems,* Volume 165, pp. 127-146.

McCarty, P., 1974. *Anaerobic processes.* Birmingham, IWA.

McCarty, P. L. & Mosey, F. E., 1991. Modelling of an anaerbic digestion process (a discussion of concepts. *Water Science and Technology,* 24(8), pp. 17-33.

Moosbrugger, R. E., C, W. M., Ekama, G. A. & Marais, G., 1993. Weak acid/bases and pH control in anaerobic systems - A review. *Water SA,* 19(1), pp. 29-40.

Murphy, C. B., 1957. Metal chelates of glycine and glycine peptides. *Biological Chemistry,* 226(1), pp. 37-50.

Musvoto, E. V., Ekama, G. A., Wentzel, M. C. & Loewenthal, R., 2000. Extension and application of the three-phase weak acid/base kinetic model to the aeration treatment of anaerobic digester liquors. *Water SA,* 26(4), pp. 417-438.

Naja, G., Mustin, C., Volesky, B. & Berthelin, J., 2005. A high-resolution titrator: a new approach to studying binding sites of microbial biosorbents. *Water Research,* Volume 39, pp. 579-588.

Nelson, P. O., Chung, A. K. & Hudson, M. C., 1981. Factors affecting the fate of heavy metals in the activated sludge process. *Water Pollution Control Federation,* 53(8), pp. 1323-1333.

Oreskes, N., Shrader-Frechette, K. & Belitz, K., 1994. Verification, Validation and Confirmation of Numerical Models in the Earth Sciences. *Science, New Series,* 263(5147), pp. 641-646.

Pagnanelli, F., Veglio, F. & Toro, L., 2004. Modelling of the acid-base properties of natural and sythetic adsorbent materials used for heavy metal removal from aqueous solutions. *Chemosphere,* 54(7), pp. 905-915.

Parkhurst, D. L. & Appelo, C. A. J., 1999. *User's guide to PHREEQC (version 2)--A computer program for speciation, batch-reaction, one-dimensional transport, and inverse geochemical calculations,* s.l.: U.S. Geological Survey Water-Resources Investigations Report 312.

Peterson, B., Gernaey, K. & Vantolleghem, P. A., 2001. Practical identifiability of model parameters by combined respirometric-titrimetric measurements. *Water Science and Technology,* 43(7), pp. 347-355.

Plette, A. C. C., v. R. W., Benedetti, M. F. & Van der Wal, A., 1995. pH Dependent Charging Behaviour of Isolated Cell Walls of a Gram-Positive Soil Bacetrium. *Journal of Colloid and Interface Science,* 173(2), pp. 354-363.

Reichert, P. B., Borchardt, D., Henze, M., Rauch, W., Shanahan, P., Somlyódy, L., Vanrolleghem, P., 2001. *River Water Quality Model No. 1. Scientific & Technical Report No. 12,* London: IWA Task Group.

Rice, E. W., Baird, R. B., Eaton, A. D. & Clesceri, L. S., 1989. *Standard Methods for the Examination of Water and Wastewater.* 17 ed. Washington D.C: American Public Health Association.

Ruiz-Herrera, J., 1992. *Fungal Cell Wall: Structure, Synthesis and Assem.* Mexico: CRC Press.

Saltelli, A., Ratto, M., Andres, T., Campolongo, F., Cariboni, J., Gatelli, D., Saisana, M., Tarantola, S.,008. *Global sensitivity analysis. The Primer.* London: Wiley.

Seders, L. A. & Fien, J. B., 2011. Proton biding of bacterial exudates determined through potentionmetic titrations. *Chemical Geology ,* Volume 285, pp. 115-123.

Sharon, N., 1969. The bacteria cell wall. *Scientific American,* 220(5), pp. 92-98.

Sotemann, S. W., van Rensburg, P., Ristow, N. E., Wentzel, M. C., Loewenthal, R. E., Ekama, G. A., 2005. Integrated chemical/physical and biological processes modelling Part 2 - Anaerobic digestion of sewage sludges. *Water SA,* 31(4), pp. 545-568.

Sposito, G. & Coves, J., 1988. *SOILCHEM: A computer program for the calculation of chemical equilibria in soil solutions and other natural water systems,* s.l.: Riverside, Kearney foundation of soil science, University of California.

Sposito, G. & Mattigod, S. V., 1979. *GEOCHEM, a computer program for calculating chemical equilibria in soil solutions and other natural water systems,* s.l.: University of California .

Sreekrishnan, T. R., 1993. Kinetics of heavy-metal bioleaching from sewage-sludge. 1. Effects of process parameters. *Water Research ,* 27(11), pp. 1641-1651.

Stumm, W. & Morgan, J. J., 1996. *Aquatic Chemistry: Chemical Equilibria and Rates in Natural Waters.* New York: John Wiley and Sons.

Talbot, D. R., House, W. A. & Pethybridge, W. A., 1990. Prediction of the temperature dependence of electrical conductance for river waters. *Water Research ,* 24(10), pp. 1295-1304.

Tang, S. & Wang, Y., 2002. A paramater estimation program for the error-in-variable model. *Ecological Modelling,* Volume 156, pp. 225-236.

Tien, C. T., 1987. *Chemical Reactions Between Some Heavy Metal Ions and Sludge Particulate.* Newark: University Delaware.

Tien, C. T. & Huang, C. P., 1991. Formation of surface complexes between heavy metal and sludge particles. *Heavy metal in the Environment,* pp. 295-311.

Tsang, C., 1991. The Modelling Process and Model Validation. *Ground Water ,* 29(6).

van Langerak, E. P. A., 1998. Effects of high calcium concentrations on the development of methanogenic sludge in upflow anaerobic sludge bed (UASB) reactors. *Water Research ,* 32(4), pp. 1255-1263.

Voet, D. & Voet, J. G., 1990. *Biochemistry.* New York: John Wiley and Sons.

Wang, J., Huang, C. P., Allen, H. E. & Takiyama, L. R., 1998. Acid characteristics of dissolved organic matter in wastewater. *Water Environment Research,* 70(5), pp. 1041-1048.

Wentzel, M. C., 1992. Processes and modelling of nitrification dentirification biological excess phosphorus removal systems—A review. *Water Science and Technology ,* 25(6), pp. 59-82.

Wolery, T. J., 1992. *EQ3NR, a computer program for geochemical aqueous speciation-solubility calculations: Theoretical manual, user`s guide, and related documentation (Version 7.0),* CA United States: s.n.

Yun, Y. S., 2004. Characterisation of Functional Groups of Protonated Sargassum polycystum Bomass Capable of Binding Protons and Metal Ions. *Journal of Microbiology and Biotechnology,* 14(1), pp. 29-34.

Appendices

Appendix 1 Experimental resources

1.1 Materials and methods expansion

Table A 1-1: Typical ion concentrations in mammalian cytosol and blood (Lodish, 1999)

Ion	Concentration in cytosol (mM)
Potassium	139
Sodium	12
Chloride	4
Bicarbonate	12
Amino acids in proteins	138
Magnesium	0.8
Calcium	<0.0002

1.1.1. Experimental data

The titration data can be found on the USB provided. A description of the files can be seen below:

Table A 1-2: Experimental data description

File(s)	Description
2a.xls 3a.xls 3b.xls blankb.xls pH probe response time calculation.xls	These files were used to calculate the pH probe response time and contain the calculations and experimental data. This response time was applied in phase 3.
120411trial2.xls 120411trial2a.xls 120411trial2b.xls 120411trial2c.xls 130411trial1.xls 130411trial2.xls 130411trial3.xls 130411trial4.xls 130411trial5.xls 130411trial6.xls	These files contain the experimental data used in phase 1 for the glycine titration experiments.
040511trial1.xls 040511trial2.xls 040511trial3.xls 040511trial4.xls 040511trial5.xls 050511trial1.xls 050511trial2.xls 050511trial3.xls	These files contain the experimental data used in phase 2 for the yeast titration experiments.
190411trial1.xls 190411trial2.xls 190411trial3.xls 190411trial4.xls 190411trial5.xls 190411trial6.xls 190411trial7.xls	These files contain the experimental data used in phase 2 for the washed anaerobic sludge titration experiments.

081013yeastacid1.xls 081013yeastacid1.xls 081013yeastacid2.xls 081013yeastacid3.xls 081013yeastacid4.xls 081013yeastacid5.xls 081013yeastacid6.xls 081013yeastacid7.xls 081013yeastacid10.xls	These files contain the experimental data used in phase 3 for the yeast titration experiments.
Temperatureanalysis.xls Titrationspeedanalysis.xls	These files contain the analysis of the effect of temperature and titration speed on the experimental titration curve
081013yeastbase8b.xls 081013yeastbase8c.xls 081013yeastmeasure8a.xls 081013yeastmeasure8b.xls 081013yeastmeasure8c.xls	These files contain the experimental data for the estimation of carbon dioxide exchange.
Total and volatile solids results.xls	This file contains the total solid, volatile solid and fixed solid results for the experiments conducted during the study

Appendix 2 **Additional simulated and experimental titration curves**

Figures A-2.1 – A-2.3 show the 3 of the 7 sample set titrations, not shown in Section 5.2, used in the establishment of the UKZiNe description. Figure A-2.4 shows the experimental titrations of the anaerobic sludge for 3 sludge concentrations in a mixed salt background solution.

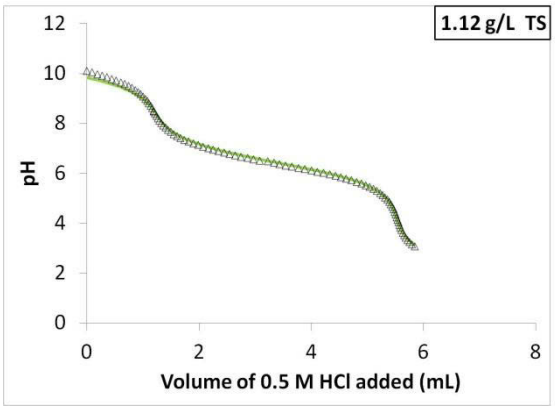

Figure A 2-1: Establishment of UKZiNe parameters by fitting the model (solid line) to experimental titration(points) of a yeast suspension (Background of 12.5 mmol/L $CO_3^{=}$ and 4 mmol/L PO_4^{-3}) for phase 2

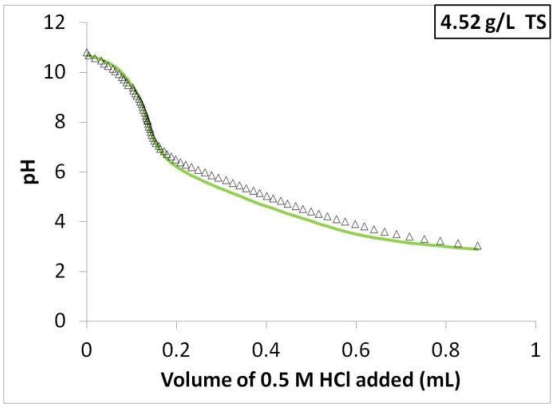

Figure A 2-2: Establishment of UKZiNe parameters by fitting the model (solid line) to experimental titration(points) of yeast biomass in a NaOH solution for phase 2

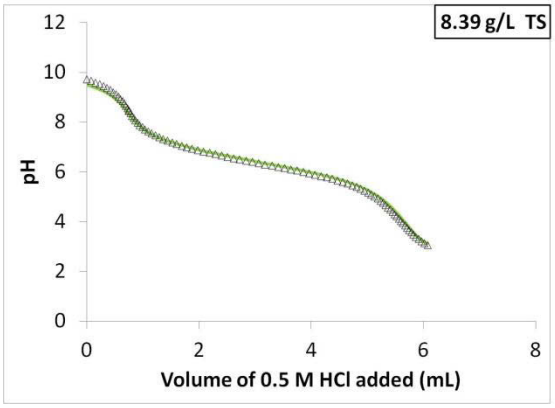

Figure A 2-3: Establishment of UKZiNe parameters by fitting the model (solid line) to experimental titration(points) of a yeast suspension (Background of 12.5 mmol/L $CO_3^=$ and 4 mmol/L PO_4^{-3}) for phase 2

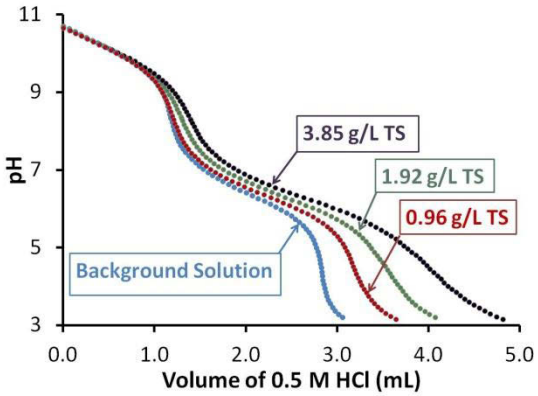

Figure A 2-4: Experimental titration results for washed anaerobic sludge in 5 mmol/L $CO_3^=$ and 1.6 mmol/L PO_4^{-3}

Appendix 3 **Uncertainty analysis**

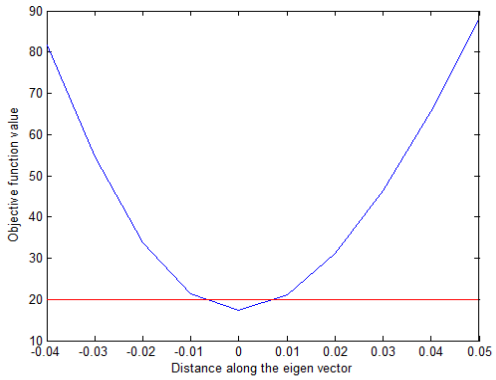

Figure A 3-1: Eigenvector diagram 1 in phase 2

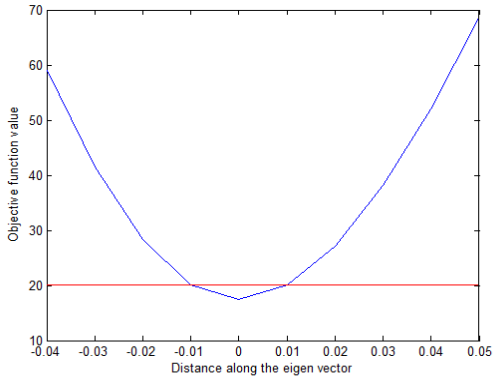

Figure A 3-2: Eigenvector diagram 2 in phase 2

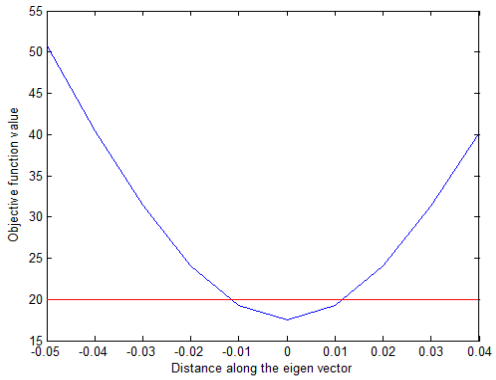

Figure A 3-3: Eigenvector diagram 3 in phase 2

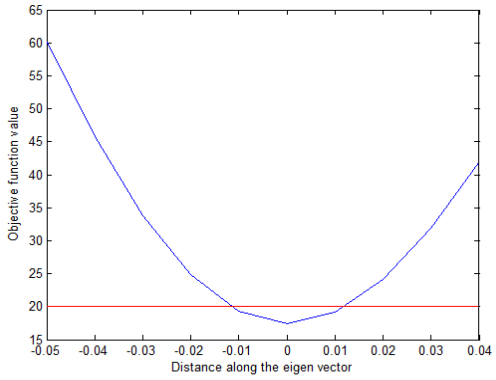

Figure A 3-4: Eigenvector diagram 4 in phase 2

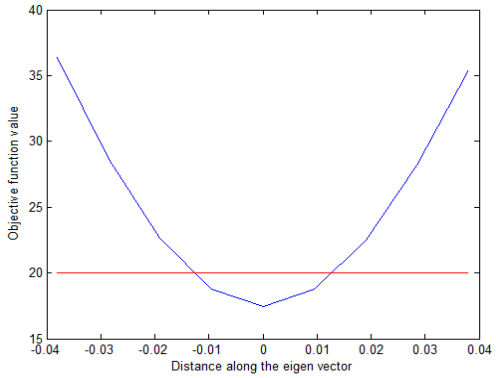

Figure A 3-5: Eigenvector diagram 5 in phase 2

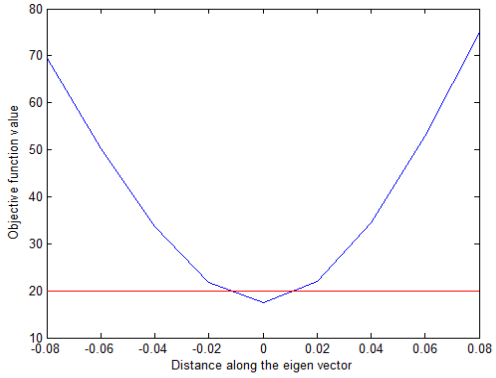

Figure A 3-6: Eigenvector diagram 6 in phase 2

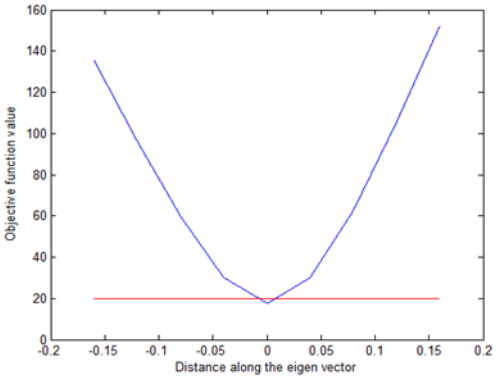

Figure A 3-7: Eigenvector diagram 7 in phase 2

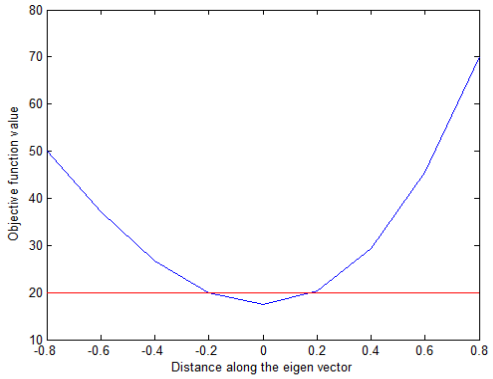

Figure A 3-8: Eigenvector diagram 8 in phase 2

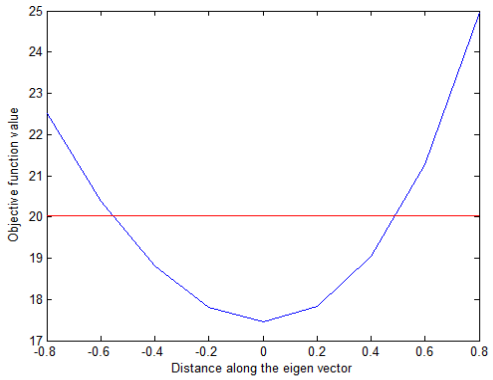

Figure A 3-9: Eigenvector diagram 9 in phase 2

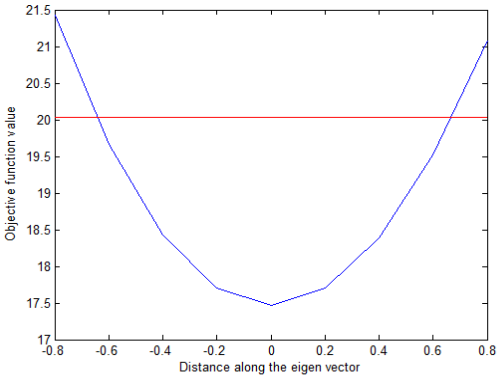

Figure A 3-10: Eigenvector diagram 10 in phase 2

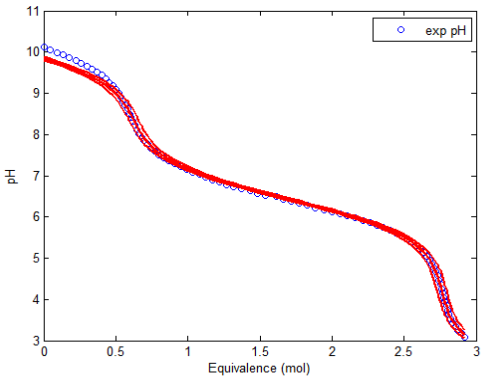

Figure A 3-11: Experimental data (blue points) with the uncertainty range of simulations plotted in red (solid line) for a 1.12 g/L TS yeast suspension (Background of 12.5 mmol/L $CO_3^{=}$ and 4 mmol/L PO_4^{-3})

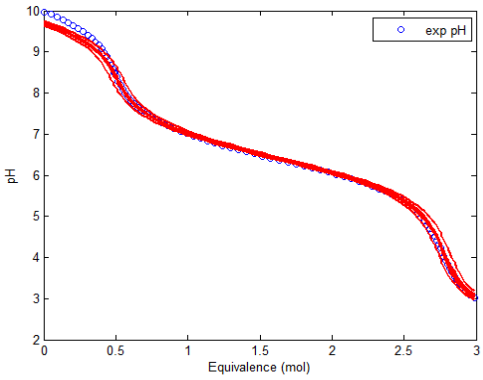

Figure A 3-12: Experimental data (blue points) with the uncertainty range of simulations plotted in red (solid line) for a 4.37 g/L TS yeast suspension (Background of 12.5 mmol/L $CO_3^{=}$ and 4 mmol/L PO_4^{-3})

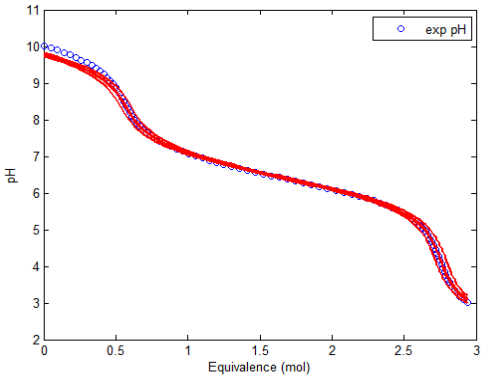

Figure A 3-13: Experimental data (blue points) with the uncertainty range of simulations plotted in red (solid line) for a 2.29 g/L TS yeast suspension (Background of 12.5 mmol/L $CO_3^{=}$ and 4 mmol/L PO_4^{-3})

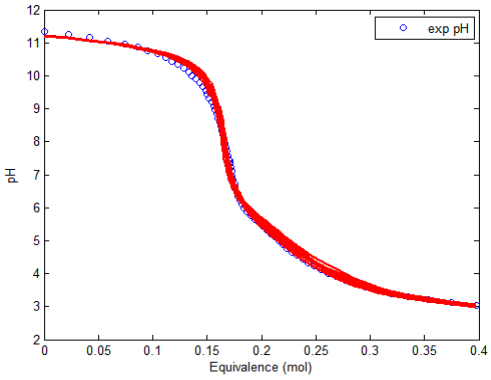

Figure A 3-14: Experimental data (blue points) with the uncertainty range of simulations plotted in red (solid line) for a 2.28 g/L TS yeast suspension

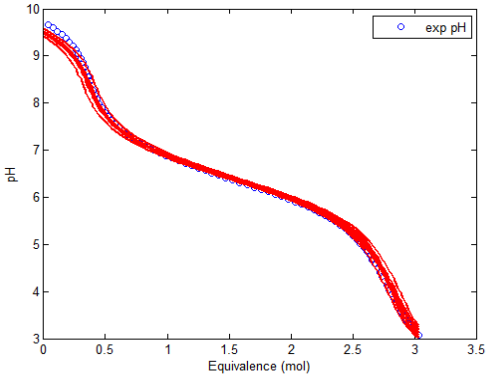

Figure A 3-15: Experimental data (blue points) with the uncertainty range of simulations plotted in red (solid line) for a 8.39 g/L TS yeast suspension (Background of 12.5 mmol/L $CO_3^{=}$ and 4 mmol/L PO_4^{-3})

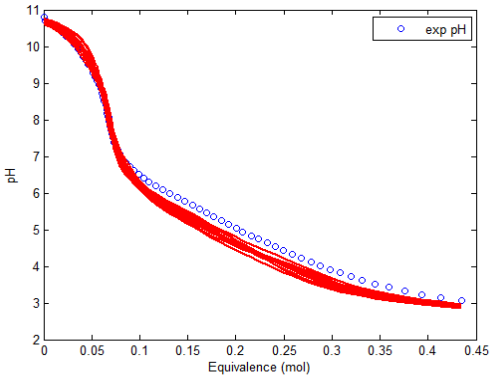

Figure A 3-16: Experimental data (blue points) with the uncertainty range of simulations plotted in red (solid line) for a 4.52 g/L TS yeast suspension

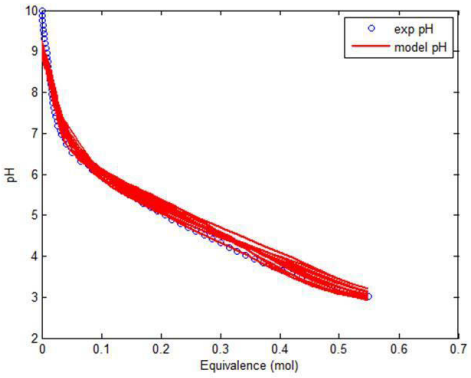

Figure A 3-17: Experimental data (blue points) with the uncertainty range of simulations plotted in red (solid line) for a 8.69 g/L TS yeast suspension

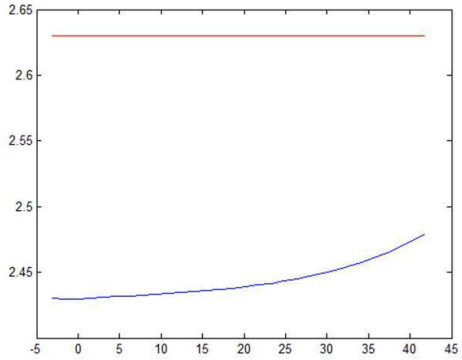

Figure A 3-18: Eigenvector diagram 1 in phase 3

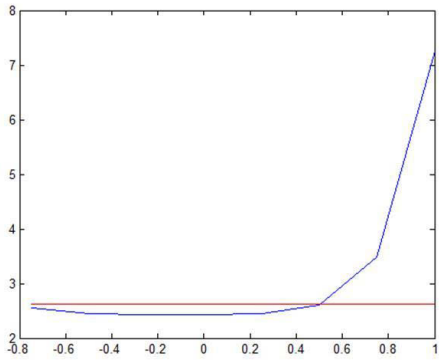

Figure A 3-19: Eigenvector diagram 2 in phase 3

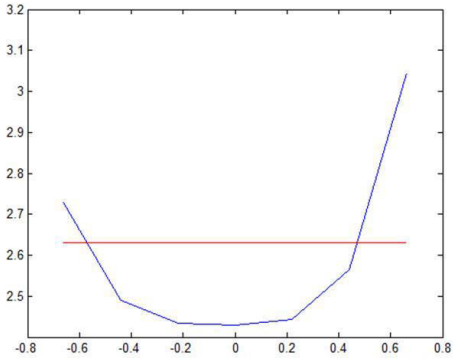

Figure A 3-20: Eigenvector diagram 3 in phase 3

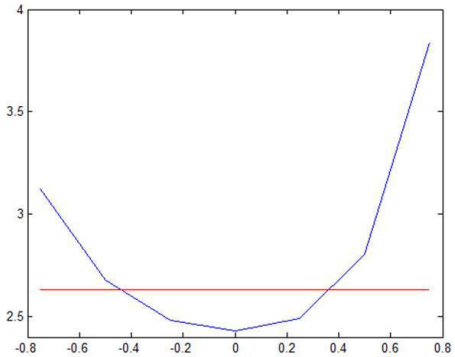

Figure A 3-21: Eigenvector diagram 4 in phase 3

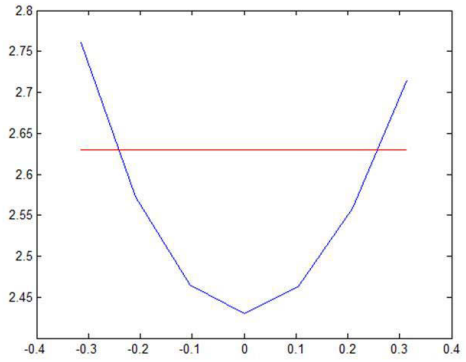

Figure A 3-22: Eigenvector diagram 5 in phase 3

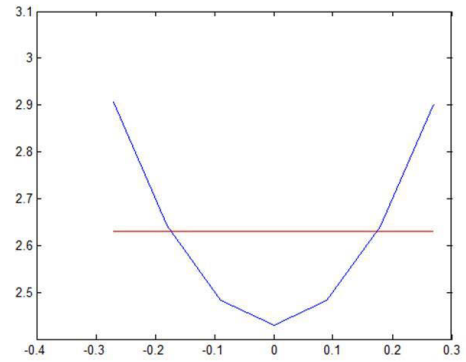

Figure A 3-23: Eigenvector diagram 6 in phase 3

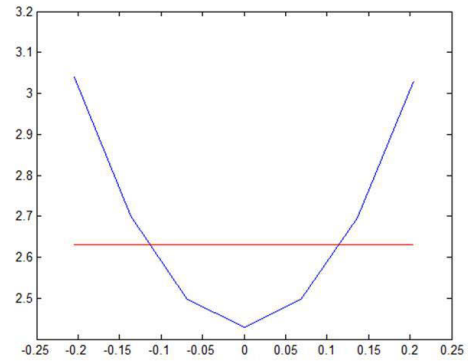

Figure A 3-24: Eigenvector diagram 7 in phase 3

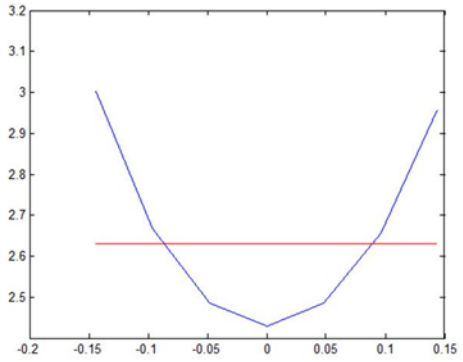

Figure A 3-25: Eigenvector diagram 8 in phase 3

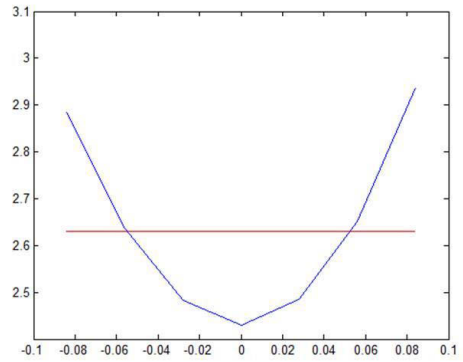

Figure A 3-26: Eigenvector diagram 9 in phase 3

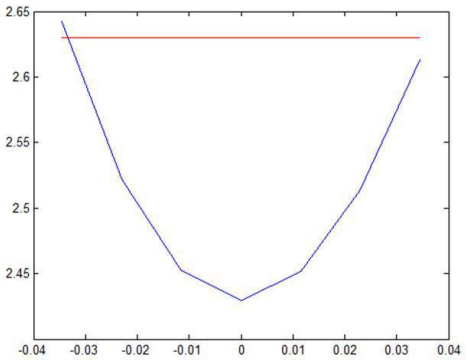

Figure A 3-27: Eigenvector diagram 10 in phase 3

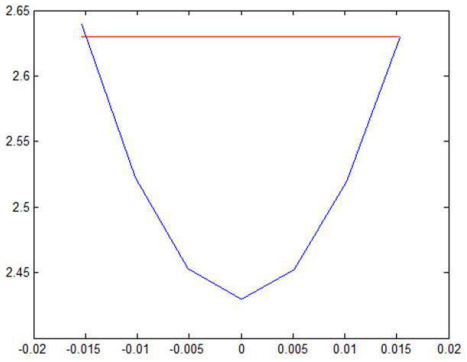

Figure A 3-28: Eigenvector diagram 11 in phase 3

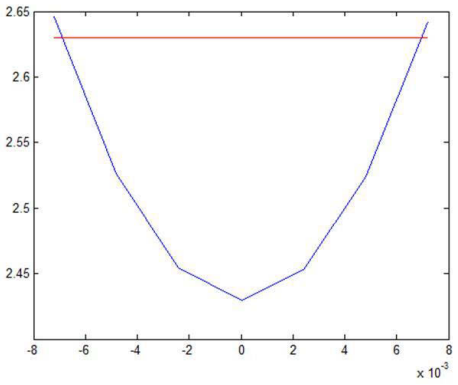

Figure A 3-29: Eigenvector diagram 12 in phase 3

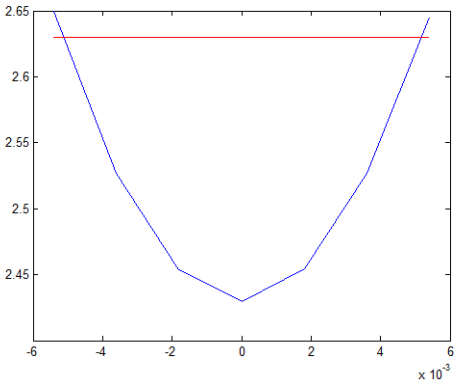

Figure A 3-30: Eigenvector diagram 13 in phase 3

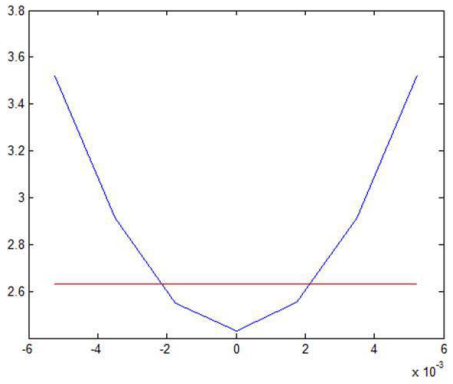

Figure A 3-31: Eigenvector diagram 14 in phase 3

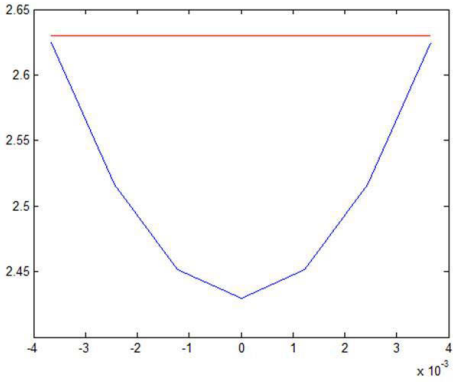

Figure A 3-32: Eigenvector diagram 15 in phase 3

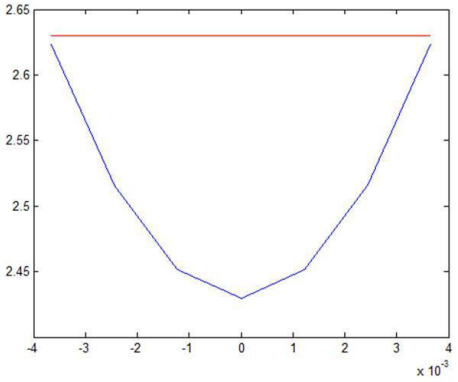

Figure A 3-33: Eigenvector diagram 16 in phase 3

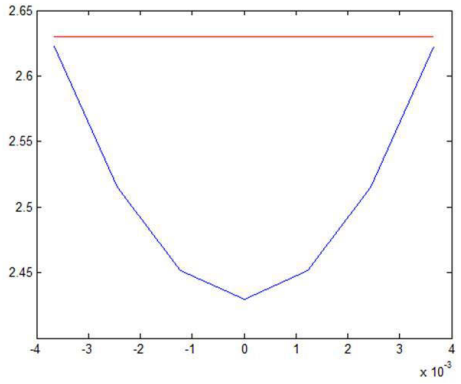

Figure A 3-34: Eigenvector diagram 17 in phase 3

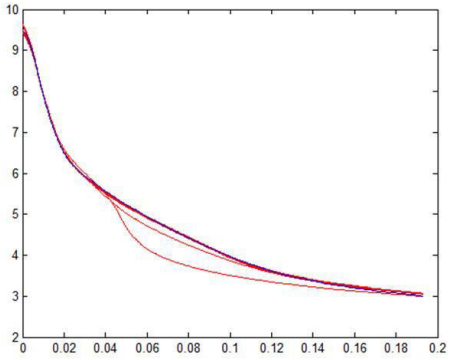

Figure A 3-35: Experimental data (blue points) with the uncertainty range of simulations plotted in red (solid line) for a 6.35 g/L TS yeast suspension

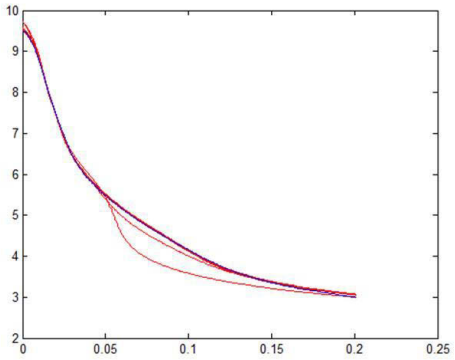

Figure A 3-36: Experimental data (blue points) with the uncertainty range of simulations plotted in red (solid line) for a 6.44 g/L TS yeast suspension

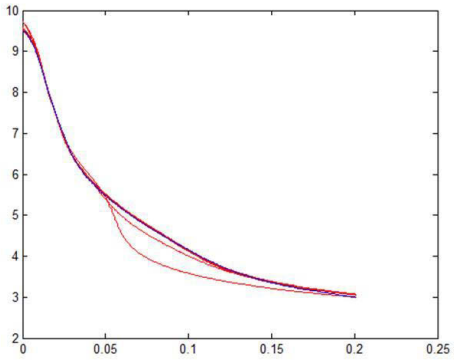

Figure A 3-37: Experimental data (blue points) with the uncertainty range of simulations plotted in red (solid line) for a 6.31 g/L TS yeast suspension

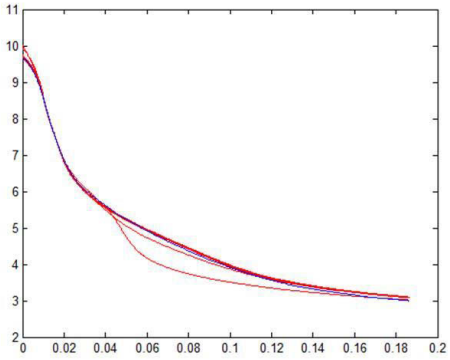

Figure A 3-38: Experimental data (blue points) with the uncertainty range of simulations plotted in red (solid line) for a 6.35 g/L TS yeast suspension

Table A 3-1: Parameter correlation for phase 2

	U1[11]	U2	U3	U4	Alk[12]1	Alk2	Alk3	Alk4	Alk5	Alk6	Alk7
U1	1.00	-0.83	0.34	-0.10	0.18	0.50	0.32	0.86	0.69	0.86	0.87
U2	-0.83	1.00	-0.64	0.22	-0.13	-0.34	-0.23	-0.45	-0.45	-0.47	-0.47
U3	0.34	-0.64	1.00	-0.54	0.05	0.13	0.09	0.13	0.17	0.16	0.18
U4	-0.10	0.22	-0.54	1.00	-0.01	-0.03	-0.02	-0.03	-0.05	-0.04	-0.05
Alk1	0.18	-0.13	0.05	-0.01	1.00	0.09	0.06	0.17	0.13	0.17	0.17
Alk2	0.50	-0.34	0.13	-0.03	0.09	1.00	0.17	0.50	0.38	0.50	0.50
Alk3	0.32	-0.23	0.09	-0.02	0.06	0.17	1.00	0.32	0.24	0.32	0.32
Alk4	0.86	-0.45	0.13	-0.03	0.17	0.50	0.32	1.00	0.72	0.99	0.99
Alk5	0.69	-0.45	0.17	-0.05	0.13	0.38	0.24	0.72	1.00	0.72	0.72
Alk6	0.86	-0.47	0.16	-0.04	0.17	0.50	0.32	0.99	0.72	1.00	0.99
Alk7	0.87	-0.47	0.18	-0.05	0.17	0.50	0.32	0.99	0.72	0.99	1.00

[11] U1-4 – Corresponds with the site concentrations for U-COO1, U-COO2, U-PO4 and U-NH3 respectively
[12] Alk – Alkalinity for the respective sample sets

Table A 3-2: Parameter correlation for phase 3

	U1	**U2**	**U3**	**U4**	**pK_a1**[13]	**pK_a2**	**pK_a3**	**pK_a4**	**Rate**[14]	**Alk1**	**Alk2**	**Alk3**	**Alk4**	**Ini1**[15]	**Ini2**	**Ini3**	**Ini4**
U1	1.00	-0.99	0.27	-0.27	0.97	0.98	-0.36	-0.31	-0.05	-0.60	-0.59	-0.59	-0.60	-0.77	-0.76	-0.77	-0.76
U2	-0.99	1.00	-0.27	0.21	-0.98	-0.93	0.27	0.25	-0.02	0.65	0.66	0.66	0.66	0.67	0.67	0.67	0.67
U3	0.27	-0.27	1.00	0.07	0.23	0.30	-0.28	0.01	0.80	0.01	-0.22	-0.19	-0.02	-0.51	-0.54	-0.51	-0.58
U4	-0.27	0.21	0.07	1.00	-0.22	-0.33	0.67	1.00	0.10	0.09	0.06	0.07	0.07	0.45	0.44	0.45	0.43
pK_a1	0.97	-0.98	0.23	-0.22	1.00	0.91	-0.29	-0.25	-0.03	-0.75	-0.74	-0.75	-0.75	-0.66	-0.66	-0.66	-0.65
pK_a2	0.98	-0.93	0.30	-0.33	0.91	1.00	-0.45	-0.37	-0.08	-0.54	-0.52	-0.52	-0.53	-0.87	-0.86	-0.87	-0.85
pK_a3	-0.36	0.27	-0.28	0.67	-0.29	-0.45	1.00	0.70	-0.02	0.11	0.11	0.11	0.10	0.70	0.70	0.70	0.70
pK_a4	-0.31	0.25	0.01	1.00	-0.25	-0.37	0.70	1.00	0.07	0.10	0.08	0.08	0.08	0.50	0.49	0.50	0.48
Rate	-0.05	-0.02	0.80	0.10	-0.03	-0.08	-0.02	0.07	1.00	0.16	-0.13	-0.09	0.13	-0.05	-0.09	-0.04	-0.14
Alk1	-0.60	0.65	0.01	0.09	-0.75	-0.54	0.11	0.10	0.16	1.00	0.88	0.89	0.92	0.33	0.30	0.30	0.29
Alk2	-0.59	0.66	-0.22	0.06	-0.74	-0.52	0.11	0.08	-0.13	0.88	1.00	0.92	0.89	0.31	0.34	0.31	0.33

[13] pK_a1-pK_a4 – Corresponds respectively with pK_a's for U-COO1, U-COO2, U-PO4 and U-NH3
[14] Rate – Carbon dioxide exchange rate
[15] Ini 1-4 –Corresponds with the initial carbon dioxide dissolved in solution for the respective sample sets

Alk3	-0.59	0.66	-0.19	0.07	-0.75	-0.52	0.11	0.08	-0.09	0.89	0.92	1.00	0.90	0.32	0.32	0.34	0.32
Alk4	-0.60	0.66	-0.02	0.07	-0.75	-0.53	0.10	0.08	0.13	0.92	0.89	0.90	1.00	0.30	0.30	0.30	0.31
Ini1	-0.77	0.67	-0.51	0.45	-0.66	-0.87	0.70	0.50	-0.05	0.33	0.31	0.32	0.30	1.00	0.99	0.99	0.99
Ini2	-0.76	0.67	-0.54	0.44	-0.66	-0.86	0.70	0.49	-0.09	0.30	0.34	0.32	0.30	0.99	1.00	0.99	0.99
Ini3	-0.77	0.67	-0.51	0.45	-0.66	-0.87	0.70	0.50	-0.04	0.30	0.31	0.34	0.30	0.99	0.99	1.00	0.99
Ini4	-0.76	0.67	-0.58	0.43	-0.65	-0.85	0.70	0.48	-0.14	0.29	0.33	0.32	0.31	0.99	0.99	0.99	1.00

Table A 3-3: Objectives values at the limits for phase 2 (Figures A 3-11 to A 3-17) generated from the regression of the parameters

Dataset 1	Dataset 2	Dataset 3	Dataset 3	Dataset 5	Dataset 6	Dataset 7
0.76	0.90	0.71	4.70	1.10	5.32	6.54
0.76	0.89	0.70	4.71	1.07	5.46	6.45
0.76	0.89	0.70	2.63	1.06	6.57	7.42
0.76	0.90	0.71	2.66	1.11	6.30	7.59
3.32	0.90	0.70	2.44	1.08	5.27	6.31
3.32	0.90	0.70	2.44	1.08	5.27	6.31
0.76	0.89	0.70	2.44	1.08	6.39	7.76
0.76	0.90	0.70	2.45	1.09	6.27	7.86
0.76	0.90	3.27	2.44	1.08	5.27	6.31
0.76	0.90	3.27	2.44	1.08	5.27	6.31
0.76	3.46	0.70	2.44	1.08	5.27	6.32
0.76	3.46	0.70	2.44	1.08	5.27	6.31
0.76	0.90	0.70	2.44	3.64	5.26	6.32
0.76	0.90	0.70	2.44	3.64	5.28	6.31
0.77	0.73	0.60	2.46	0.54	9.79	5.15
0.77	1.26	0.88	3.32	2.17	2.19	9.45
0.75	0.91	0.73	5.40	1.24	7.55	3.45
0.78	0.94	0.70	1.24	1.08	5.63	9.67
0.79	1.04	0.80	1.51	1.42	6.29	8.18
0.75	0.93	0.67	4.52	1.18	6.49	5.49
0.76	0.87	0.71	2.79	1.06	6.86	6.99
0.76	0.96	0.72	3.99	1.21	5.69	6.70

Table A 3-4: Objectives values at the limits for phase 3 (Figures A 3-35 to A 3-38) generated from the regression of the parameters

Dataset 1	Dataset 2	Dataset 3	Dataset 4	Total of Datasets
5.10	5.11	5.74	5.29	21.2
52.0	49.7	54.3	45.4	201
0.36	0.58	0.68	1.01	2.63
0.36	0.58	0.68	1.01	2.63
0.59	0.42	0.65	0.97	2.63
0.59	0.38	0.71	0.94	2.63
0.72	0.57	0.70	0.63	2.63
0.37	0.37	1.07	0.82	2.63
0.44	0.35	0.83	1.02	2.63
0.62	0.53	0.67	0.81	2.63
0.55	0.52	0.73	0.83	2.63
0.53	0.54	0.73	0.83	2.63
0.48	0.48	0.87	0.81	2.63
0.46	0.45	0.86	0.85	2.63
0.47	0.51	0.76	0.89	2.63
0.55	0.46	0.92	0.70	2.63
0.69	0.30	0.72	0.92	2.63
0.36	0.63	0.84	0.80	2.63
0.54	0.45	0.60	1.05	2.63
0.50	0.50	0.98	0.65	2.63
0.50	0.50	1.00	0.63	2.63
0.50	0.47	0.54	1.12	2.63
0.42	0.54	0.71	0.96	2.63
0.60	0.41	0.83	0.79	2.63
0.31	0.62	0.67	1.02	2.63
0.71	0.32	0.84	0.76	2.63
0.52	0.47	0.77	0.87	2.63
0.51	0.48	0.76	0.88	2.63
0.47	0.57	0.73	0.86	2.63
0.47	0.57	0.73	0.86	2.63
0.46	0.44	0.82	0.91	2.63
0.47	0.42	0.83	0.91	2.63
0.60	0.43	0.77	0.84	2.63
0.60	0.43	0.77	0.84	2.63

Table A 3-5: Parameter standard deviations for phase 2

U-COO1 site concentration	0.0349
U-COO2 site concentration	0.0296
U-PO4 site concentration	0.0680
U-NH3 site concentration	0.0421
Dataset 1 alkalinity	0.0008
Dataset 2 alkalinity	0.0012
Dataset 3 alkalinity	0.0009
Dataset 4 alkalinity	0.0041
Dataset 5 alkalinity	0.0017
Dataset 6 alkalinity	0.0078
Dataset 7 alkalinity	0.0100

Table A 3-6: Parameter standard deviations for phase 3

U-COO1 site concentration	0.1237
U-COO2 site concentration	0.2807
U-PO4 site concentration	0.0179
U-NH3 site concentration	1.1505
U-COO1 pK_a	0.0116
U-COO2 pK_a	0.0373
U-PO4 pK_a	0.0021
U-NH3 pK_a	0.0357
CO2 exchange rate	0.0323
Dataset 1 alkalinity	0.0037
Dataset 2 alkalinity	0.0035
Dataset 3 alkalinity	0.0035
Dataset 4 alkalinity	0.0037
Dataset 1 initial CO_2 in solution	0.2067
Dataset 2 initial CO_2 in solution	0.1466
Dataset 3 initial CO_2 in solution	0.0974
Dataset 4 initial CO_2 in solution	42.422

The very high standard deviation (42.422) for the initial CO_2 concentration in Table A3-6 is an artefact of the non-linearity of the model and the numerical differentiation.

Appendix 4 **Model script**

A collection of MATLAB files can be found on the USB provided. A description of the files is provided in the table below:

Table A 4-1: MATLAB files

File	**Description**
PHResUKZiNeOctCO3.m	This file calls the Excel experimental data and sets up the experimental data to be used within the regression/speciation
SetupSpeciationUKZiNeOctCO3.m	This file initializes all the variables to be used within the regression/speciation
FitUKZiNeOctCO3.m	This file is used to setup and activate the parameter regression. The file allows for kinetics or no kinetics to be present in the regression.
MultiTitrationObjOctCO3.m	This file is called by the regression and determines whether the objective function is the minimum for the regression to continue
ObjectiveTitrationUKZiNeAlkOctCO3.m	This file calculates the objective function and uses the speciation model to determine the simulated results.
IntegrateModelOct.m UKHderivOct.m ElectrodederivOct.m	This file is called by the objective function and is used only when kinetics are included in the model. This file accounts for the kinetics of the model (i.e. mass transfer as well as the pH electrode lag)
UKZiNe: SpeciationUKZINE.cpp UKZINE_pHAlkalinity_Arrays.cpp UKZINE_Speciation_Arrays.cpp Glycine: SpeciateGlycine.cpp	This file is called by the objective function to perform the speciation of the model.
Bufferintensitycalc.m	This file calculates the buffer intensity for the

	experimental curve as well as simulated curve
FitUKZiNeCO31a1.m	Provides the speciated values for Bufferintensitycalc.m with biomass included
FitUKZiNeCO31b1.m	Provides the speciated values for Bufferintensitycalc.m with biomass not included
explore. m	This is the file that calculates the uncertainty analysis once the regression is completed(i.e. once FitUKZiNeOctCO3.m is run)
MultiTitrationObjExplore.m	This file is called by explore.m and is used in exploring the different parameter sets and objective values
MultiTitrationObjPlot.m	This file is called by explore.m and plots the parameter sets from the uncertainty range as well as the experimental titration for comparison
secant.m	This file is called by explore.m and finds the secant for the uncertainty analysis

Appendix 5 Formulating and adapting the ionic speciation model

5.1 Phase 1

Reactions:

$HGly \rightarrow H^+ + Gly^-$ Equation 2-14

$H_2Gly^+ \rightarrow H^+ + HGly$ Equation 2-15

$MgGly^+ \rightarrow Mg^{2+} + Gly^-$ Equation 4-1

$CaGly^+ \rightarrow Ca^{2+} + Gly^-$ Equation 4-2

$CaHGly \rightarrow Ca^{2+} + HGly$ Equation 4-3

Construction of the mass balance of the model:

Calculation of thermodynamic equilibrium constants (kt):

The thermodynamic equilibrium constants, at infinite dilution, are calculated using the following equations:

$$LogKt = Logkt(25^0C) - \Delta H * T_{correction}$$ Equation A-1

where $T_{correction} = \frac{1}{T(experiment)} - \frac{1}{298.15}(2.303*8.314)$ Equation A-2

$$Kt(component) = 10^{LogKt}$$ Equation A-3

Table A 5-1: Thermodynamic data for the glycine reactions (Kiss, et al., 1991)

Reaction	logKt (25^0 C)	ΔH (KJ mol^{-1})
$HGly \rightarrow H^+ + Gly^-$	-9.778	44350.4
$H_2Gly^+ \rightarrow H^+ + HGly$	-2.35	4100.3
$MgGly^+ \rightarrow Mg^{2+} + Gly^-$	-2.08	-4184
$CaGly^+ \rightarrow Ca^{2+} + Gly^-$	-1.39	4184
$CaHGly \rightarrow Ca^{2+} + HGly$	-0.322	-8368

Calculation of equilibrium constants using ion activity coefficients:

$$K(HGly) = \frac{Kt(HGly)*gam0}{gam1*gam1}$$ Equation A-4

$$K(H_2Gly^+) = \frac{Kt(H_2Gly^+)}{gam0}$$ Equation A-5

$$K(MgGly) = \frac{Kt(MgGly)}{gam2}$$ Equation A-6

$$K(CaGly) = \frac{Kt(CaGly)}{gam2}$$ Equation A-7

$$K(CaHGly) = \frac{Kt(CaHGly)}{gam0}$$ Equation A-8

where

$$gam0 = 10^{0.1I}$$ Equation A-9

$$gam1 = 10^{-1.825*10^6*78.3*T(experiment)^{-1,5}*\frac{I^{0.5}}{1+I^{0.5}}}$$ Equation A-10

$$gam2 = 10^{4gam1}$$ Equation A-11

Kt: Thermodynamic equilibrium constant; I: Ionic strength; T: Temperature

Calculation of glycine component concentration:

$$[HGly] = \frac{[HGly]_{total}}{(1+\frac{2K(H_2O)}{K(H_2Gly)*[OH]}+\frac{[Ca]}{K(CaHGly)}+\frac{K(HGly)*[OH]*(1+\frac{[Mg]}{K(MgGly)}+\frac{[Ca]}{K(CaGly)})}{K(H_2O)}}$$ Equation A-12

Calculation of the hydrogen balance used to calculate the absolute error between the results and the last iteration's results:

$$Error = [H]*\left(1+\frac{2[HCO_3]}{K(H_2CO_3)}+\frac{[Ac]}{K(HAc)}+\frac{[Pr]}{K(HPr)}+\frac{2[HPO_4]}{K(H_2PO_4)}+\frac{2[Mg]*[HPO_4]}{K(MgH_2PO_4)}\right)+[HCO_3]*$$
$$\left(1+\frac{[Ca]}{K(CaHCO_3)}+\frac{[Mg]}{K(MgHCO_3)}+\frac{[Na]}{K(NaHCO_3)}\right)+[HPO_4]*\left(1+\frac{[Mg]}{K(MgHPO_4)}+\frac{[Ca]}{K(CaHPO_4)}+\right.$$
$$\left.\frac{[Na]}{K(NaHPO_4)}+\frac{3[H]*[H]}{\boldsymbol{K(H_3PO_4)}}\right)-[OH]*\left(1+\frac{[Ca]}{K(CaOH)}+\frac{[Mg]}{K(MgOH)}\right)-\frac{[NH_4]*K(NH_4)}{[H]}+[HGly]*(1+$$
$$\frac{[Ca]}{K(CaHGly)}+\frac{2[H]}{K(H_2Gly)})-[H]_{total}$$ Equation A-13

5.2 Phase 2 & 3

Reactions:

U1-COO^- + H^+ → U1-COOH Equation 5-1

U2-COO^- + H^+ → U2-COOH Equation 5-2

U3-PO_4^{2-} + H^+ → U3-PO_4^- Equation 5-3

U4-NH_3^+ → U4-NH_2 + H^+ Equation 5-4

Construction of the mass balance of the model:

Calculation of thermodynamic equilibrium constants (Kt):

The thermodynamic equilibrium constants, at infinite dilution, are calculated using Equations A-1 to A-3.

Table A 5-2: Thermodynamic data for the UKZiNe reactions

Reaction	log$Kt(25^0$ C) – Phase 2	Regressed log$Kt(25^0$ C) - Phase 3	ΔH (KJ mol^1)
U1-COO $^-$+ H^+ → U1-COOH	4.35	4.586	0
U2-COO $^-$+ H^+ → U2-COOH	5.65	5.339	0
U3-PO_4^{2-} + H^+ → U3-PO_4^-	7.198	7.698	0
U4-NH_3^+ → U4-NH_2 + H^+	-9.244	-10.646	0

Calculation of equilibrium constants using ion activity coefficents:

$K(U1) = Kt(U1) * gam1$ Equation A-14

$K(U2) = Kt(U2) * gam1$ Equation A-15

$K(U3) = Kt(U3) * gam1$ Equation A-16

$K(U4H) = \frac{Kt(U4H)}{gam1}$ Equation A-17

where

$gam1 = 10^{-Adh*(\frac{\sqrt{I}}{1+\sqrt{I}}-0.3I)}$ Equation A-18

$Adh = 1.82\ X\ 10^6(\epsilon T)^{-3/2}$ Equation A-19

ϵ: dielectric constant ; Kt: Thermodynamic equilibrium constant; I: Ionic strength; T: Temperature

Calculation of UKZiNe component concentration:

$[U1] = \frac{[U1]_{total}}{1+K(U1)*[H]}$ Equation A-20

$[U2] = \frac{[U2]_{total}}{1+K(U2)*[H]}$ Equation A-21

$[U3] = \frac{[U3]_{total}}{1+K(U3)*[H]}$ Equation A-22

$[U4H] = \frac{[U4H]_{total}}{1+K(U4H)*[H]}$ Equation A-23

Calculation of the hydrogen balance used to calculate the absolute error between the results and the last iteration's results:

$$Error = [H] * \left(1 + \frac{2[HCO_3]}{K(H_2CO_3)} + \frac{[Ac]}{K(HAc)} + \frac{[Pr]}{K(HPr)} + \frac{2[HPO_4]}{K(H_2PO_4)} + \frac{2[Mg]*[HPO_4]}{K(MgH_2PO_4)}\right) + [HCO_3] * \left(1 + \frac{[Ca]}{K(CaHCO_3)} + \frac{[Mg]}{K(MgHCO_3)} + \frac{[Na]}{K(NaHCO_3)}\right) + [HPO_4] * \left(1 + \frac{[Mg]}{K(MgHPO_4)} + \frac{[Ca]}{K(CaHPO_4)} + \frac{[Na]}{K(NaHPO_4)} + \frac{3[H]*[H]}{\boldsymbol{K(H_3PO_4)}}\right) - [OH] * \left(1 + \frac{[Ca]}{K(CaOH)} + \frac{[Mg]}{K(MgOH)}\right) - \frac{[NH_4]*K(NH_4)}{[H]} + \frac{[U1]}{K(U1)*[H]} + \frac{[U2]}{K(U2)*[H]} + \frac{[U3]}{K(U3)*[H]} - \frac{[U4H]*K(U4H)}{[H]} - [H]_{total}$$ Equation A-24

Appendix 6